Electronic supplementary information (ESI) for:

Solid state structure and properties of phenyl diketopyrrolopyrrole derivatives

Joshua Humphreys,[a,b] Flavia Pop,[a,b§] Paul A. Hume,[c] Alanna S. Murphy,[a,b] William Lewis,[b¶] E. Stephen Davies,[b] Stephen P. Argent,[b] and David B. Amabilino*[a,b]

[a] The GSK Carbon Neutral Laboratories for Sustainable Chemistry, The University of Nottingham Jubilee Campus, Triumph Road, Nottingham NG7 2TU, UK.

School of Chemistry, University of Nottingham, Nottingham NG7 2RD, UK. E-mail: David.Amabilino@nottingham.ac.uk.

[c] MacDiarmid Institute for Advanced Materials and Nanotechnology and School of Chemical and Physical Sciences, Victoria University of Wellington, Wellington 6010, New Zealand

§ Current Address MOLTECH-Anjou, UMR 6200, CNRS, Univ. Angers, 2bd Lavoisier, 49045 Angers, France

¶Current address Chemistry Building, The University of Sydney, Eastern Avenue NSW 2006, Australia

Contents

1. Experimental section
2. ^{1}H NMR Spectra
3. ^{13}C NMR Spectra
4. IR Spectra
5. Mass Spectra
6. Electrochemistry
7. Crystallographic tables and data
8. Computational data
9. Supporting figures
10. Supporting tables
11. References

Experimental section

General Methods and Materials. All commercially available reagents and solvents were used as received. Chromatography purifications were performed using Sigma-Aldrich Silica Gel (pore size 60Å, particle size 40- 63 μm) and thin-layer chromatography (TLC) was carried out on E. Merck silica gel plates, irradiated using UV light (365 nm). NMR spectra were acquired on a Bruker AV400, Bruker AV(III)500 or Bruker DPX300 spectrometers and NMR spectra were recorded at room temperature. All chemical shifts are reported in δ parts per million (ppm), using the solvent residual signal as an internal standard and the coupling constant values (J) are reported in Hertz (Hz). The following abbreviations are used for signal multiplicities: s, singlet; d, doublet; t, triplet; m, multiplet; and b, broad. ESI-MS were recorded using a Bruker micro-TOF II instrument. Infra-red spectra were recorded on a Bruker Tensor 27 instrument equipped with a Pike GladiATR attachment with a diamond crystal. Melting points were determined on a Stuart SMP20 Melting Point Apparatus. Elemental analysis (CHN) was performed by the University of Nottingham, School of Chemistry Microanalytical Service on an Exeter Analytical CE- 440 instrument.

The band gap was calculated from the onset of the optical absorption of the film using the equation: $Eg = 1240 / \lambda_{onset}$ [eV].

For PhOMeDPP *N*-Hex and PhOBocDPP *N*-Boc, single crystals were selected and mounted using Fomblin® (YR-1800 perfluoropolyether oil) on a polymer-tipped MiTeGen MicroMountTM and cooled rapidly to 120 K in a stream of cold N_2 using an Oxford Cryosystems open flow cryostat.[1] Single crystal X-ray diffraction data were collected on an Oxford Diffraction GV1000 (AtlasS2 CCD area detector, mirror-monochromated Cu-Kα radiation source; λ = 1.54184 Å, ω scans). Cell parameters were refined from the observed positions of all strong reflections and absorption corrections were applied using a Gaussian numerical method with beam profile correction (CrysAlisPro).[2] Structures were solved within Olex2[3] by dual space iterative methods (SHELXT)[4] and all non-hydrogen atoms refined by full-matrix least-squares on all unique F2 values with anisotropic displacement parameters (SHELXL).[5] Hydrogen atoms were refined with constrained geometries and riding thermal parameters. Structures were checked with checkCIF.[6] CCDC-2005929 and 2005925 contains the supplementary data for these compounds. This data can be obtained free of charge from The Cambridge Crystallographic Data Centre via www.ccdc.cam.ac.uk/data_request/cif. For PhOMeDPP *N*-Boc X-ray diffraction measurements were performed in Experiments Hutch 1 (EH1) of Beamline I19, at Diamond Light Source.[7] The data were collected at a wavelength of 0.6889 Å on a Fluid Film Devices 3-circle fixed-chi diffractometer using a Dectris Pilatus 2M detector. The crystal was mounted on a MiTeGen MicroMountTM using a perfluoropolyether oil, and cooled for data collection by a Cryostream nitrogen-gas stream.[1] The collected frames were integrated using XIA26 software[8] and the data were

corrected for absorption effects using AIMLESS,[9] an empirical method. Structures were solved within Olex2[3] by dual space iterative methods (SHELXT)[4] and all non-hydrogen atoms refined by full-matrix least-squares on all unique F2 values with anisotropic displacement parameters (SHELXL).[5] Hydrogen atoms were refined with constrained geometries and riding thermal parameters. The terminal OMe group is disordered over two positions. The occupancies of the two components were refined competitively, converging to a ratio of 0.51:0.49.Structures were checked with checkCIF.[6] CCDC-2005924contains the supplementary data for these compounds. This data can be obtained free of charge from The Cambridge Crystallographic Data Centre via www.ccdc.cam.ac.uk/data_request/cif. For PhOHDPP *N*-Hex, a single crystal was selected and mounted using Fomblin® (YR-1800 perfluoropolyether oil) on a polymer-tipped MiTeGen MicroMountTM and cooled rapidly to 120 K in a stream of cold N_2 using an Oxford Cryosystems open flow cryostat.[1] Single crystal X-ray diffraction data was collected on an Oxford Diffraction GV1000 (TitanS2 CCD area detector, mirror-monochromated Cu-Kα radiation source; λ = 1.54184 Å, ω scans). Cell parameters were refined from the observed positions of all strong reflections and absorption corrections were applied using a Gaussian numerical method with beam profile correction (CrysAlisPro).[2] The structure was solved within Olex2[3] by dual space iterative methods (SHELXT)[4] and all non-hydrogen atoms refined by full-matrix least-squares on all unique F2 values with anisotropic displacement parameters (SHELXL).[5] The structure was checked with checkCIF.[6] CCDC-2005927 contains the supplementary data for this compounds. This data can be obtained free of charge from The Cambridge Crystallographic Data Centre via www.ccdc.cam.ac.uk/data_request/cif. For PhOTHPDPP *N*-Hex and PhOMeDPP *N*-2MB, single crystals were selected and mounted using Fomblin® (YR-1800 perfluoropolyether oil) on a polymer-tipped MiTeGen MicroMountTM and cooled rapidly to 120 K in a stream of cold N_2 using an Oxford Cryosystems open flow cryostat.[1] Single crystal X-ray diffraction data were collected on an SuperNova Duo diffractometer (Atlas CCD area detector, mirror-monochromated Cu-Kα radiation source; λ = 1.54184 Å or mirror-monochromated Mo-Kα radiation source; λ = 0.71073 Å; ω scans). Cell parameters were refined from the observed positions of all strong reflections and absorption corrections were applied using a Gaussian numerical method with beam profile correction (CrysAlisPro).[2] Structures were solved within Olex2[3] by dual space iterative methods (SHELXT)[4] and all non-hydrogen atoms refined by full-matrix least-squares on all unique F2 values with anisotropic displacement parameters (SHELXL).[5] For PhOTHPDPP *N*-Hex, conformational disorder is modelled for the hexyl and phenol-tetrahydropyran moieties. Large quantities of restraints have been applied to the geometries and displacement parameters of these two regions of disorder to aid refinement of sensible models. The hexyl chain is disordered over two overlapping conformations, the occupancies of which have been refined and constrained to sum to unity resulting in values of 0.68(1) and 0.32(1).

The phenol-tetrahydropyran moiety is disordered between two overlapping diastereomeric conformations of the group. The occupancies of these conformations are refined and constrained to sum to unity resulting in values of 0.85(1) and 0.15(1). The molecule lies on a two-fold symmetry element meaning that all three possible diastereomers R,R S,S and R,S are likely to be present in the crystal, and in unequal amounts. The atoms of the minor occupancy disorder component of the phenol-tetrahydropyran moiety are modelled with isotropic displacement parameters; all other non-hydrogen atoms are modelled anisotropically. Rigid bond and similarity restraints have been applied to the displacement parameters of the disordered atoms. The geometries of the disorder components have been restrained to have similar geometries (SAME, SADI). The phenol ring systems are restrained to have planar geometries and planar connections to the adjacent atoms (FLAT). The C-C bond length of the terminal two carbon atoms in both disorder components are restrained to a target value of 1.5 A (DFIX). All hydrogen atoms were geometrically placed and refined using a riding model. The structures were checked with checkCIF.[6] CCDC-2005930 and 2005928 contains the supplementary data for this compounds. This data can be obtained free of charge from The Cambridge Crystallographic Data Centre via www.ccdc.cam.ac.uk/data_request/cif. For PhOHDPP *N*--2MB, a single crystal was selected and mounted using Fomblin® (YR-1800 perfluoropolyether oil) on a polymer-tipped MiTeGen MicroMountTM and cooled rapidly to 120 K in a stream of cold N_2 using an Oxford Cryosystems open flow cryostat.[1] Single crystal X-ray diffraction data were collected on an XtaLAB PRO MM007 (PILATUS3 R 200K Hybrid Pixel Array detector, mirror-monochromated Cu-Kα radiation source; λ = 1.54184 Å, ω scans). Cell parameters were refined from the observed positions of all strong reflections and absorption corrections were applied using a Gaussian numerical method with beam profile correction (CrysAlisPro).[2] The structure was solved within Olex2[3] by dual space iterative methods (SHELXT)[4] least squares refinement of the structure was carried using (SHELXL).[5] Structures were checked with checkCIF.[6] CCDC-2005926 contains the supplementary data for these compounds. These data can be obtained free of charge from The Cambridge Crystallographic Data Centre via www.ccdc.cam.ac.uk/data_request/cif.

UV/Vis absorption studies were performed using a Cary 5000 UV-Vis-NIR Absorption spectrometer. Emission studies were performed using an Edinburgh Instruments FLS980 Photoluminescence spectrometer. For quantum yield studies, fluorescence spectra were recorded as aerated solutions using a Jobin Yvon Horiba FluoroMax-3 spectrometer at ambient temperature in a 1cm pathlength quartz cuvette.

Quantum yields were calculated by comparison with the fluorescence observed for fluorescein (F = 91 in NaOH) under identical conditions of irradiation.[10] . Cyclic voltammetric studies were carried out using an Autolab PGSTAT20 potentiostat and in some cases an EmStat3 potentiostat. Standard cyclic

voltammetry was carried out under an atmosphere of argon using a three-electrode arrangement in a single compartment cell. A glassy carbon working electrode, a Pt wire secondary electrode and a saturated calomel reference electrode, chemically isolated from the test solution *via* a bridge tube containing electrolyte solution and fitted with a porous Vycor frit, were used in the cell when using the Autolab PGSTAT20 potentiostat. For the EmStat3 potentiostat a three electrode set up consisting of a platinum wire counter electrode, a platinum disc working electrode and a Ag/AgCl wire quasi reference electrode was used. Redox potentials are quoted versus the ferrocenium-ferrocene couple, which was used as an internal reference.[11] Acetonitrile was utilised as solvent for PhOMeDPP *N*-Hex, PhOMeDPP *N*-2MB and PhOTHPDPP *N*-Hex, dimethylformamide was used for PhOHDPP *N*-Hex and PhOHDPP *N*-2MB and dichloromethane for PhOMeDPP *N*-Boc and PhOBocDPP *N*-Boc. Tetrabutylammoniumhexafluorphosphae was employed as supporting electrolyte for all electrochemical experiments. HOMO and LUMO levels were calculated using the equations[12]:

E_{HOMO} = - (E_{onset}(ox) + 4.8 [eV]) and E_{LUMO} = -(E_{onset}(red) + 4.8 [eV]).

The band gap is calculated using the equation

$E_g = E_{HOMO} - E_{LUMO}$ [eV].

Alternatively, the band gap can also be calculated from the onset of the optical absorption of the film using the equation:

$E_g = 1240 / \lambda_{onset}$ [eV].

Electronic structure calculations were performed using Gaussian 09.[13] Electronic coupling calculations used molecular geometries taken from the crystal structures and used the B3LYP exchange-correlation functional and 6-311G(d,p) basis set with an ultrafine integration grid. Calculations of reorganisation energies used the larger 6-311+(d,p) basis set, with alkyl groups replaced with methyl to speed up geometry optimisation. Coupling values were calculated by 3 different methods (DIPRO,[14] monomer projection[15] and Fock matrix),[16] which all provided comparable values. Mobilities were calculated using a sum-over-neighbours approach using rate constants derived from Marcus theory.[17]

PhOMeDPP *N*-H

3,6-Bis(4-methoxyphenyl)-2,5-dihydropyrrolo[3,4-c]pyrrole-1,4-dione

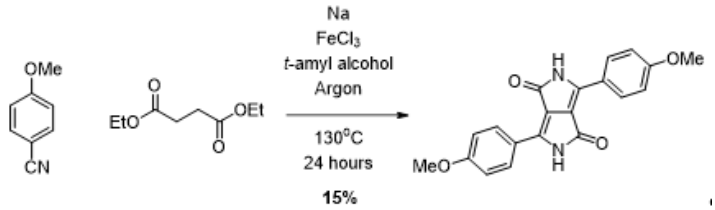

Sodium (8.75g, 0.380 mol) and a catalytic amount of iron chloride were added to anhydrous t-amyl alcohol (170 ml, 2.40 mol) and the mixture was heated at 120°C for 1 hour under an argon atmosphere, whilst stirring until all the sodium had dissolved. The solution was then cooled to around 80°C and 4-methoxybenzonitrile (25.0g, 0.188 mol) added. The reaction was then heated slowly to 130°C and once it had reached this temperature, a solution of diethyl succinate (16.0 ml, 96.1 mmol) in *t*-amyl alcohol (42.5 ml, 0.388 mol) was added via syringe pump over 3 hours. Once added, the reaction was heated at 130°C overnight. Upon completion, the reaction mixture was cooled to 50°C and glacial acetic acid (100 ml, 1.75 mol) added and the solution was heated at refluxfor 1 hour. The solid was separated by filtration (No. 4 porosity glass sinter), washed with hot methanol and dried in vacuo to afford the known product as a red solid (9.40 g, 2.70 mol, 14.5%), which had the following data in agreement with the literature[18,19]: Mp: >250 °C; ν max (ATR-IR) 3125 (NH stretch) , 3086 (CH stretch), 3018 (CH stretch), 2983 (CH stretch), 2855 (CH stretch), 1634 (C=O) , 1594 (C=C stretch), 1512, 1446, 1339, 1304, 1267, 1189, 1147, 1022, 946, 911, 865, 830, 754, 628, 602, 501 cm^{-1};^{1}H NMR (400 MHz, DMSO-d_6) δ 11.17 (2H, bs, NH), 8.46-8.44 (4H, m, ArH), 7.14-7.11 (4H, m, ArH), 3.85 (6H, s, OMe) ppm;

General synthesis route for *N*-alkylation of PhOMeDPP *N*-H

3,6-Bis(4-methoxyphenyl)-2,5-dihydropyrrolo[3,4-c]pyrrole-1,4-dione (500 mg, 1.44 mmol) was added to caesium carbonate (2 g, 6.14mmol) and alkyl halide (6.24 mmol) in anhydrous acetonitrile (20 ml) and the mixture was heated to 85°C, whilst stirring under an inert atmosphere for 24 hours. The solvent was then removed under reduced pressure. Dichloromethane (100 ml) was added and the remaining unreacted starting material filtered off using a No. 4 porosity glass sintered crucible. The solution was washed with water (200 ml), the organic phase was separated and the aqueous phase was washed with dichloromethane (2 x100 ml). The organic extracts were combined and dried ($MgSO_4$). The solution was filtered, and concentrated under reduced pressure. The crude product was purified by column chromatography using an eluent system of 95:5 CH_2Cl_2: ethyl acetate to yield the pure product.

PhOMeDPP *N*-2MB

3,6-Bis(4-methoxyphenyl)-2,5-bis((S)-2-methylbutyl)-2,5- dihydropyrrolo[3,4-c]pyrrole-1,4-dione

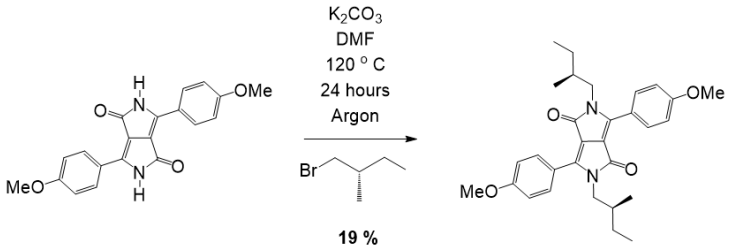

The compound was synthesised using the general method for *N*-alkylation of **PhOMeDPP *N*-H** using (S)-(+)-1-bromo-2-methylbutane as alkyl halide to yield the product as an orange crystalline solid (133 mg, 0.273 mmol, 19%). The product is novel and has: Mp: 222°C; (ESI-MS): Found [M+ H]+ 489.2754 and $C_{30}H_{37}N_2O_4$ requires 489.2748; ν max (ATR-IR) 3073 (CH stretch), 3010 (CH stretch), 2954 (CH stretch), 1660 (C=O), 1601(C=C stretch), 1564, 1508, 1456, 1419, 1349, 1304, 1257, 1176, 1123, 1084, 1026, 966, 917, 871, 836, 791, 735, 653, 595, 527, 478 cm^{-1}; ^{1}H NMR (300 MHz, $CDCl_3$) δ 7.80 (4H, d, J 8.5 Hz, ArH), 7.03 (4H, d, J 8.5 Hz, ArH), 3.89 (6H, s, OMe), 3.81-3.64 (4 H, m, NCH_2), 1.70-1.60 (2 H, m, CH), 1.35-0.98 (4 H, m, CH_2), 0.81-0.73 (12 H, m, RCH_3) ppm; ^{13}C NMR (75MHz, $CDCl_3$) δ 163.0, 161.6, 147.9, 130.5, 121.1, 114.2, 110.0 , 55.4, 47.7, 34.5, 26.9 , 16.8, 11.1 ppm; Elemental analysis: calcd for $C_{30}H_{37}N_2O_4$: C, 73.74; H, 7.43; N, 5.73%; found: C, 72.8; H, 7.42; N, 5.64%

PhOMeDPP *N*-Hex

2,5-Dihexyl-3,6-bis(4-methoxyphenyl)-2,5-dihydropyrrolo[3,4- c]pyrrole-1,4-dione

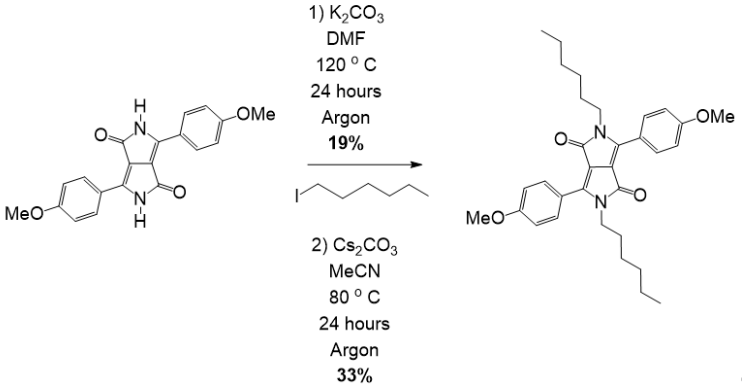

The compound was synthesised using the general method for *N*-alkylation of **PhOMeDPP *N*-H** using hexyl iodide as alkyl halide to yield the product as an orange solid (250 mg, 0.484 µmol, 34%). This compound is known[18] and the ^{1}H NMR is in agreement with the literature, but it is not fully characterised. The compound has: Mp: 163°C; ESI-MS found: [M+ H]+ 517.3072 and $C_{32}H_{41}N_2O_4$ requires M 517.3061; νmax (ATR-IR) 3067 (CH stretch), 3010(CH stretch), 2962(CH stretch), 2927(CH stretch), 2855(CH stretch), 1666 (C=O), 1607 (C=C stretch), 1566, 1506, 1454, 1380, 1341, 1304, 1255, 1178, 1119, 1084, 1024, 962, 836, 781, 737, 655, 587, 538, 507, 478, 420 cm^{-1}; ^{1}H NMR (300 MHz, $CDCl_3$) δ 7.85 (4 H, d, J 9.0 Hz, ArH), 7.06 (4 H, d, J 9.0 Hz, ArH), 3.91 (6 H, s, OMe), 3.78 (4 H, t, J 6.0 Hz, NCH_2), 1.68-1.59 (4 H, m, CH_2), 1.28-1.22 (12 H, m, CH_2), 0.86 (6 H, t, J 6.0 Hz, Me) ppm; ^{13}C NMR (75MHz, $CDCl_3$) δ 162.9, 161.7, 147.7, 130.6, 120.8 , 114.4, 108.9, 55.5, 42.1, 31.3, 29.5, 26.5, 22.5, 14.0 ppm; Elemental analysis: calcd for $C_{32}H_{41}N_2O_4$: C, 74.39; H, 7.80; N, 5.42%; found: C, 74.21; H, 7.79; N, 5.42%.

PhOMeDPP *N*-Boc

Di-*tert*-butyl 3,6-bis(4-methoxyphenyl)-1,4-dioxopyrrolo[3,4- c]pyrrole-2,5(1H,4H)-dicarboxylate

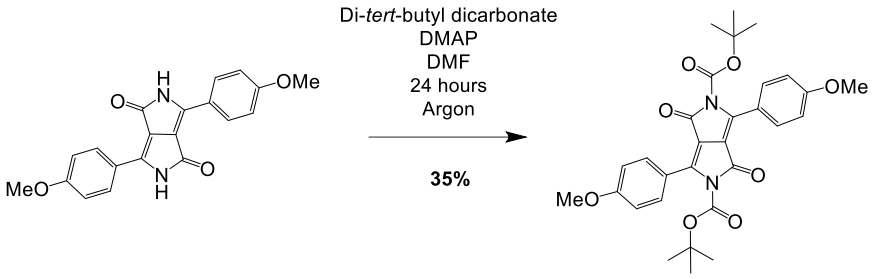

3,6-Bis(4-methoxyphenyl)-2,5-dihydropyrrolo[3,4-c]pyrrole-1,4-dione (1.0g, 2.9 mmol), di-*tert*-butyldicarbonate (1.25g, 5.44mmol) and 4-dimethylaminopyridine (0.70g, 5.73 mmol) were dissolved in anhydrous DMF (50 ml) and the mixture was stirred at room temperature under an inert atmosphere for 24 hours. Once this time had elapsed, the reaction mixture was washed with water (200 ml) and the solution was filtered (No. 4 porosity glass sinter), to remove unreacted starting material. The excess solvent was removed under reduced pressure. The crude product was then purified by column chromatography using an eluent system of 95:5 petroleum ether: ethyl acetate to yield the pure product a yellow solid (560mg, 1.02 mmol, 35 %). The product is novel and has: Mp: decomposed 120° C ; ESI-MS found: $[M+ H]^+$ 549.2247 and $C_{30}H_{33}N_2O_8$ requires M 549.2231; νmax (ATR-IR) 3073 (CH stretch), 2989(CH stretch), 2933 (CH stretch), 1747(C=O), 1708(C=O DPP), 1625 (C=C stretch), 1599, 1508, 1461, 1370, 1257, 1207, 1178, 1141, 1053, 1024, 876, 834, 766, 733, 661, 608, 550, 513, 484 cm^{-1}; ^1H NMR (400 MHz, $CDCl_3$) δ 7.76 (4 H, d, *J* 8.0 Hz, ArH), 6.99 (4 H, d, *J* 8.0 Hz, ArH), 3.88 (6 H, s, OMe), 1.47 (18 H, s, Me) ppm; ^{13}C NMR (75MHz, $CDCl_3$) δ 162.2, 159.8, 148.6, 145.3, 130.5, 120.7, 113.9, 111.0, 102.0, 85.0, 55.5, 27.6 ppm

PhOTHPDPP *N*-H

3,6-Bis(4-((tetrahydro-2H-pyran-2-yl)oxy)phenyl)-2,5-dihydropyrrolo[3,4-c]pyrrole-1,4-dione

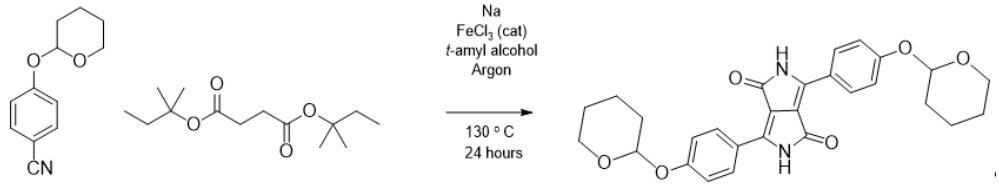

Sodium (3.92 g, 1.70 mol) and a catalytic amount of iron chloride were added to anhydrous *t*-amyl alcohol (112 ml, 1.02 mol) and heated at 120°C for 1 hour, under an argon atmosphere, whilst stirring, until all the sodium had dissolved. The solution was then cooled to around 80°C and 4-(tetrahydro-2-pyran-2H-yloxy) benzonitrile (17.3 g, 8.46 mol) [20] added. The reaction was then heated slowly to 130 ° C and once it had reached this temperature a solution of di-*tert* amyl succinate (10.5 ml, 4.79 mmol) in *t*-amyl alcohol (28.0 ml, 0.256 mol) was added *via* syringe pump over 3 hours. The reaction was heated at 130°C overnight. Upon completion, the reaction mixture was cooled and hot methanol added. The solid was separated by filtration(No. 4 porosity glass sinter) and washed with hot methanol and dried in vacuo to afford the pure product as a red solid (11.9 g, 2.43 mmol, 28.7 %). This compound is known[20] ; ^1H NMR (400 MHz, DMSO-d_6) δ 11.11 (2H, s, NH), 8.43 (4H, d, *J* 7.8 Hz, ArH), 7.17 (4H, d, *J* 7.8 Hz, ArH),5.63 (2H,m, OCH), 3.79-3.69 (2H, m, OCH), 3.64 – 3.56 (2H, m, OCH), 1.95-1.48 (12H, m, CH and CH_2) ppm

PhOTHPDPP *N*-Hex

2,5-Dihexyl-3,6-bis(4-((tetrahydro-2H-pyran-2-yl)oxy)phenyl)-2,5-dihydropyrrolo[3,4-c]pyrrole-1,4-dione

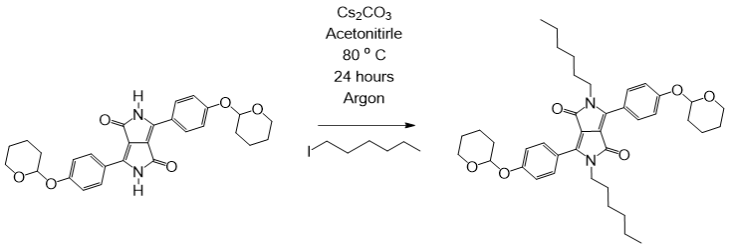

3,6-Bis(4-((tetrahydro-2H-pyran-2-yl)oxy)phenyl)-2,5-dihydropyrrolo[3,4-c]pyrrole-1,4-dione (500 mg, 1.02 mmol) was added to a mixture of caesium carbonate (1.42 g, 4.35 mmol) and hexyl iodide (0.94 g, 4.42 mmol) in anhydrous acetonitrile (20 ml) and the reaction mixture was heated to 85°C, whilst stirring under an inert atmosphere for 24 hours. The mixture was then evaporated to dryness under reduced pressure. Dichloromethane (100 ml) was added and unreacted starting material filtered off (No. 4 porosity glass sinter). The solution was washed with water (200 ml), the organic phase was separated and the aqueous phase was washedwith dichloromethane (2 x100 ml). The organic extracts were combined and dried ($MgSO_4$).The solution was filtered and concentrated under reduced pressure. The crude product was purified by column chromatography using an eluent system of 95:5 DCM: ethyl acetate to yield the pure product as an orange crystalline solid (121 mg, 0.18mmol, 18%). This compound is novel and has: Mp: 144°C; ESI-MS found: $[M+Na]^+$ 679.3715 and $C_{40}H_{52}N_2O_6Na$ requires M 679.3718; νmax (ATR-IR) 2931 (CH stretch), 2855 (CH stretch), 1765 (C=O), 1739 (C=C stretch), 1660, 1609, 1508, 1454, 1358, 1279, 1242, 1201, 1176, 1088, 1036, 958, 919, 847, 764, 737, 655, 630, 603, 562, 538, 499, 470 cm^{-1}; ^1H NMR (300 MHz, $CDCl_3$) δ 7.80 (4H, d, *J* 8.9 Hz, ArH), 7.18 (4H, d, *J* 8.9 Hz, ArH), 5.51 (2H, t, *J* 3.1 Hz, OCH), 3.90 (2H, ddd, *J* = 12.4, 9.6, 3.0 Hz, OCH), 3.79 – 3.71 (4H, m, NCH_2), 3.67 – 3.59 (2H, m, OCH), 2.07 – 1.95 (2H, m, CH), 1.94 – 1.83 (4H, m, CH_2), 1.77 – 1.57 (10H, m, CH and CH_2), 1.31 – 1.17 (12H, m, CH_2), 0.87 – 0.79 (6H, m, CH_3) ppm ; ^{13}C NMR (75 MHz, $CDCl_3$) δ 163.1, 159.4, 147.9, 130.6, 121.6, 116.7, 109.1, 96.4, 62.3, 42.2, 31.4, 30.4, 29.6, 26.6, 25.3, 22.6, 18.8, 14.1 ppm.

General synthesis of PhOHDPP *N*-R by deprotection of PhOMeDPP *N*-R

3,6-Bis(4-methoxyphenyl)-2,5-bis((S)-2-methylbutyl)-2,5-dihydropyrrolo[3,4-c]pyrrole-1,4-dione (100mg, 0.20 mmol) was dissolved in dichloromethane (5 ml) and the solution was cooled to -20°C whilst stirring under an argon atmosphere. Once this temperature had been reached, a solution of boron tribromide (0.1 ml, 1.05 mmol) in dichloromethane (3 ml) was added dropwise and the reaction mixture was allowed to warm to room temperature, continuing stirring for 24 hours. Upon completion, the reaction mixture was quenched with water (20 ml) and an orange solid precipitated. The solid was separated by filtration (No. 4 porosity glass sinter) and washed with 10 % sodium hydroxide (10 ml) and 2M hydrochloric acid (10 ml) and dried in vacuo to yield the pure product

PhOHDPP *N*-Hex

2,5-Dihexyl-3,6-bis(4-hydroxyphenyl)-2,5-dihydropyrrolo[3,4- c]pyrrole-1,4-dione

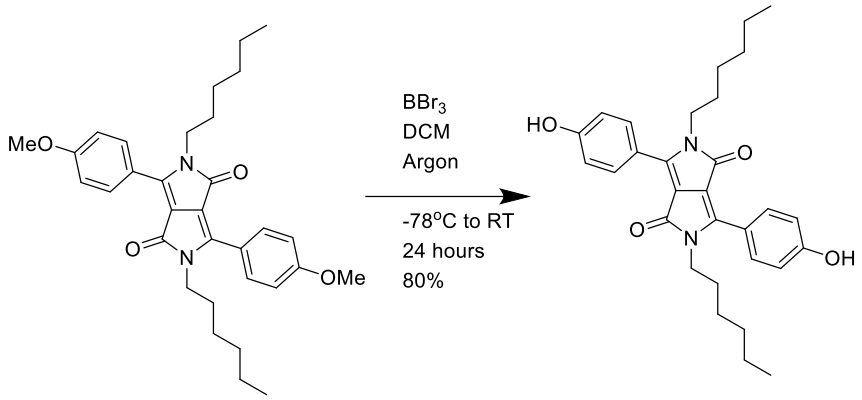

The compound was synthesised using the general method for deprotection of **PhOMeDPP *N*-R** to yield the pure product as a red solid (75mg , 0.15 mmol, 81%). This compound is known[18] and the ^{1}H NMR is in agreement with the literature but it is not fully characterised. The compound has: Mp: 225°C; ESI-MS found: $[M- H]^-$ 487.2717 and $C_{30}H_{35}N_2O_4$ requires M 487.2675; γ max (ATR-IR) 3187 (OH stretch), 3024 (CH stretch), 2917(CH stretch), 2851(CH stretch), 2746(CH stretch), 2678(CH stretch), 1664 (C=O), 1592 (C=C stretch), 1514, 1444, 1374, 1277, 1232, 1178, 1098, 1005, 960, 892, 843, 764, 705, 647, 595, 521, 490, 447 cm^{-1}; ^{1}H NMR (300 MHz, DMSO-d_6) δ 10.29 (2H, s, Ar-OH), 7.73 (4 H, d, *J* 8.7 Hz, ArH), 6.93 (4 H, d, *J* 8.7 Hz, ArH), 3.71 (4 H, t, *J* 7.0 Hz, NCH_2), 1.45-1.40 (4 H, m, CH_2), 1.18-1.13 (12 H, m, CH_2), 0.79 (6 H, t, *J* 7.0 Hz, Me) ppm; ^{13}C NMR (75 MHz, DMSO-d_6) δ 161.8, 160.2, 147.1, 130.6, 118.63, 115.6, 107.3, 48.5, 30.5, 28.4, 25.6, 21.8, 13.8 ppm;

PhOHDPP *N*-2MB

3,6-Bis(4-hydroxyphenyl)-2,5-bis((S)-2-methylbutyl)-2,5- dihydropyrrolo[3,4-c]pyrrole-1,4-dione

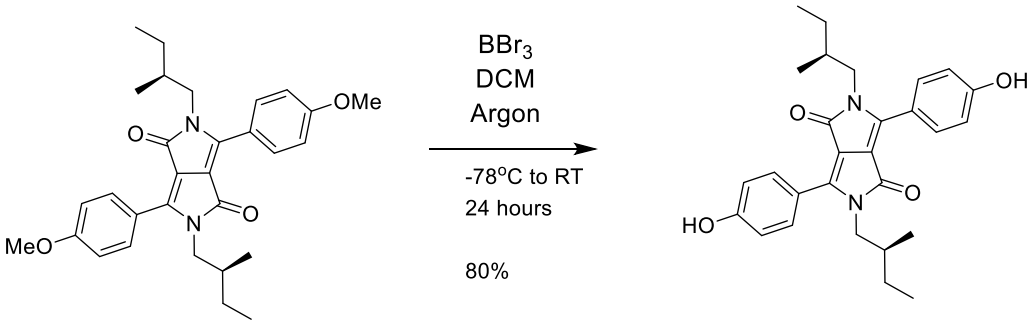

The compound was synthesised using the general method for deprotection of **PhOMeDPP *N*-R** to yield the pure product as a red solid (74 mg, 0.16 mmol, 80 %). The product is novel and has: Mp: >250°C; ESI-MS found: $[M+ H]^+$ 461.2452 and $C_{30}H_{33}N_2O_4$ requires M 461.2435; ν max (ATR-IR) 3232 (OH stretch), 3180 (CH stretch), 2962(CH stretch), 2876 (CH stretch), 1640 (C=O), 1588 (C=C stretch), 1514, 1444, 1378, 1347, 1275, 1230, 1174, 1094, 970, 917, 840, 740, 639, 593, 521, 439 cm^{-1}; ^{1}H NMR (300 MHz, DMSO-d_6) δ 10.26 (2H , s, Ar-OH) 7.76 (4 H, d, *J* 8.8 Hz, ArH), 6.93 (4 H, d, *J* 8.8 Hz, ArH), 3.78-3.59 (4 H, m, NCH_2), 1.47-1.41 (2H, m, CH), 1.25-0.96 (4 H, m, CH_2), 0.73-0.63 (12 H, m, Me) ppm; ^{13}C NMR (75 MHz, DMSO-d_6) δ 162.0, 160.0, 147.3, 130.6, 118.9, 115.6, 107.4, 46.1, 33.9, 26.3, 16.6, 10.8 ppm

PhOHDPP *N*-H

3,6-Bis(4-hydroxyphenyl)-2,5-dihydropyrrolo[3,4-c]pyrrole-1,4-dione

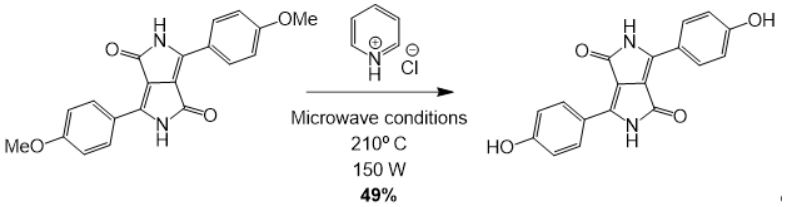

3,6-Bis(4-methoxyphenyl)-2,5-dihydropyrrolo[3,4-c]pyrrole-1,4-dione (500 mg, 1.44 mmol) and pyridinium hydrochloride (500 mg, 4.3 mmol) were degassed in a microwave vial. The vial was then heated (210°C) and stirred under microwave irradiation (150 W) for 15 minutes then cooled and held at 160 °C for 5 minutes. The cycle was then repeated. The progress of the reaction was monitored between cycles by ^{1}H NMR until no starting material remained. Typically, 3 cycles were sufficient to ensure complete conversion. The desired material was produced in good yield after washing with water and CH_2Cl_2 to yield the pure product as a red solid (225 mg, 0.70 mmol, 49%). This compound is known[20] and the ^{1}H NMR is in agreement with the literature but it is not fully characterised. The compound has Mp: >250°C; MALDI-TOF MS found M 320.119 and $C_{18}H_{12}N_2O_4$ requires M 320.0797; ν_{Max} (ATR-IR) 3102 (v.broad OH stretch), 3045 (v.broad NH stretch), 2958 (CH stretch), 2929 (CH stretch), 2839 (CH stretch), 2775 (CH stretch), 1636 (C=O), 1578 (C=C stretch), 1512, 1454, 1432, 1384, 1333, 1283, 1246, 1187, 1143, 1106, 1034, 948, 876, 838, 793, 756, 670, 630, 604, 509, 461 cm^{-1}; ^{1}H NMR (400 MHz, DMSO-d_6) δ 11.01 (2 H, s, NH), 10.36 (2H, s, OH), 8.35 (4H, d, *J* 8 Hz, ArH), 6.90 (4H, d, *J* 8 Hz, ArH) ppm ; ^{13}C NMR (100 MHz, DMSO-d_6) δ 162.5, 160.7, 143.0, 129.9, 119.2, 115.8, 108.4 ppm;

PhOBocDPP *N*-Boc

Di-*tert*-butyl 3,6-bis(4-((*tert*-butoxycarbonyl)oxy)phenyl)-1,4-dioxopyrrolo[3,4-c]pyrrole-2,5(1H,4H)-dicarboxylate

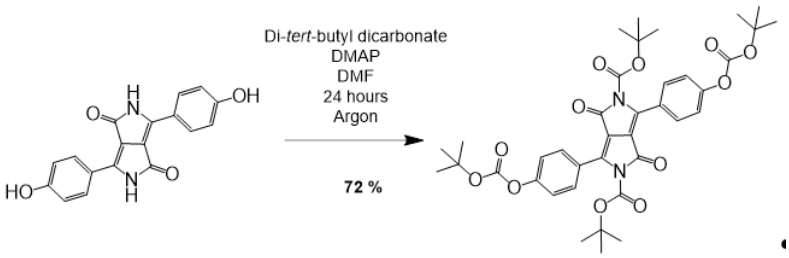

3,6-Bis(4-hydroxyphenyl)-2,5-dihydropyrrolo[3,4-c]pyrrole-1,4-dione (0.65g, 2.03 mmol), di-*tert*-butyldicarbonate (2.09 g, 9.58 mmol) and 4-dimethylaminopyridine (0.2 g , 1.64 mmol) were dissolved in anhydrous DMF (50 ml) and the solution was stirred at room temperature, under an argon atmosphere. Once this time had elapsed, the reaction mixture was washed with water (200 ml) and the solution was filtered (No. 4 porosity glass sinter) to remove unreacted starting material. The solvent was removed under reduced pressure. The crude product was then purified by column chromatography, using an eluent system of 95:5 petroleum ether: ethyl acetate, to yield the pure product an orange solid (1.05 g, 1.46 mmol, 72 %). The product is novel and has: Mp: 190°C ; ESI-MS found: $[M+Na]^+$ 743.2763 and $C_{38}H_{44}N_2O_{12}Na$ requires M 743.2786; νmax (ATR-IR) 2981(CH stretch), 1747 (C=O), 1708 (C=O DPP), 1621(C=C stretch), 1510, 1458, 1370, 1341, 1273, 1222, 1137, 1065, 956, 888, 836, 781, 744, 696, 659, 628, 564, 507, 476 cm^{-1}; ^{1}H NMR (400 MHz, $CDCl_3$) δ 7.78(4 H, d, *J* 8.9 Hz, ArH), 7.31 (4 H, d, *J* 8.9 Hz, ArH), 1.57 (18 H, s, $O(Me)_3$), 1.42 (18 H, s, $O(Me)_3$) ppm; ^{13}C NMR (100 MHz, $CDCl_3$) δ 159.5,153.5, 151.0, 148.1, 145.4, 130.1, 125.7, 121.4, 112.4, 85.6, 84.3, 27.8, 27.7 ppm

1. ^{1}H NMR Spectra

^{1}H NMR spectrum of **PhOMeDPP *N*-H** in D_6-DMSO

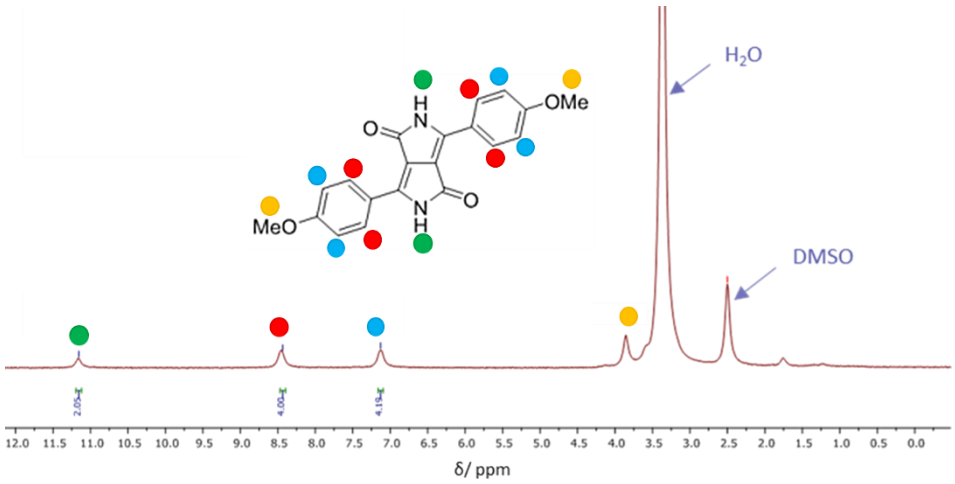

^{1}H NMR spectrum of **PhOMeDPP *N*-2MB** in $CDCl_3$

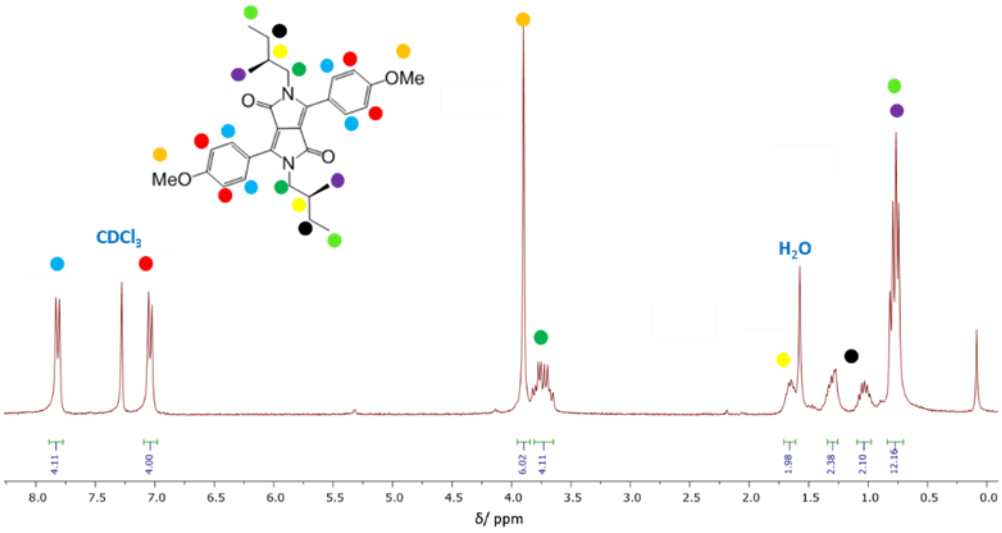

^{1}H NMR spectrum of **PhOMeDPP *N*-Hex** in $CDCl_3$

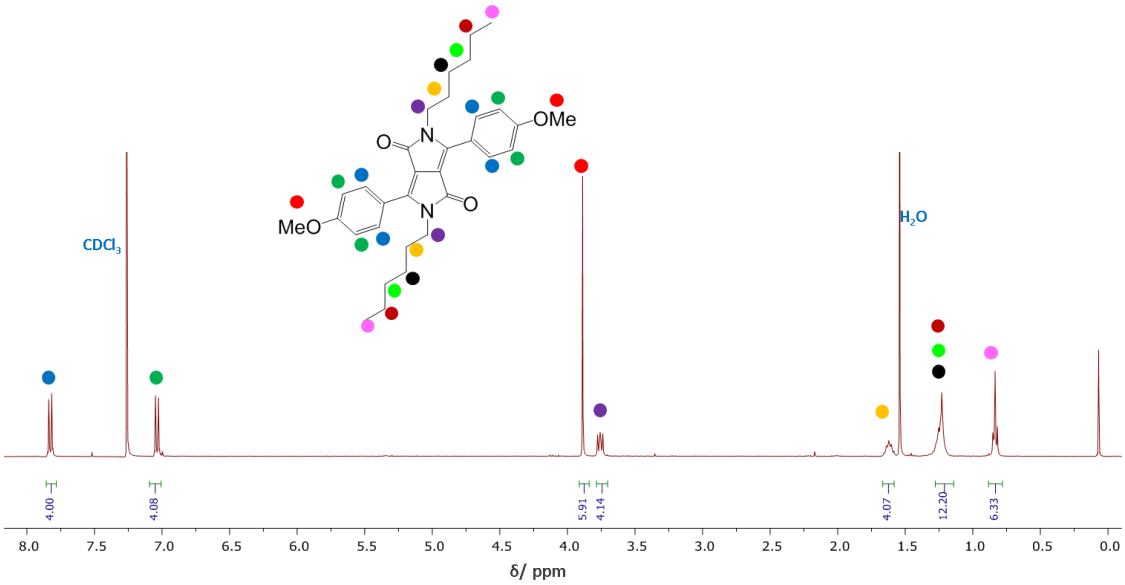

^{1}H NMR spectrum of **PhOMeDPP *N*-Boc** in $CDCl_3$

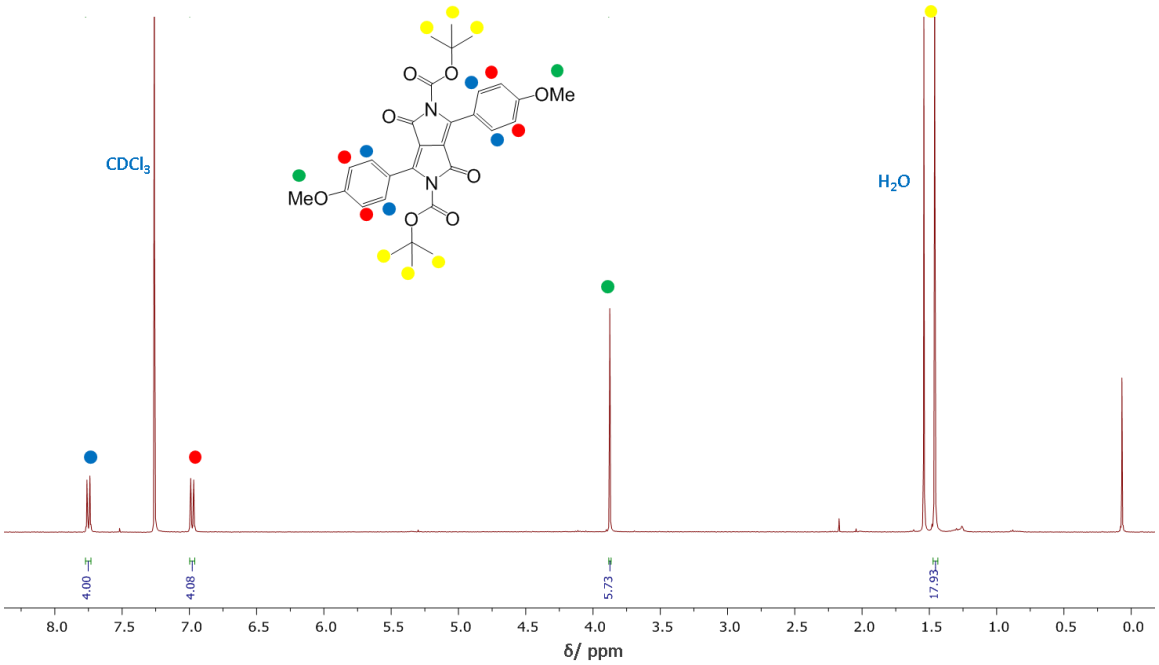

^{1}H NMR spectrum of **PhOTHPDPP *N*-H** in D_6-DMSO

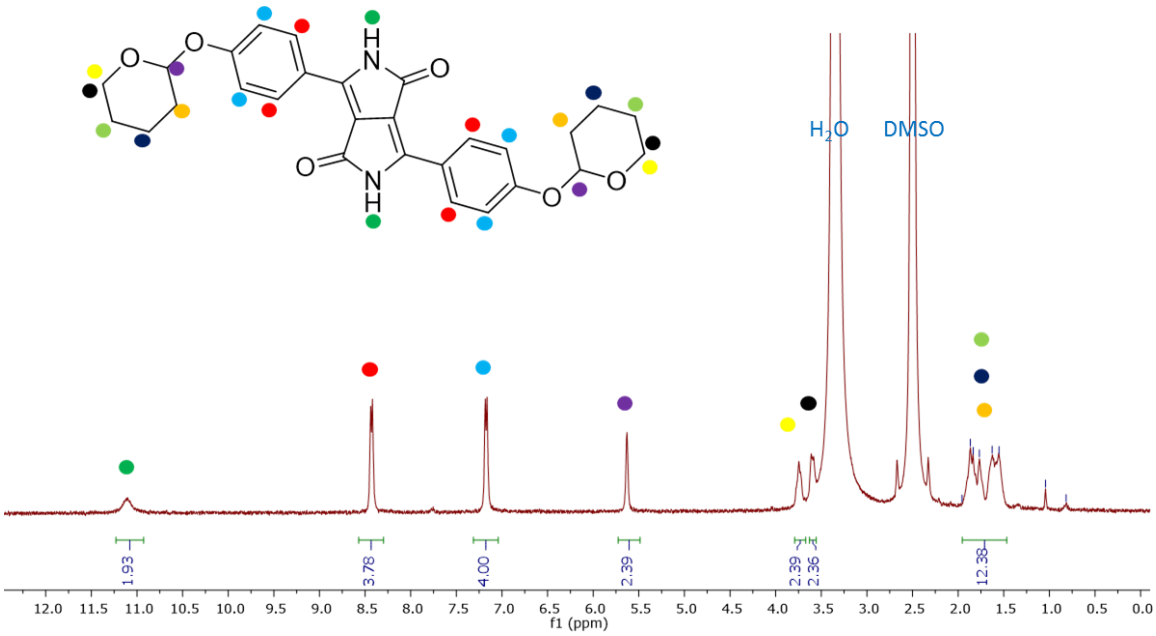

^{1}H NMR spectrum of **PhOTHPDPP *N*-Hex** in $CDCl_3$

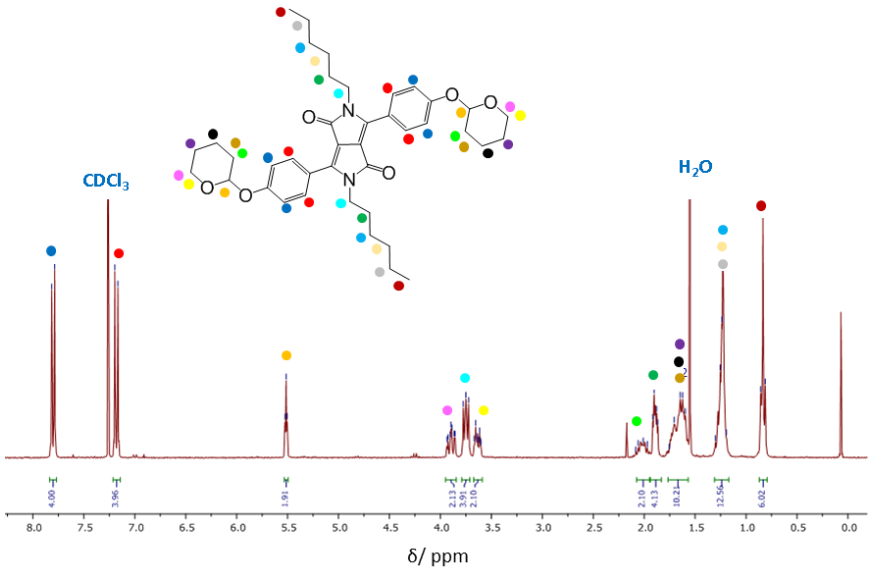

^{1}H NMR spectrum of **PhOHDPP *N*-Hex** in D_6-DMSO

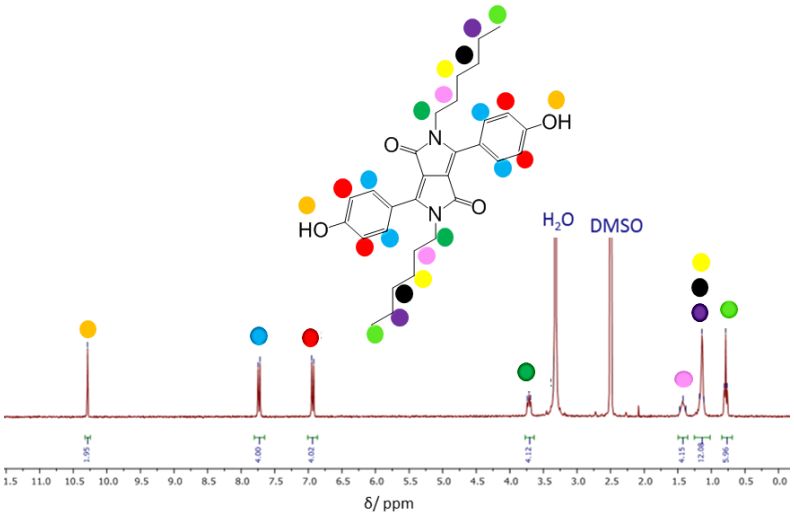

^{1}H NMR spectrum of **PhOHDPP *N*-2MB** in D_6-DMSO

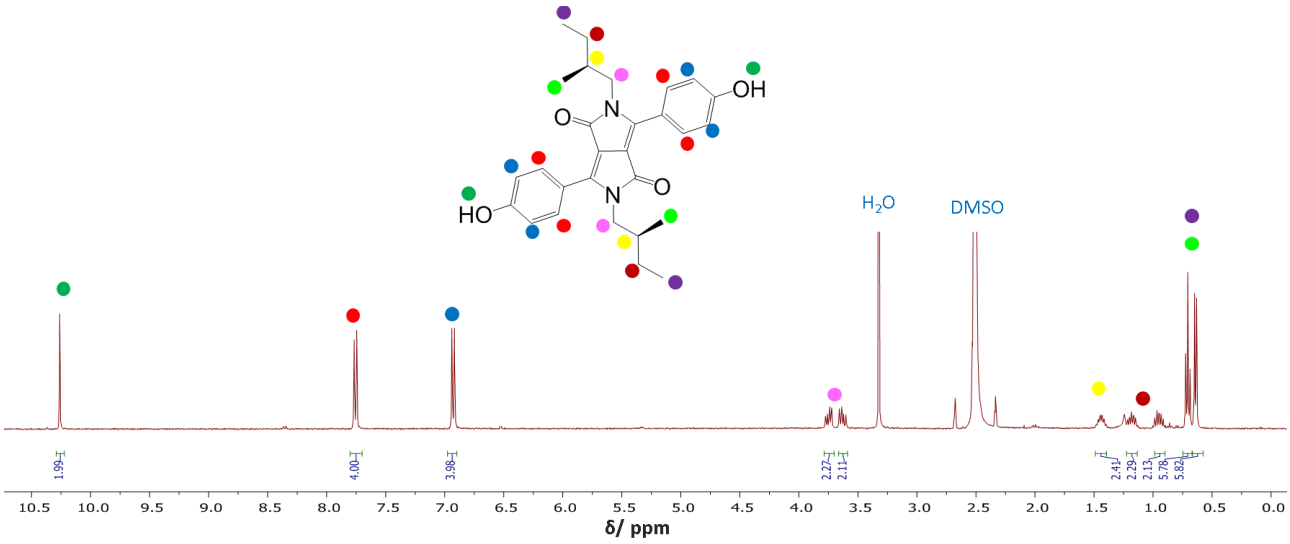

^{1}H NMR spectrum of **PhOHDPP *N*-H** in D_6-DMSO

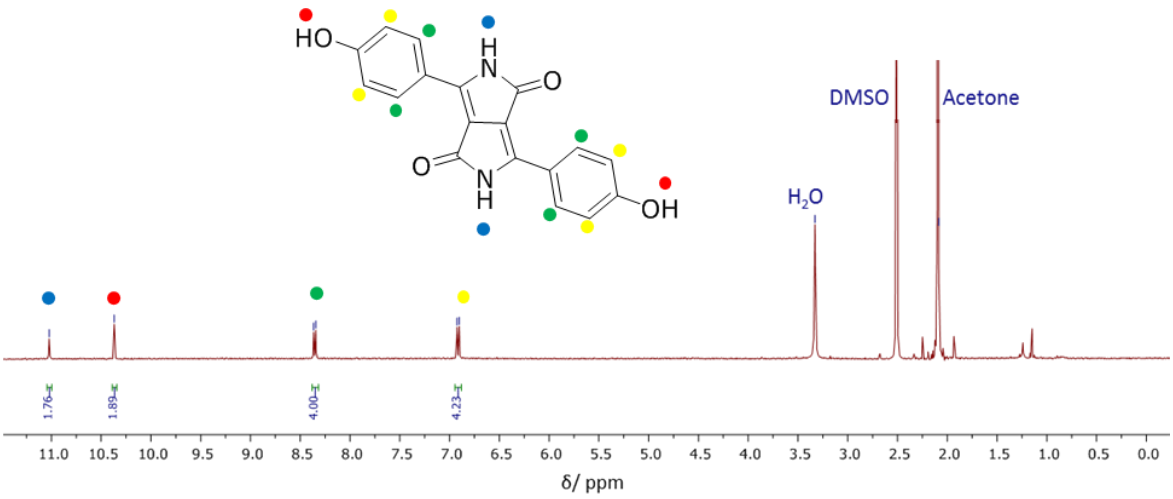

^{1}H NMR spectrum of **PhOBocDPP *N*-Boc** in $CDCl_3$

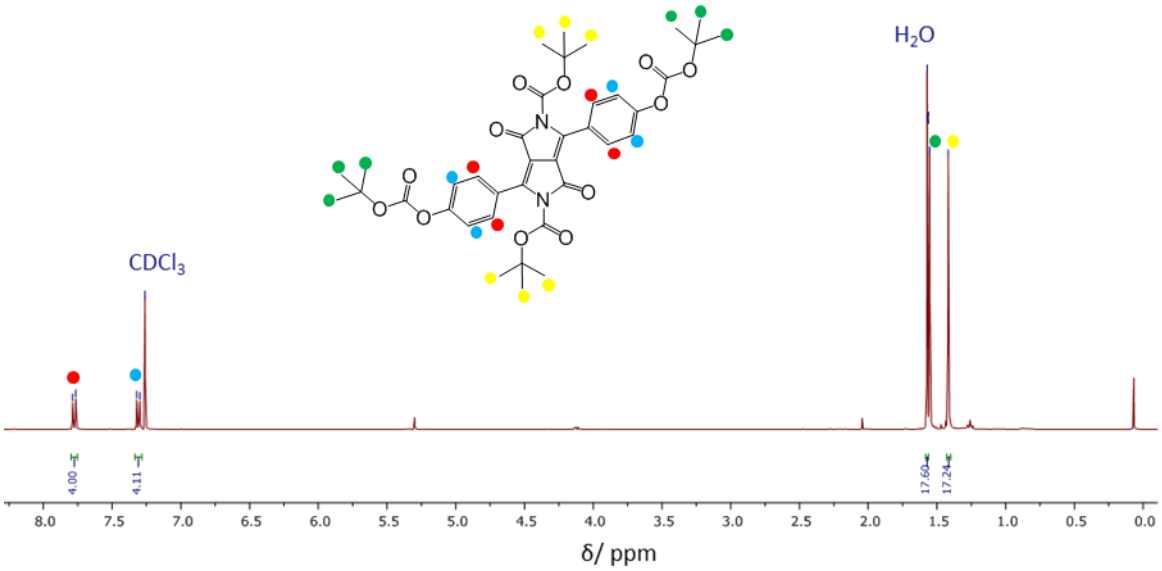

2. ^{13}C NMR Spectra

^{13}C NMR spectrum of **PhOMeDPP *N*-2MB** in $CDCl_3$

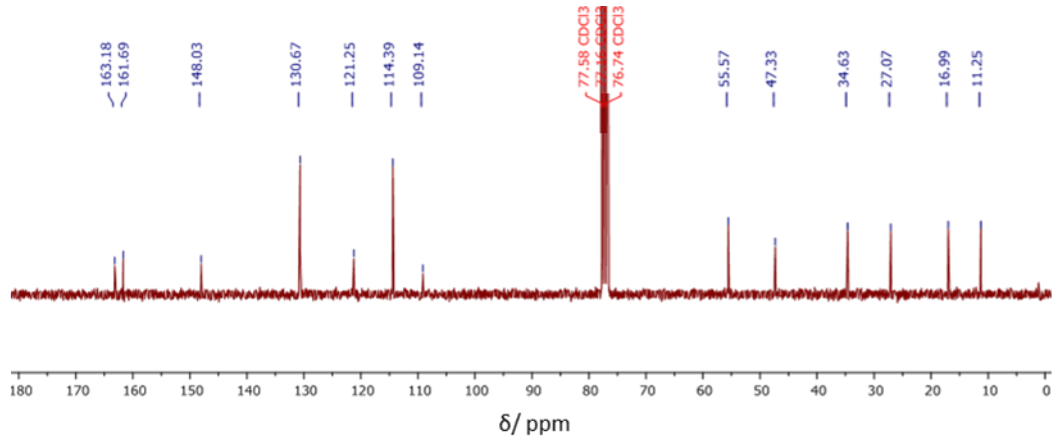

^{13}C NMR spectrum of **PhOMeDPP *N*-Hex** in $CDCl_3$

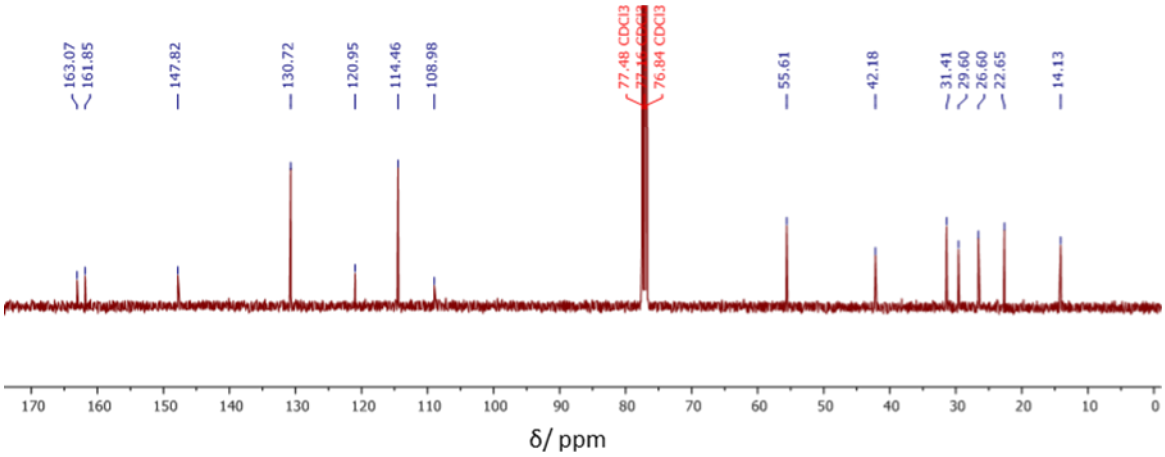

^{13}C NMR spectrum of **PhOMeDPP *N*-Boc** in $CDCl_3$

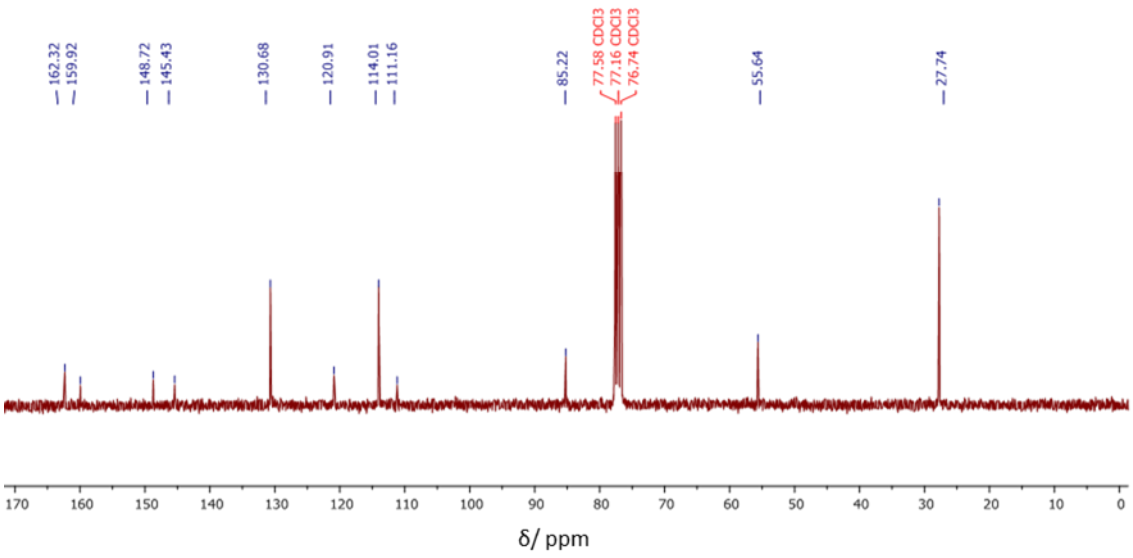

^{13}C NMR spectrum of **PhOTHPDPP *N*-Hex** in $CDCl_3$

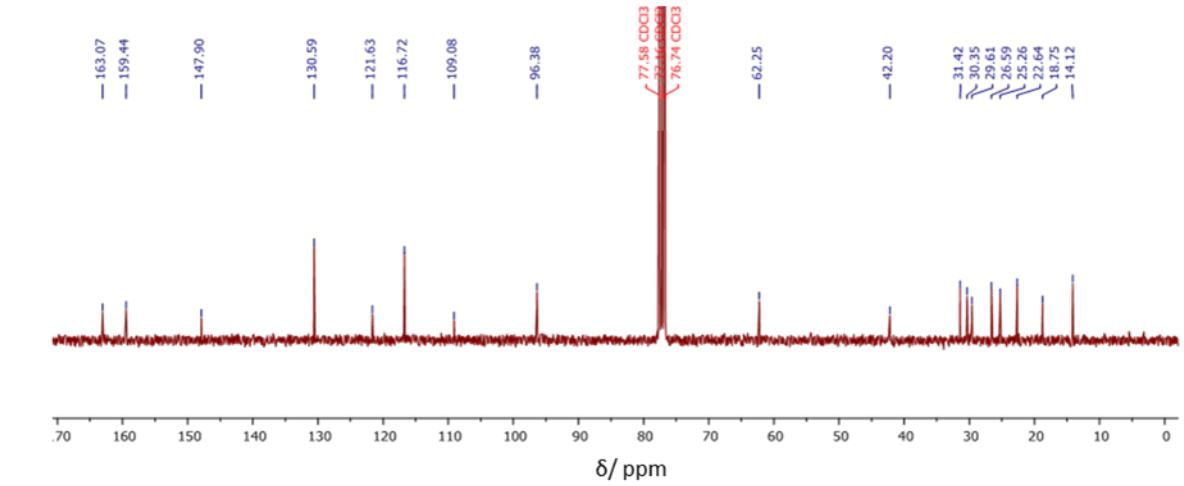

^{13}C NMR spectrum of **PhOHDPP *N*-Hex** in D_6-DMSO

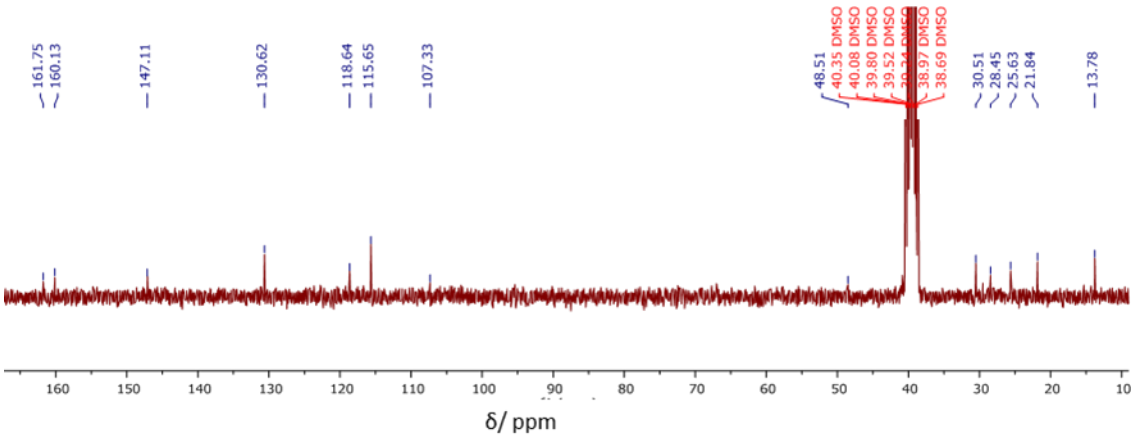

^{13}C NMR spectrum of **PhOHDPP *N*-2MB** in D_6-DMSO

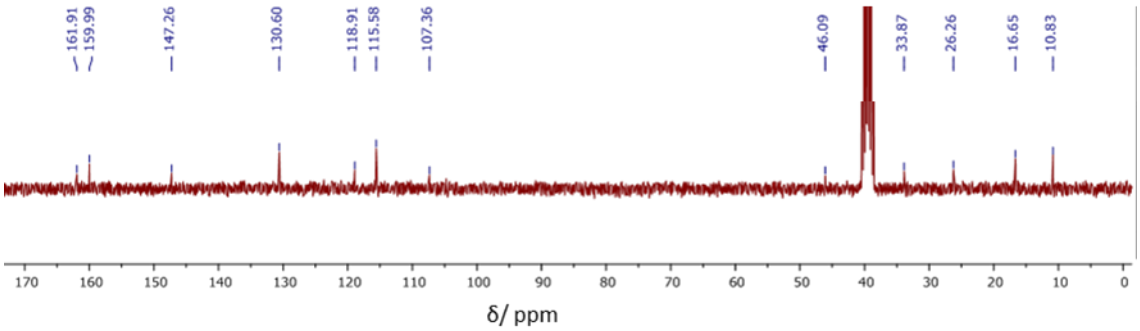

^{13}C NMR spectrum of **PhOHDPP *N*-H** in D_6-DMSO

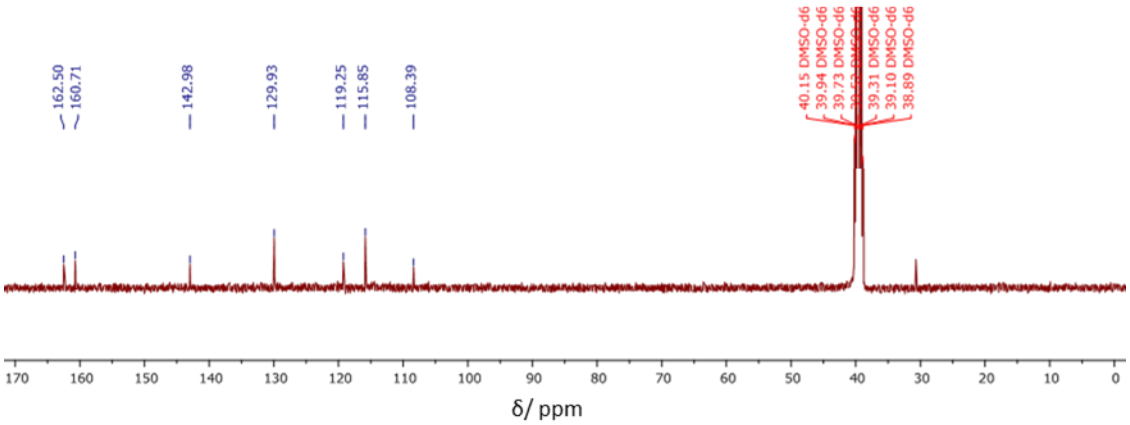

^{13}C NMR spectrum of **PhOBocDPP *N*-Boc** in $CDCl_3$

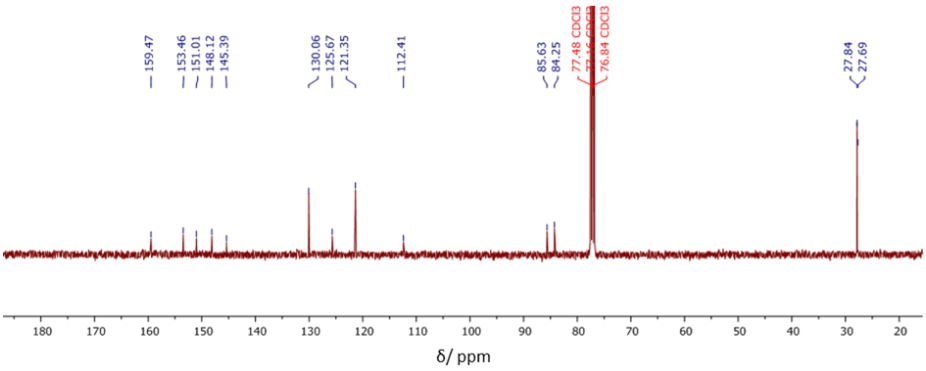

3. IR Spectra

FT-IR spectrum of **PhOMeDPP *N*-H**

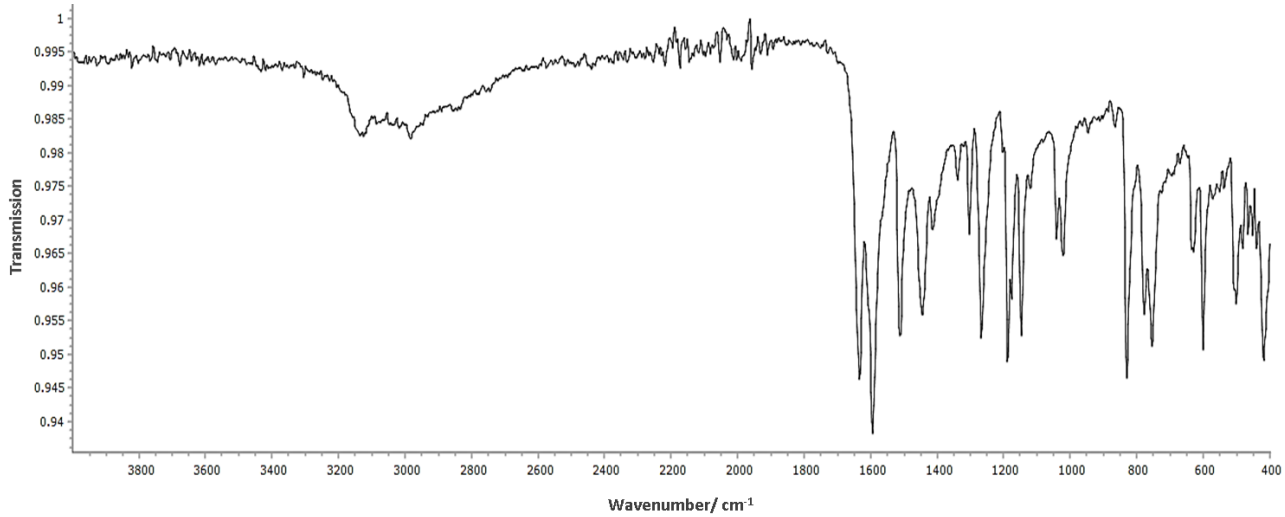

FT-IR spectrum of **PhOMeDPP *N*-2MB**

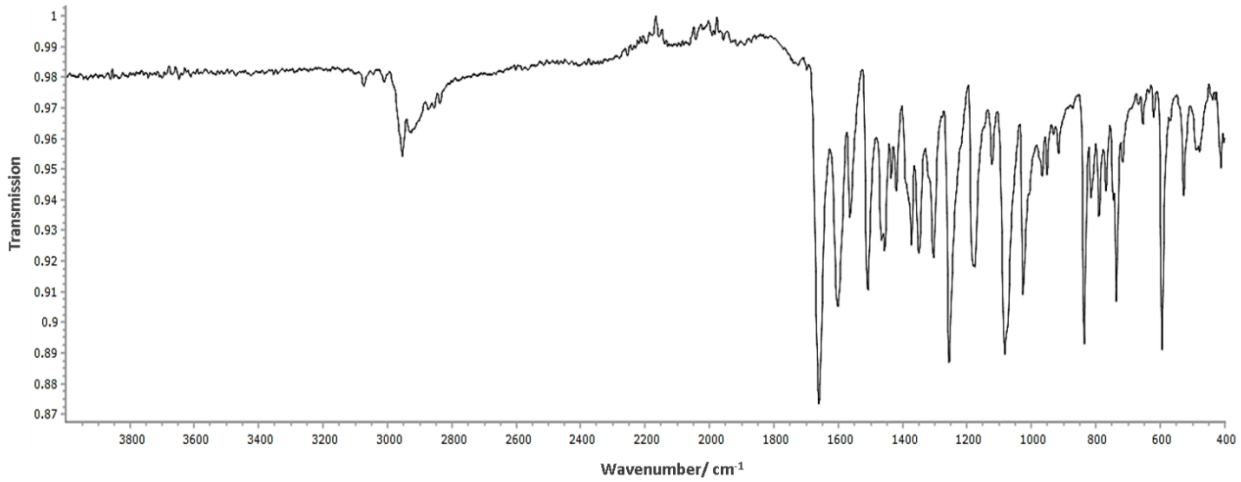

FT-IR spectrum of **PhOMeDPP *N*-Hex**

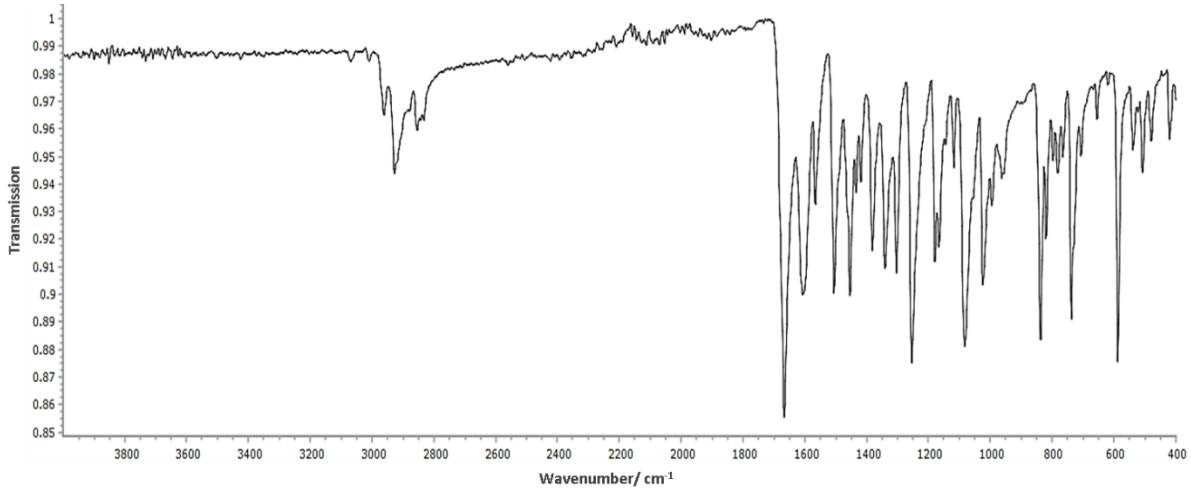

FT-IR spectrum of **PhOMeDPP *N*-Boc**

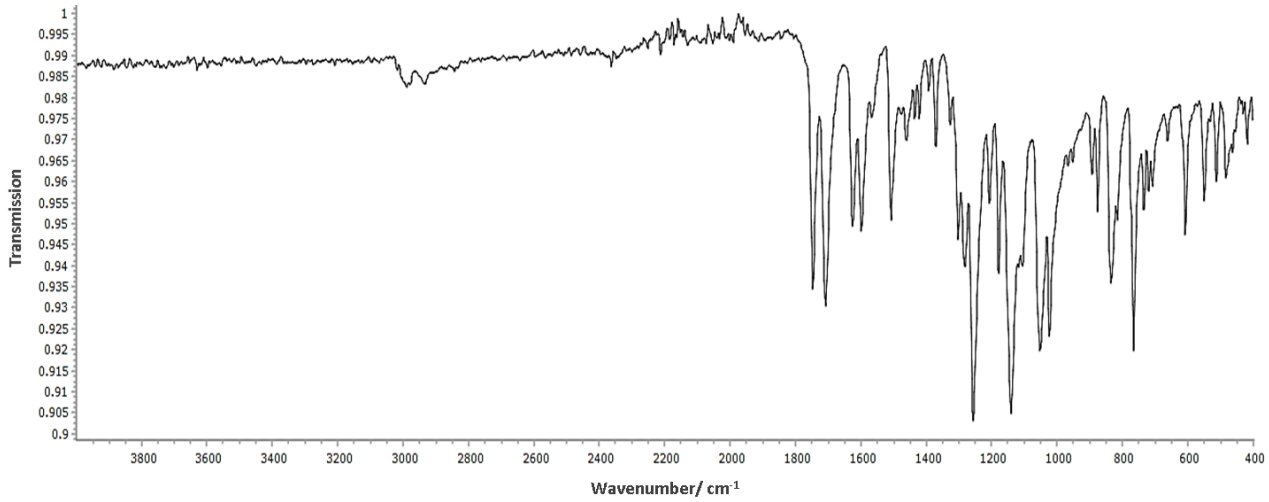

FT-IR spectrum of **PhOTHPDPP *N*-Hex**

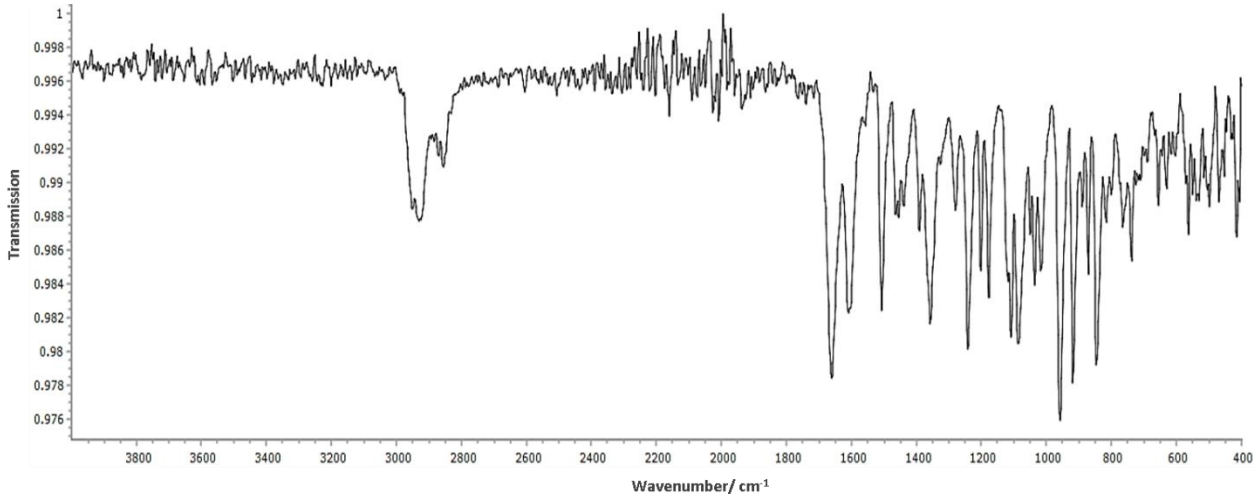

FT-IR spectrum of **PhOHDPP *N*-Hex**

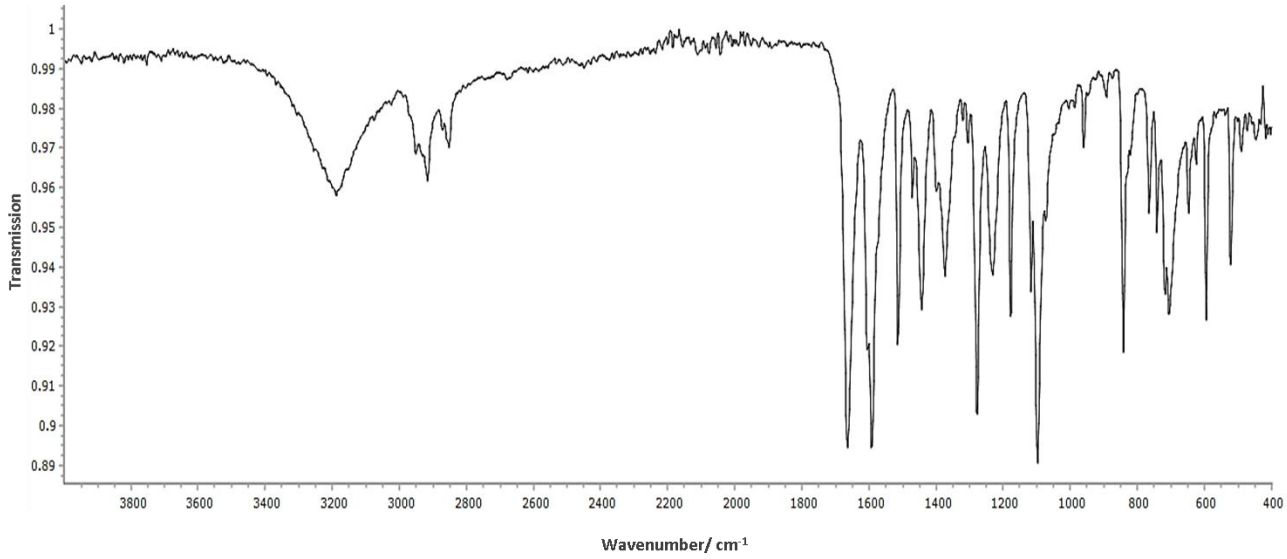

FT-IR spectrum of **PhOHDPP *N*-2MB**

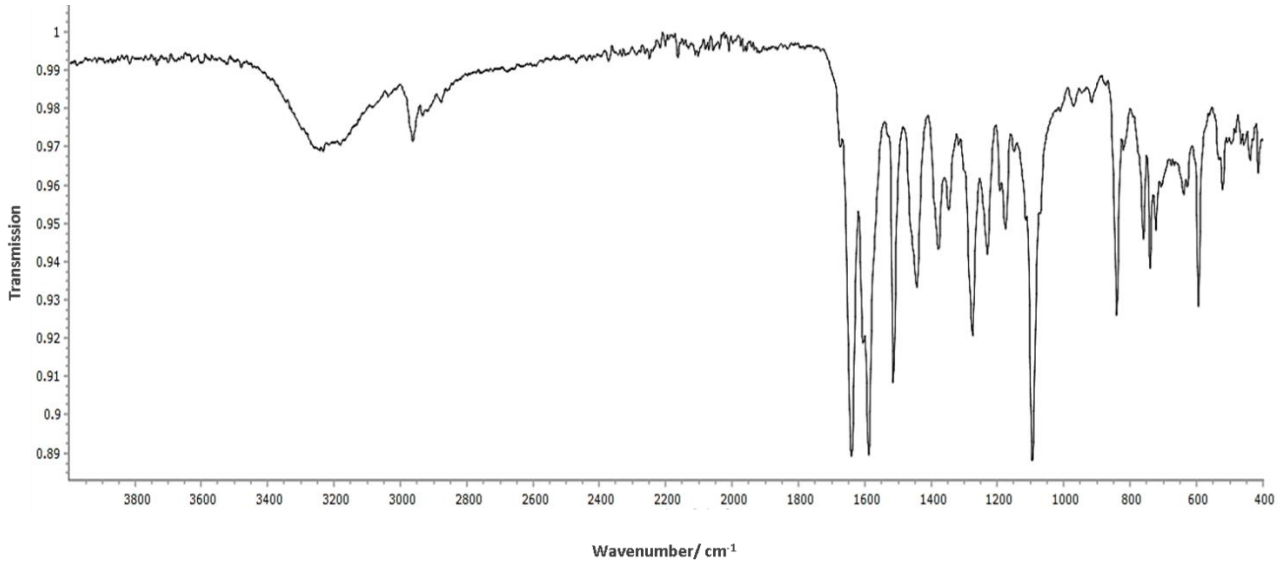

FT-IR spectrum of **PhOHDPP *N*-H**

FT-IR spectrum of **PhOBocDPP *N*-Boc**

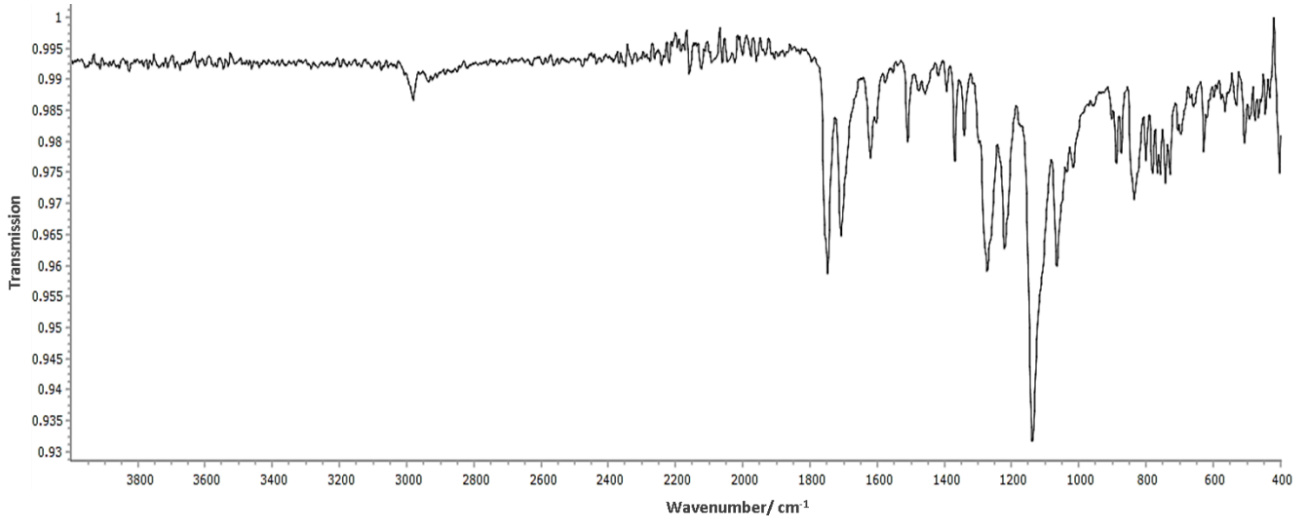

4. Mass Spectra

ESI-MS of **PhOMeDPP *N*-2MB**

Ionisation Mode ESI Positive Instrument Bruker MicroTOF

+MS, 1.0-1.2min #(74-88)

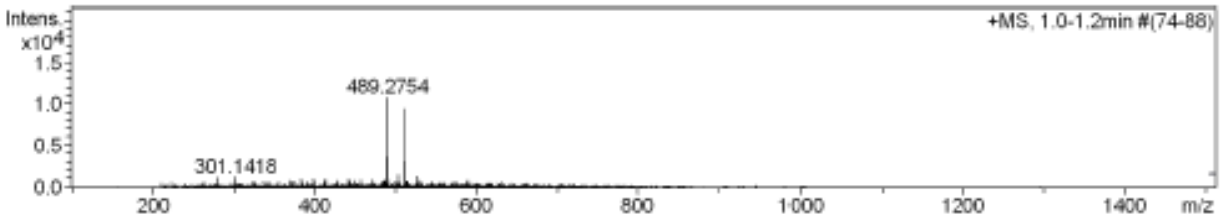

#	m/z	I %
1	279.0966	10.0
2	301.1418	10.6
3	383.3059	8.8
4	398.1944	8.5
5	411.0953	7.1
6	413.2966	7.6
7	427.3401	7.1
8	441.3506	8.0
9	443.3366	7.1
10	457.3457	7.1
11	471.3612	7.5
12	485.3784	7.7
13	489.2754	100.0
14	490.2786	33.6
15	491.2834	7.2
16	503.2936	13.7
17	511.2574	87.9
18	512.2611	29.4
19	525.2745	11.3
20	589.4077	7.7

Generate Molecular Formula Parameters

No of Most Intense MS Peaks Analysed 5

Charge	Tolerance	sigma_limit	Calibration
+1	6 ppm	0.08	TRUE

Formula Min C 25 H 26 N 2 O 4 **Formula Max** C30 H36 N2 O4 H Na

#	meas. m/z	theo. m/z	|Err|[ppm]	Sigma	Formula
1	489.2754	489.2748	1.30	0.0055	C 30 H 37 N 2 O 4
2	511.2574	511.2567	1.30	0.0021	C 30 H 36 N 2 Na 1 O 4

Note: Sigma fits < 0.05 indicates high probability of correct MF

ESI-MS of **PhOMeDPP *N*-Hex**

Ionisation Mode	ESI	Positive	Instrument	Bruker MicroTOF

+MS, 1.0-1.2min #(74-88)

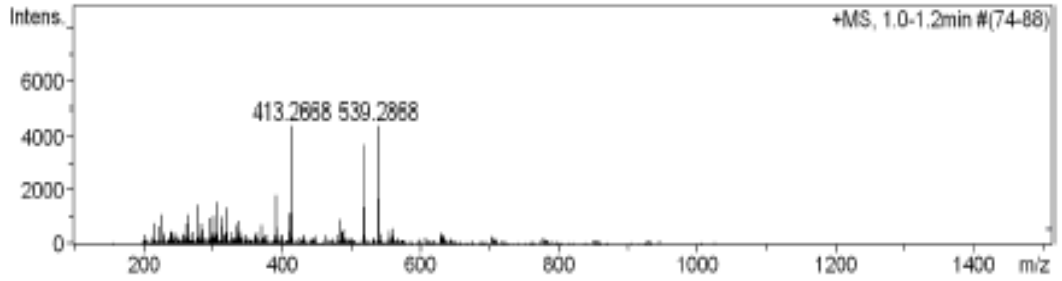

#	m/z	I %
1	217.1042	17.0
2	226.9514	24.3
3	263.0586	16.8
4	265.1584	24.0
5	279.0994	32.3
6	297.1864	21.2
7	301.1332	23.2
8	305.1503	34.7
9	314.2081	22.7
10	319.1665	29.9
11	337.0765	19.0
12	391.2843	41.1
13	411.0943	25.1
14	413.2668	100.0
15	414.2692	25.1
16	485.1137	19.9
17	517.3072	84.2
18	518.3096	30.6
19	539.2868	100.0
20	540.2912	37.2

Generate Molecular Formula Parameters

Charge	Tolerance	sigma limit	H/C Ratio	Electron Conf.	Nitrogen Rule	Chrom.BackGround	Calibration
+1	6 ppm	0.08	3 - 0	both	false	false	TRUE

Expected Formula C32 H40 N2 O4 **Adduct(s):** H, Na, NH4, radical

#	meas. m/z	theo. m/z	|Err|[ppm]	Sigma	Formula	Adduct	Adduct Mass
1	517.3072	517.3061	2.10	0.0084	C32H41N2O4	M+H	1.0078
1	539.2868	539.2880	2.20	0.0072	C32H40N2NaO4	M+Na	22.9898

Note: Sigma fits < 0.05 indicates high probability of correct MF

ESI-MS of **PhOMeDPP *N*-Boc**

Ionisation Mode ESI Positive Instrument Bruker MicroTOF

+MS, 1.0-1.2min #(74-88)

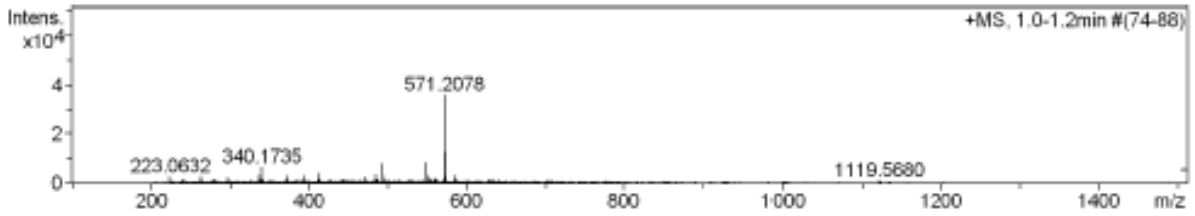

#	m/z	I %
1	223.0632	7.0
2	263.0563	6.7
3	297.0819	5.3
4	337.0744	8.4
5	340.1735	17.3
6	371.1001	7.7
7	393.1077	7.8
8	411.0933	10.0
9	411.1871	4.7
10	471.1523	5.9
11	485.1140	8.5
12	493.1599	21.6
13	494.1652	7.6
14	549.2247	22.8
15	550.2268	7.6
16	559.1331	4.9
17	571.2078	100.0
18	572.2116	35.2
19	573.2095	7.7
20	585.2243	7.9

Generate Molecular Formula Parameters No of Most Intense MS Peaks Analysed 5

Charge	Tolerance	sigma_limit	Calibration
+1	6 ppm	0.08	TRUE

Formula Min C 1 H 0 N 0 O 0 **Formula Max** C50 H100 N10 O10 H Na

#	meas. m/z	theo. m/z	|Err|[ppm]	Sigma	Formula
1	571.2078	571.2075	0.60	0.0029	C 32 H 31 N 2 O 8
		571.2064	2.50	0.0050	C 31 H 28 N 6 Na 1 O 4
		571.2061	2.90	0.0054	C 30 H 29 N 5 O 7
		571.2051	4.80	0.0074	C 29 H 26 N 9 Na 1 O 3
		571.2078	0.10	0.0083	C 33 H 30 N 3 Na 1 O 5
2	572.2116	572.2086	5.20	0.0347	C 23 H 28 N 10 O 8
		572.2089	4.70	0.0390	C 25 H 33 N 4 Na 1 O 10
		572.2100	2.80	0.0405	C 25 H 30 N 7 O 9
		572.2113	0.50	0.0504	C 27 H 32 N 4 O 10
		572.2102	2.40	0.0545	C 26 H 29 N 8 Na 1 O 6
3	549.2247	549.2231	2.90	0.0069	C 30 H 33 N 2 O 8
		549.2218	5.30	0.0094	C 28 H 31 N 5 O 7

ESI-MS of **PhOTHPDPP *N*-Hex**

Ionisation Mode	ESI	Positive	Instrument	Bruker MicroTOF

+MS, 0.7-0.9min #59-75

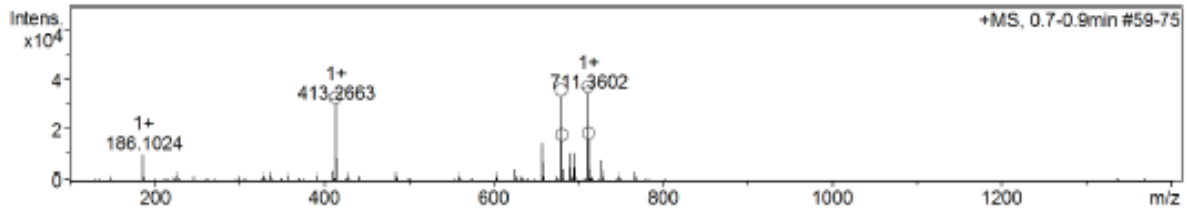

#	m/z	I %
1	186.1024	28.7
2	411.0950	9.2
3	413.2663	87.0
4	414.2695	23.9
5	485.1131	8.1
6	625.3252	11.1
7	657.3905	41.8
8	658.3936	19.6
9	679.3715	96.5
10	680.3749	43.9
11	681.3775	11.1
12	689.3790	30.8
13	690.3824	13.3
14	695.3549	30.0
15	696.3576	13.6
16	711.3602	100.0
17	712.3641	45.5
18	713.3655	12.0
19	727.3354	21.7
20	728.3391	10.2

Generate Molecular Formula Parameters

No of Most Intense MS Peaks Analysed 5

Charge	Tolerance	sigma_limit	Calibration
+1	6 ppm	0.08	TRUE

Formula Min C 1 H 0 N 0 O 0 **Formula Max** C50 H100 N10 O10 H Na

#	meas. m/z	theo. m/z	|Err|[ppm]	Sigma	Formula
1	711.3602	711.3627	3.50	0.0032	C 40 H 49 N 5 O 7
		711.3616	2.00	0.0045	C 40 H 52 N 2 Na 1 O 8
		711.3613	1.60	0.0068	C 38 H 47 N 8 O 6
		711.3616	2.00	0.0070	C 39 H 46 N 9 Na 1 O 3
		711.3640	5.40	0.0081	C 42 H 51 N 2 O 8
2	679.3715	679.3728	1.90	0.0023	C 40 H 49 N 5 O 5
		679.3718	0.40	0.0041	C 40 H 52 N 2 Na 1 O 6

ESI-MS of **PhOHDPP *N*-Hex**

Ionisation Mode	ESI	Negative	Instrument	Bruker MicroTOF

-MS, 1.0-1.2min #(74-88)

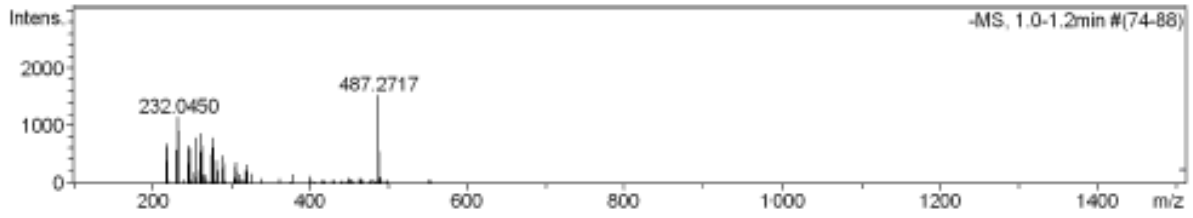

#	m/z	I %
1	217.0327	24.8
2	218.0292	44.4
3	219.0260	40.2
4	231.0479	37.5
5	232.0450	74.7
6	233.0415	59.1
7	246.0607	41.7
8	247.0565	38.6
9	255.2316	51.1
10	261.0457	35.3
11	262.0383	56.2
12	263.0344	41.0
13	275.0575	31.4
14	276.0537	51.7
15	277.0497	39.7
16	281.2478	25.3
17	290.0685	30.4
18	306.0456	22.9
19	487.2717	100.0
20	488.2753	35.5

Generate Molecular Formula Parameters

No of Most Intense MS Peaks Analysed 5

Charge	Tolerance	sigma_limit	Calibration
-1	6 ppm	0.08	TRUE

Formula Min C 1 H 0 N 0 O 0 **Formula Max** C50 H100 N10 O10 H Na

#	meas. m/z	theo. m/z	|Err|[ppm]	Sigma	Formula
1	487.2717	487.2731	2.80	0.0038	C 32 H 36 N 2 Na 1 O 1
		487.2717	0.00	0.0056	C 30 H 34 N 5 Na 1
		487.2728	2.20	0.0075	C 31 H 37 N 1 O 4
		487.2741	4.90	0.0079	C 32 H 33 N 5
		487.2715	0.60	0.0120	C 29 H 35 N 4 O 3

ESI-MS of **PhOHDPP *N*-2MB**

Ionisation Mode	ESI	Positive	Instrument	Bruker MicroTOF

+MS, 1.0-1.2min #(74-88)

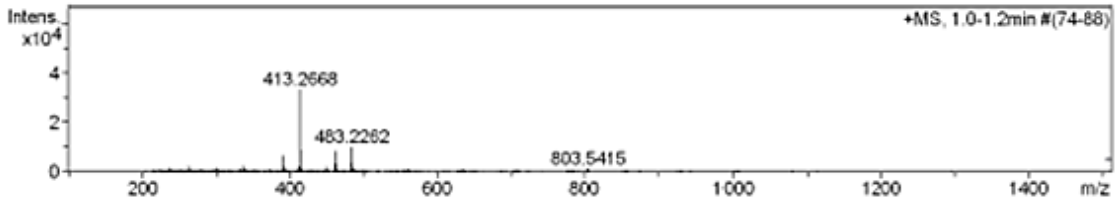

#	m/z	I %
1	236.0718	3.8
2	263.0366	5.9
3	301.1374	4.0
4	332.1098	2.8
5	337.0745	6.4
6	391.2842	19.2
7	392.2879	5.5
8	411.0944	5.3
9	413.0954	3.0
10	413.2668	100.0
11	414.2703	25.4
12	415.2723	4.0
13	450.3594	4.9
14	461.2452	24.7
15	462.2484	8.0
16	483.2262	29.7
17	484.2291	9.5
18	485.1123	4.0
19	559.1349	3.0
20	803.5415	3.5

Generate Molecular Formula Parameters

No of Most Intense MS Peaks Analysed 5

Charge	Tolerance	sigma_limit	Calibration
+1	6 ppm	0.08	TRUE

Formula Min C 1 H 0 N 0 O 0 **Formula Max** C50 H100 N10 O10 H Na

#	meas. m/z	theo. m/z	|Err|[ppm]	Sigma	Formula
1	413.2668	413.2649	4.60	0.0022	C 22 H 36 N 3 Na 1 O 3
		413.2662	1.40	0.0056	C 24 H 38 Na 1 O 4
		413.2660	2.10	0.0058	C 22 H 33 N 6 O 2
		413.2646	5.30	0.0059	C 20 H 31 N 9 O 1
		413.2645	5.30	0.0090	C 21 H 37 N 2 O 6
2	483.2262	483.2265	0.70	0.0036	C 28 H 29 N 5 O 3
		483.2254	1.50	0.0048	C 28 H 32 N 2 Na 1 O 4
		483.2251	2.10	0.0057	C 26 H 27 N 8 O 2
		483.2268	1.30	0.0084	C 29 H 28 N 6 Na 1
		483.2278	3.50	0.0098	C 30 H 31 N 2 O 4
3	414.2703	414.2684	4.40	0.0204	C 16 H 38 N 4 O 8
		414.2698	1.20	0.0236	C 18 H 40 N 1 O 9
		414.2687	3.80	0.0279	C 17 H 37 N 5 Na 1 O 5
		414.2698	1.20	0.0340	C 17 H 34 N 8 O 4
		414.2700	0.50	0.0345	C 19 H 39 N 2 Na 1 O 6
4	461.2452	461.2435	3.70	0.0081	C 28 H 33 N 2 O 4
		461.2438	3.10	0.0082	C 29 H 32 N 3 Na 1 O 1
		461.2451	0.10	0.0086	C 31 H 34 Na 1 O 2
		461.2448	0.80	0.0089	C 29 H 29 N 6
		461.2424	6.00	0.0114	C 27 H 30 N 6 Na 1

MALDI of **PhOHDPP *N*-H**

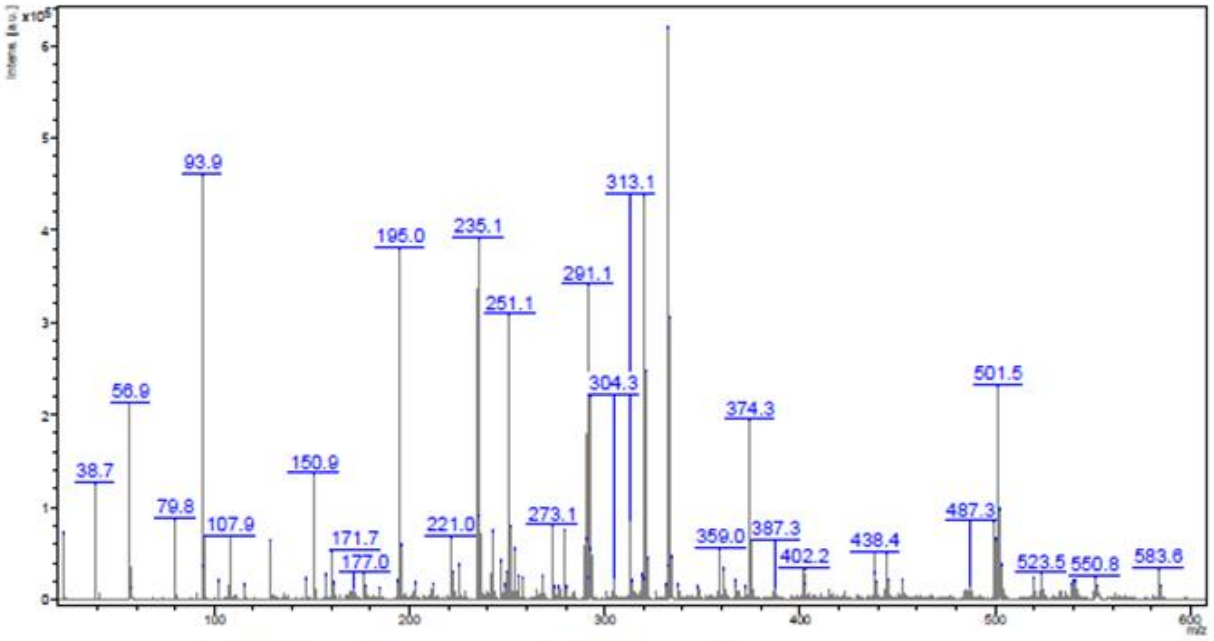

m/z	Rel. Intens.	Intens.	m/z	Rel. Intens.	Intens.
752.827	4	22939.00	367.247	3	19039.50
751.826	7	42171.00	367.080	2	13672.50
584.583	2	12992.00	361.039	5	31921.50
583.578	5	31475.00	359.040	9	53462.00
551.857	2	12913.50	348.152	2	12673.50
550.845	4	22963.50	337.934	2	14151.50
541.478	3	18373.50	334.227	7	44803.50
540.454	3	18715.50	333.234	49	304251.50
539.449	2	15378.50	332.698	6	34629.50
523.498	4	26602.00	332.237	100	617231.50
519.501	4	21626.00	331.214	2	14448.50
503.498	6	35600.00	322.101	7	43281.50
502.495	16	96606.00	321.095	40	245424.50
501.489	37	229253.00	320.553	3	20353.50
500.488	10	64081.00	320.091	71	437037.50
499.476	13	81896.00	319.080	4	25506.50
487.284	2	13120.00	314.131	3	18347.50
452.988	3	19251.50	313.124	14	85537.50
445.413	3	19905.50	304.301	4	21694.00
444.419	8	48632.50	293.115	9	52849.00
439.362	3	17508.50	292.093	35	218980.00
438.622	4	27199.50	291.533	4	21969.00
438.351	8	49517.50	291.074	55	339120.00
403.156	3	15671.50	290.095	10	64435.00
402.166	5	31870.50	280.080	2	12763.00
387.346	2	12668.50	279.074	12	73324.00
387.042	2	12990.50	276.244	2	12308.00
375.291	10	62276.50	274.130	2	12026.00
374.282	31	192009.50	273.126	13	77865.00
372.296	2	12825.50	268.160	4	23988.00

ESI-MS of **PhOBocDPP *N*-Boc**

Ionisation Mode	ESI	Positive	Instrument	Bruker MicroTOF

+MS, 0.6-0.7min #51-62

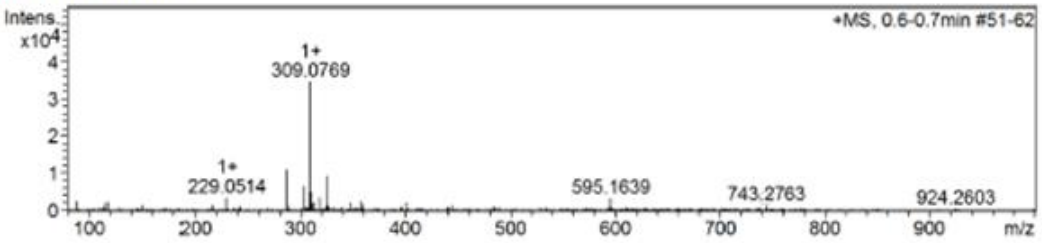

#	m/z	I %
1	88.0754	7.8
2	116.0713	6.5
3	118.0863	7.2
4	215.1228	5.1
5	229.0514	10.4
6	287.0936	32.1
7	288.0990	4.9
8	304.1202	19.6
9	309.0769	100.0
10	310.0782	14.9
11	311.0761	6.2
12	313.2336	6.6
13	318.1353	10.9
14	325.0489	27.1
15	348.1478	6.6
16	357.2541	7.7
17	360.1488	5.3
18	401.2857	6.8
19	445.3109	4.5
20	595.1639	9.9

Generate Molecular Formula Parameters

Charge	Tolerance	sigma limit	H/C Ratio	Electron Conf.	Nitrogen Rule	Chrom.BackGround	Calibration
+1	6 ppm	0.08	3 - 0	both	false	false	TRUE

Expected Formula C38 H44 N2 O12 **Adduct(s):** H, Na, NH4, C3H5N2, radical

#	meas. m/z	theo. m/z	[Err][ppm]	Sigma	Formula	Adduct	Adduct Mass
1	743.2763	743.2786	3.20	0.0698	C38H44N2NaO12	M+Na	22.9898

Note: Sigma fits < 0.05 indicates high probability of correct MF

5. Electrochemistry

Cyclic voltammogram of **PhOMeDPP *N*-2MB** in acetonitrile at 100 mV/s scan rate

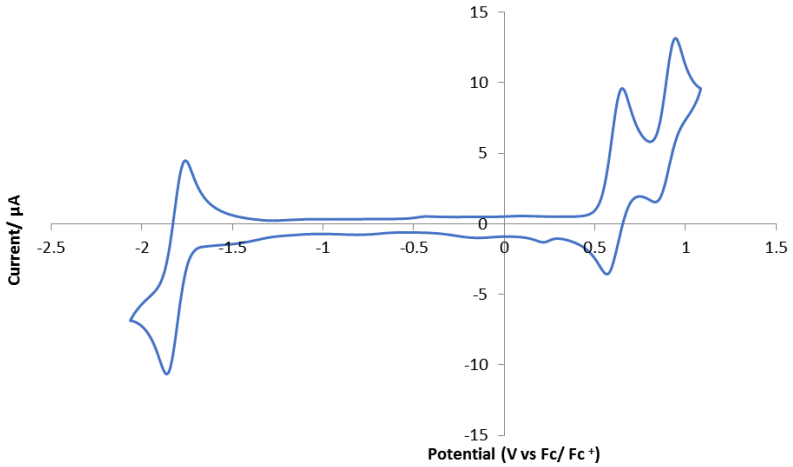

Cyclic voltammogram of **PhOMeDPP *N*-Hex** in acetonitrile at 100 mV/s scan rate

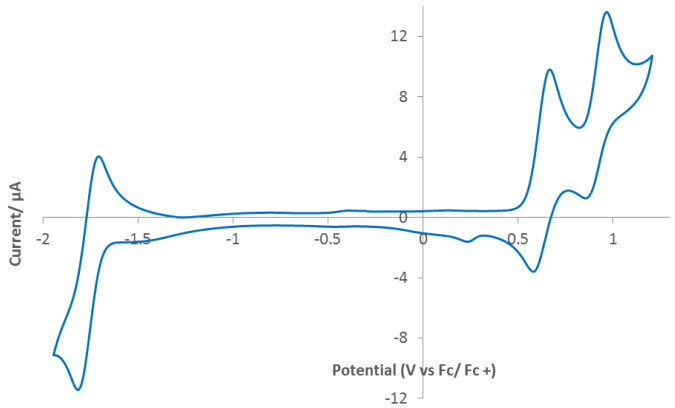

Cyclic voltammogram of **PhOMeDPP *N*-Boc** in dichloromethane at 100 mV/s scan rate

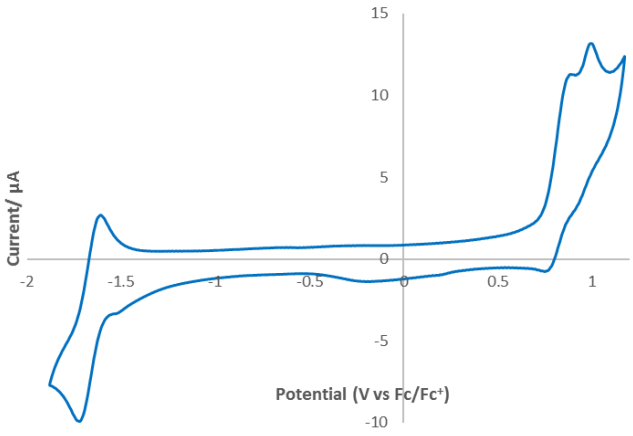

Cyclic voltammogram of **PhOHDPP *N*-Hex** in dimethylformamide at 100 mV/s scan rate

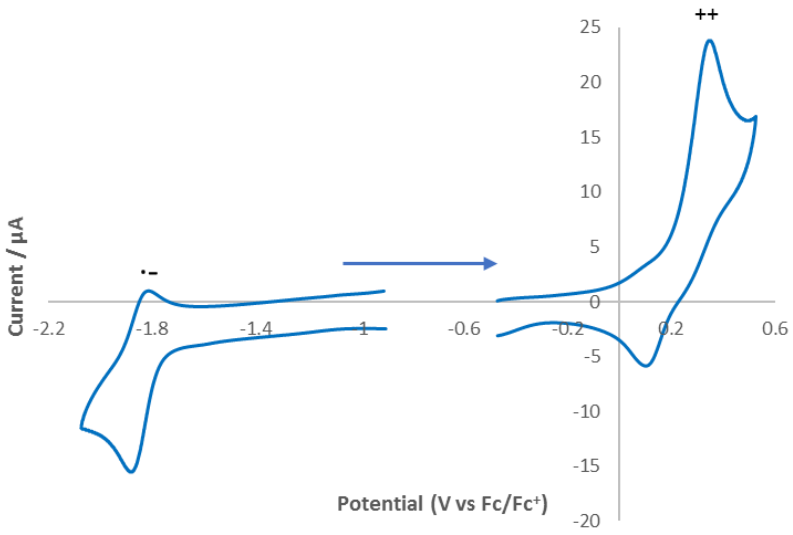

Cyclic voltammogram of **PhOHDPP *N*-2MB** in dimethylformamide at 100 mV/s scan rate

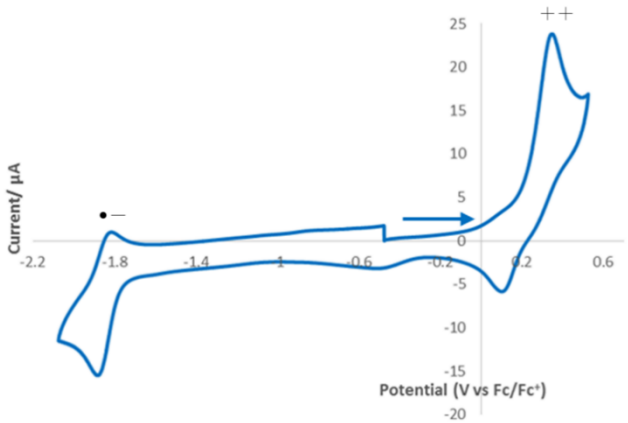

PhOTHPDPP *N*-Hex

Cyclic voltammogram of **PhOTHPDPP *N*-Hex** in acetonitrile at 100 mV/s scan rate

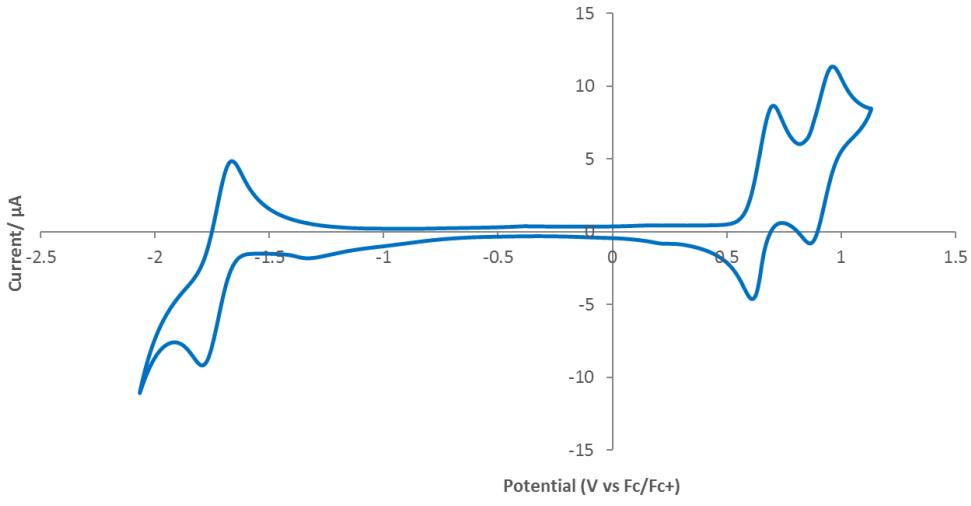

Cyclic voltammogram of **PhOBocDPP *N*-Boc** in dichloromethane at 100 mV/s scan rate

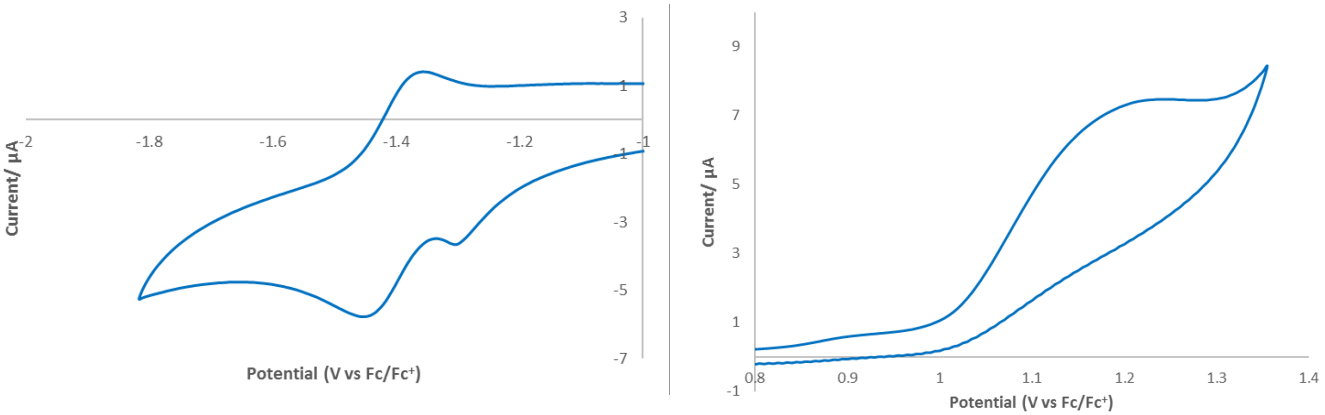

Table of potentials for oxidation and reduction processes for **PhOMeDPP *N*-2MB**, **PhOMeDPP N-Hex**, **PhOMeDPP *N*-Boc**, **PhOHDPP *N*-2MB**, **PhOHDPP *N*-Hex, PhOBocDPP *N*-Boc** and **PhOTHPDPP *N*-Hex** at 100 mV/s scan rate. Potentials in V versus Fc^+ / Fc. Values in brackets are Epa – Epc for couples.

Compound	$E_{pc\ (1st\ ox)}$ / V	$E_{pa\ (1st\ ox)}$ / V	$E_{1/2\ (1st\ ox)}$ / V	$E_{pa\ (2nd\ ox)}$ / V	$E_{pc\ (red)}$ / V	$E_{pa\ (red)}$ / V	$E_{1/2\ (red)}$ / V
PhOMeDPP *N*-2MB	+ 0.50	+ 0.59	+ 0.54 (0.09)	+ 0.84	- 1.83	- 1.73	- 1.78 (0.10)
PhOMeDPP *N*-Hex	+ 0.48	+ 0.56	+ 0.52 (0.08)	+ 0.81	- 1.84	- 1.70	- 1.77 (0.13)
PhOMeDPP *N*-Boc	+ 0.89	-	-	+ 0.98	- 1.71	- 1.62	- 1.66 (0.09)
PhOHDPP *N*-2MB	+ 0.10	+ 0.36	+ 0.23 (0.26)	-	- 1.85	- 1.82	- 1.85 (0.06)
PhOHDPP *N*-Hex	+ 0.12	+ 0.29	+ 0.21 (0.17)	-	- 1.89	- 1.81	- 1.85 (0.08)
PhOBocDPP *N*-Boc	+ 1.24	-	-	-	- 1.46	- 1.36	- 1.41 (0.10)
PhOTHPDPP *N*-Hex	+0.62	+0.70	+0.66 (0.08)	+0.96	-1.76	-1.69	-1.72 (0.07)

6. Crystallographic tables

Identification code	PhOMeDPP *N*-2MB	PhOMeDPP *N*-Hex	PhOHDPP *N*-Hex	PhOHDPP *N*-2MB
Empirical formula	$C_{30}H_{36}N_2O_4$	$C_{32}H_{40}N_2O_4$	$C_{30}H_{36}N_2O_4$	$C_{28}H_{32}N_2O_4$
Formula weight	488.61	516.66	488.61	460.55
Temperature/K	120(2)	120.00(12)	120(2)	120(2)
Crystal system	monoclinic	monoclinic	triclinic	monoclinic
Space group	$P2_1$	$P2_1/c$	P-1	$P2_1$
***a*/Å**	11.0360(8)	17.998(4)	5.2797(14)	11.3208(2)
***b*/Å**	11.6239(6)	10.8801(7)	7.831(2)	8.58917(16)
***c*/Å**	11.4808(10)	11.445(5)	16.028(3)	13.1920(3)
α/°	90	90	76.61(2)	90
β/°	118.259(11)	141.57(5)	85.29(2)	108.388(2)
γ/°	90	90	76.64(2)	90
Volume/Å³	1297.3(2)	1393.0(12)	627.0(3)	1217.25(5)
***Z* (*Z'*)**	2 (1)	2 (0.5)	1 (0.5)	2 (1)
ρ_{calc} g/cm³	1.251	1.232	1.294	1.257
μ/mm⁻¹	0.660	0.641	0.683	0.674
***F*(000)**	524.0	556.0	262.0	492.0
Crystal size/mm	0.34 × 0.2434 × 0.1397	0.15 × 0.103 × 0.027	0.141 × 0.048 × 0.036	0.196 × 0.115 × 0.061
Radiation type	CuKα	CuKα	CuKα	CuKα
2Θ range for data collection/°	8.744 to 148.84	12.766 to 117.826	11.354 to 147.158	8.23 to 156.62
Index ranges	-13 ≤ h ≤ 13, -14 ≤ k ≤ 14, -12 ≤ l ≤ 14	-19 ≤ h ≤ 15, -8 ≤ k ≤ 12, -9 ≤ l ≤ 12	-4 ≤ h ≤ 6, -9 ≤ k ≤ 9, -19 ≤ l ≤ 19	-14 ≤ h ≤ 14, -10 ≤ k ≤ 10, -16 ≤ l ≤ 16
Reflections collected	8266	2973	4095	13621
Independent reflections	4540 [R_{int} = 0.0395, R_{sigma} = 0.0403]	1605 [R_{int} = 0.0373, R_{sigma} = 0.0425]	2419 [R_{int} = 0.1408, R_{sigma} = 0.2050]	5021 [R_{int} = 0.0400, R_{sigma} = 0.0470]
Data/restraints/parameters	4540/1/331	1605/0/174	2419/0/165	5021/1/313
Goodness-of-fit on F²	1.044	1.055	0.983	1.060
Final R indexes [I>=2σ (I)]	R_1 = 0.0525, wR_2 = 0.1382	R_1 = 0.0448, wR_2 = 0.1137	R_1 = 0.0880, wR_2 = 0.1686	R_1 = 0.0395, wR_2 = 0.0997
Final R indexes [all data]	R_1 = 0.0541, wR_2 = 0.1411	R_1 = 0.0590, wR_2 = 0.1218	R_1 = 0.1663, wR_2 = 0.2184	R_1 = 0.0452, wR_2 = 0.1042
Largest diff. peak/hole / e Å⁻³	0.44/-0.28	0.17/-0.17	0.29/-0.33	0.17/-0.23
Flack parameter	0.0(2)			-0.11(13)
CCDC Deposit Number				

Identification code	**PhOTHPDPP *N*-Hex**	**PhOMeDPP *N*-Boc**	**PhOBocDPP *N*-Boc**
Empirical formula	$C_{40}H_{52}N_2O_6$	$C_{30}H_{32}N_2O_8$	$C_{38}H_{44}N_2O_{12}$
Formula weight	656.83	548.57	720.75
Temperature/K	120(2)	120(2)	120(2)
Crystal system	monoclinic	monoclinic	Monoclinic
Space group	$P2_1/c$	$P2_1/n$	$I2/a$
***a*/Å**	12.4391(17)	6.2882(2)	16.4073(9)
***b*/Å**	15.1213(15)	22.9444(5)	10.3312(4)
***c*/Å**	9.5874(8)	9.3448(2)	21.7327(10)
α/°	90	90	90
β/°	96.470(10)	96.832(2)	91.113(5)
γ/°	90	90	90
Volume/Å³	1791.9(3)	1338.68(6)	3683.2(3)
***Z* (*Z'*)**	2 (0.5)	2 (0.5)	4 (0.5)
ρ_{calc} g/cm³	1.217	1.361	1.300
μ/mm⁻¹	0.647	0.093	0.808
***F*(000)**	708.0	580.0	1528.0
Crystal size/mm	0.456 × 0.187 × 0.03	0.15 × 0.03 × 0.01	0.221 × 0.125 × 0.053
Radiation type	CuKα	synchrotron	CuKα
2Θ range for data collection/°	7.152 to 153.616	6.692 to 63.58	8.138 to 146.906
Index ranges	-15 ≤ h ≤ 15, -18 ≤ k ≤ 18, -10 ≤ l ≤ 11	-9 ≤ h ≤ 7, -35 ≤ k ≤ 34, -12 ≤ l ≤ 14	-19 ≤ h ≤ 15, -12 ≤ k ≤ 8, -20 ≤ l ≤ 27
Reflections collected	18027	16657	6992
Independent reflections	3626 [R_{int} = 0.0349, R_{sigma} = 0.0217]	4316 [R_{int} = 0.0413, R_{sigma} = 0.0333]	3595 [R_{int} = 0.0259, R_{sigma} = 0.0333]
Data/restraints/parameters	3626/1116/325	4316/0/205	3595/0/241
Goodness-of-fit on F²	1.069	1.080	1.031
Final R indexes [I>=2σ (I)]	R_1 = 0.0850, wR_2 = 0.2398	R_1 = 0.0479, wR_2 = 0.1168	R_1 = 0.0452, wR_2 = 0.1122
Final R indexes [all data]	R_1 = 0.1027, wR_2 = 0.2621	R_1 = 0.0645, wR_2 = 0.1237	R_1 = 0.0530, wR_2 = 0.1184
Largest diff. peak/hole / e Å⁻³	0.37/-0.31	0.41/-0.20	0.44/-0.27
Flack parameter			
CCDC Deposit Number			

7. Computational calculations

PhDPP *N*-H

Separation distances and electronic coupling for unique neighbouring molecules:

$R_{centre\text{-}centre}$ (Å)	V (meV)
5.5404	14.12
9.049	0.41
9.189	0.40

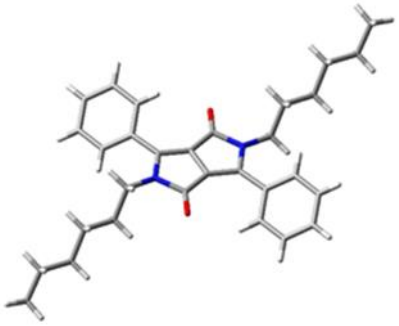

PhOMeDPP *N*-2MB

Separation distances and electronic coupling for unique neighbouring molecules:

$R_{centre\text{-}centre}$ (Å)	V (meV)
11.036	0.785
8.002	8.004
8.033	3.509

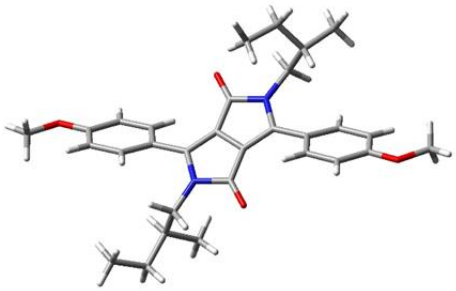

PhOMeDPP *N*-Hex

Separation distances and electronic coupling for unique neighbouring molecules:

$R_{centre\text{-}centre}$ (Å)	V (meV)
7.896	4.636
7.896	4.636
11.497	0.023

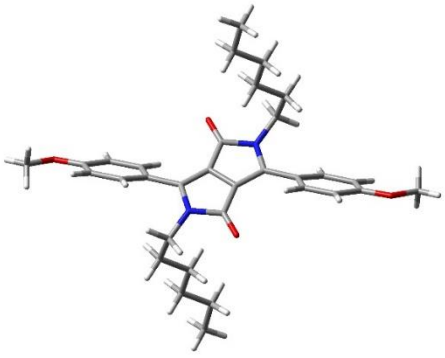

PhOMeDPP *N*-Boc

Separation distances and electronic coupling for unique neighbouring molecules:

$R_{centre\text{-}centre}$ (Å)	V (meV)
16.536	7.314
6.288	79.3
11.878	7.180

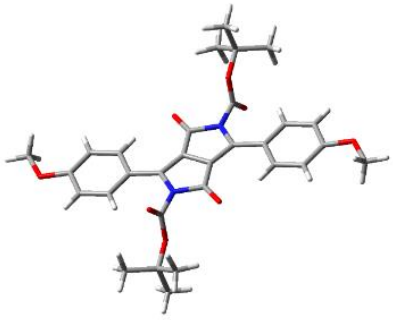

PhOHDPP *N*-Hex

Separation distances and electronic coupling for unique neighbouring molecules:

$R_{centre\text{-}centre}$ (Å)	V (meV)
16.028	0
7.831	1.407
10.407	12.231
5.280	5.564

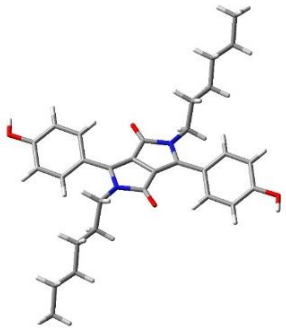

PhOHDPP *N*-2MB

Separation distances and electronic coupling for unique neighbouring molecules:

$R_{centre\text{-}centre}$ (Å)	V (meV)
11.321	2.101
8.589	8.832
8.231	0.803
8.231	0.803
10.877	0.081

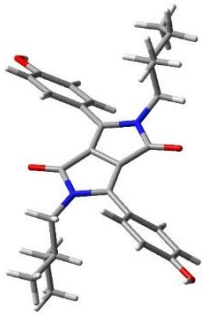

PhOTHPDPP *N*-Hex

Separation distances and electronic coupling for unique neighbouring molecules:

$R_{centre\text{-}centre}$ (Å)	V (meV)
14.83	0.086
8.95	4.855
8.95	4.86
9.59	16.451

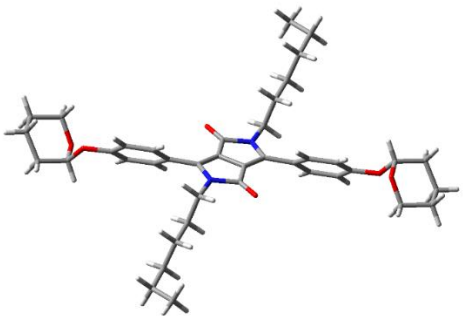

PhOBocDPP *N*-Boc
Separation distances and electronic coupling for unique neighbouring molecules:

$R_{centre\text{-}centre}$ (Å)	V (meV)
12.03	1.153
12.03	1.153
8.20	5.656
10.33	43.075

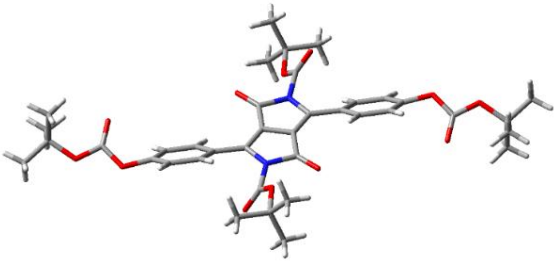

PhOMeDPP *N*-Alkyl calculated electron density distribution of frontier molecular orbitals

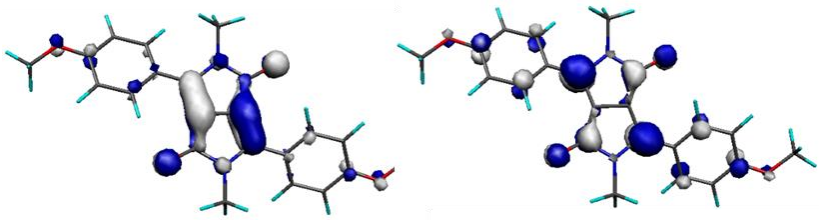

HOMO LUMO

PhOHDPP *N*-Alkyl calculated electron density distribution of frontier molecular orbitals

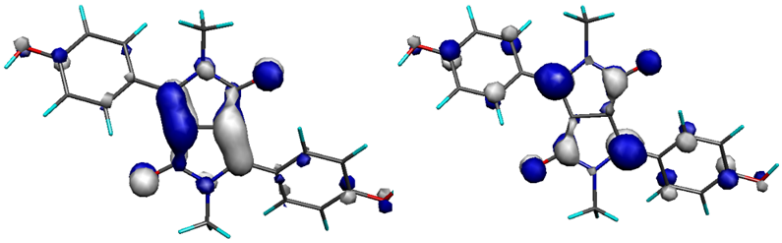

HOMO LUMO

PhOMeDPP *N*-Boc calculated electron density distribution of frontier molecular orbitals

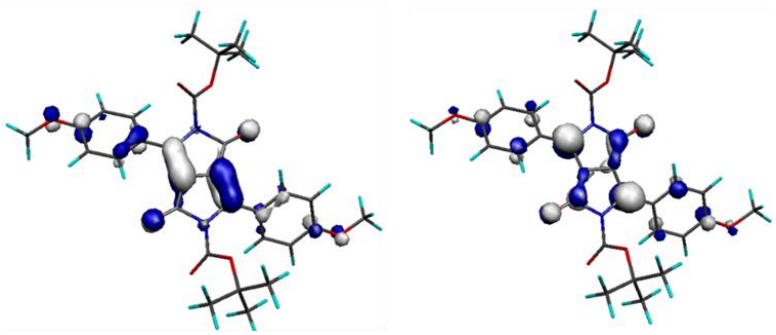

HOMO LUMO

PhOBocDPP *N*-Boc calculated electron density distribution of frontier molecular orbitals

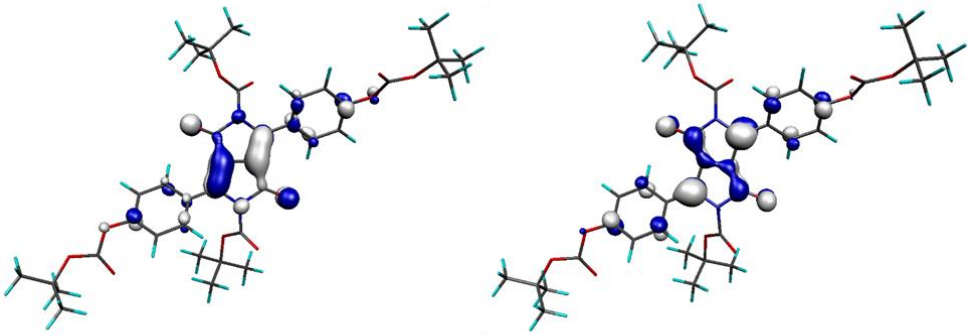

HOMO LUMO

PhOTHPDPP *N*-Hex calculated electron density distribution of frontier molecular orbitals

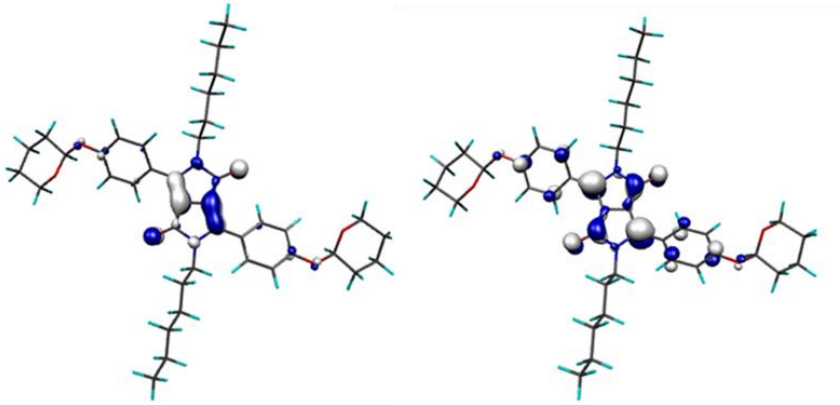

HOMO LUMO

8. Supporting Figures

Fig. S1 Example of DPP-Aryl angle calculation with a plane on the aryl ring and a plane on the connected lactam

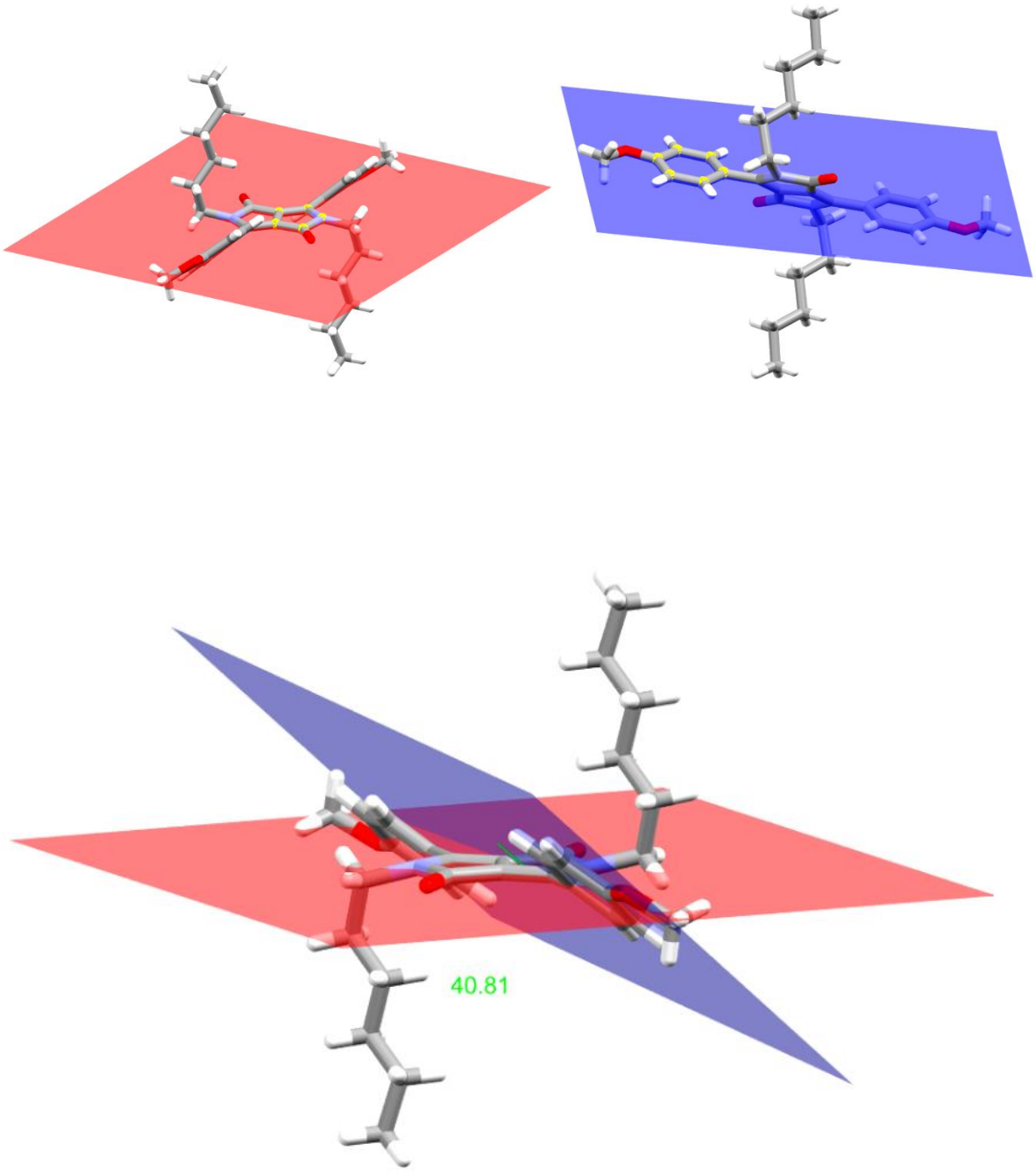

Fig. S2 Example of DPP-Alkyl angle calculation with a plane on the lactam and a plane on [Clactam – N – C(R)]

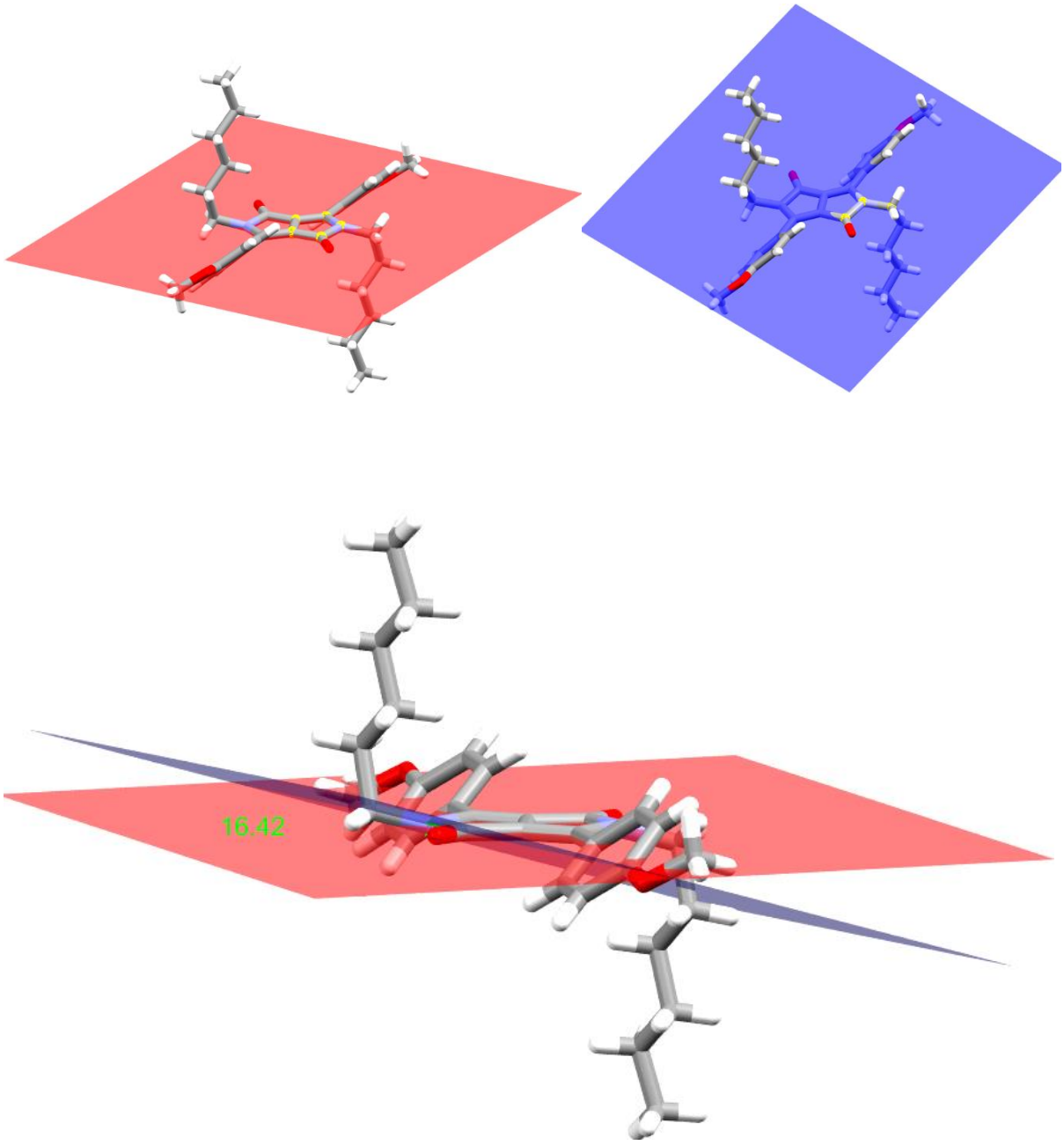

Fig. S3 Closest π–π contact of **PhDPP *N* Hex**

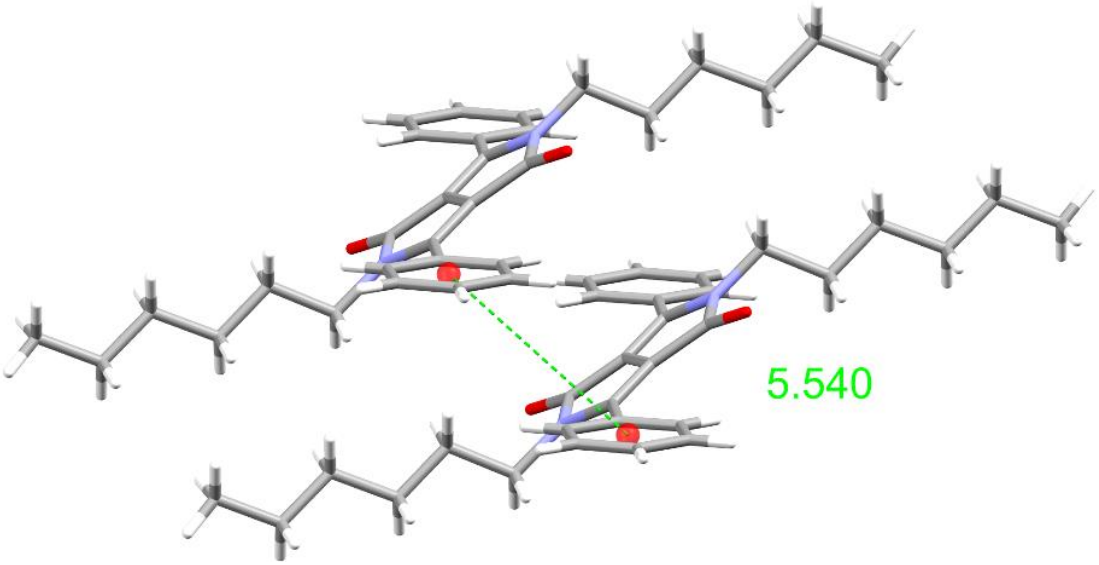

Fig. S4 Closest π–π contact of **PhOHDPP *N*-Hex**

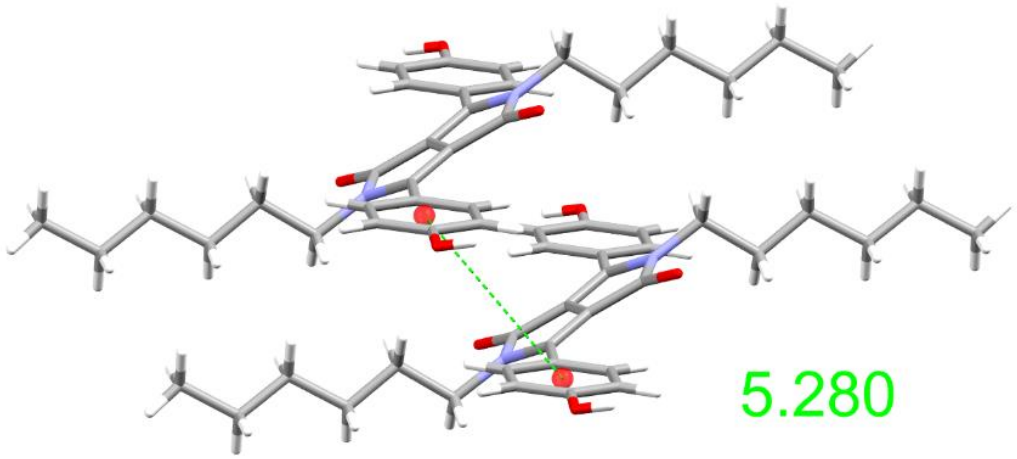

Fig. S5 Plot of Vertical Displacement vs DPP-Aryl Dihedral Angle for **PhDPP *N*-Hex**, **PhOMeDPP *N*-Hex**, **PhOHDPP *N*-Hex, PhOTHPDPP *N*-Hex, PhOHDPP *N*-2MB**, **PhOMeDPP *N*-2MB**,**PhDPP *N*-Boc, PhOMeDPP *N*-Boc** and **PhOBocDPP *N*-Boc**

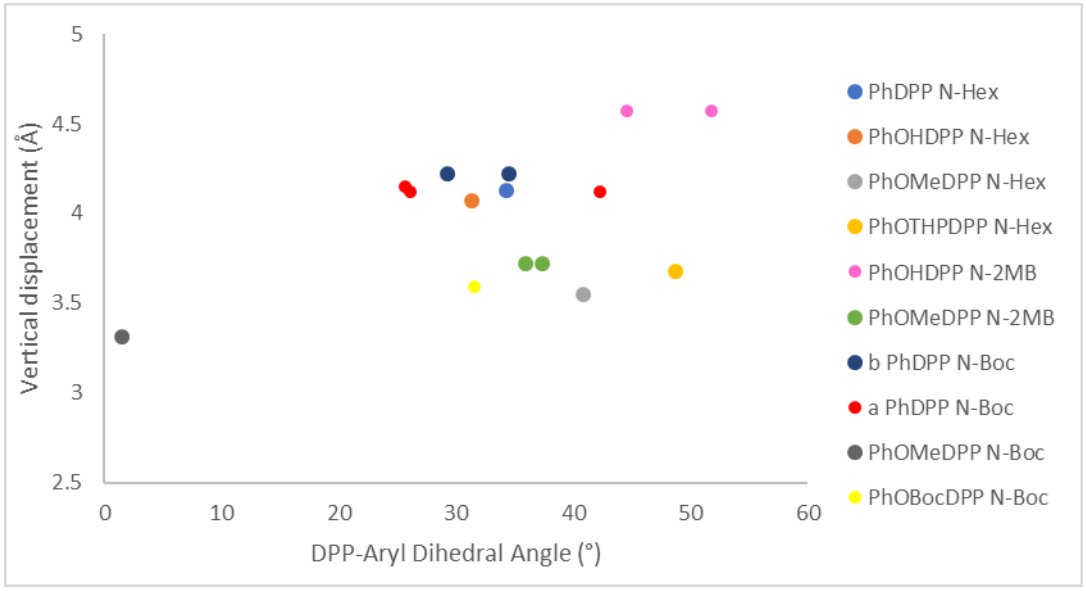

Fig. S6 Plot of Overall Displacement vs DPP-Aryl Dihedral Angle for **PhDPP *N*-Hex**, **PhOMeDPP *N*-Hex**, **PhOHDPP *N*-Hex, PhOTHPDPP *N*-Hex, PhOHDPP *N*-2MB**, **PhOMeDPP *N*-2MB**,**PhDPP *N*-Boc, PhOMeDPP *N*-Boc** and **PhOBocDPP *N*-Boc**

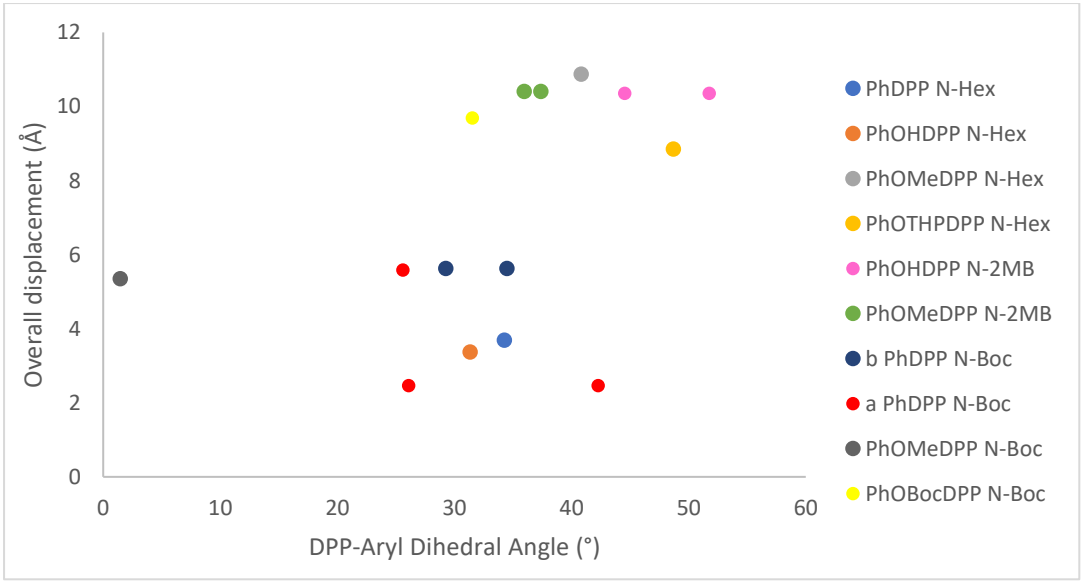

Fig. S7 Plot of Lateral Displacement vs DPP-Aryl Dihedral Angle for **PhDPP *N*-Hex**, **PhOMeDPP *N*-Hex**, **PhOHDPP *N*-Hex, PhOTHPDPP *N*-Hex, PhOHDPP *N*-2MB**, **PhOMeDPP *N*-2MB**,**PhDPP *N*-Boc, PhOMeDPP *N*-Boc** and **PhOBocDPP *N*-Boc**

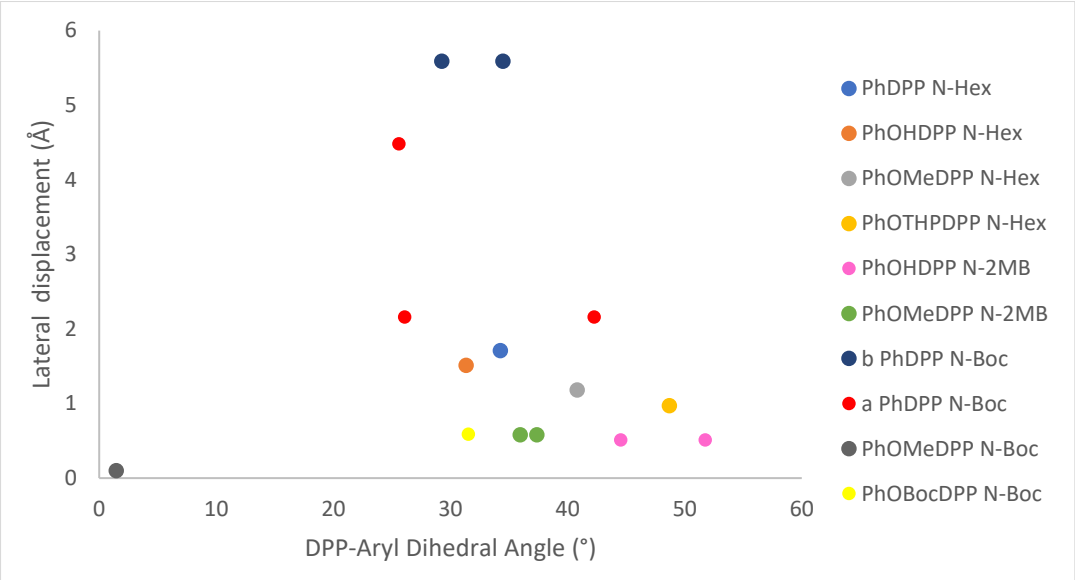

Fig. S8 Plot of Longitudinal Displacement vs DPP-Aryl Dihedral Angle for **PhDPP *N*-Hex**, **PhOMeDPP *N*-Hex**, **PhOHDPP *N*-Hex, PhOTHPDPP *N*-Hex, PhOHDPP *N*-2MB**, **PhOMeDPP *N*-2MB**,**PhDPP *N*-Boc, PhOMeDPP *N*-Boc** and **PhOBocDPP *N*-Boc**

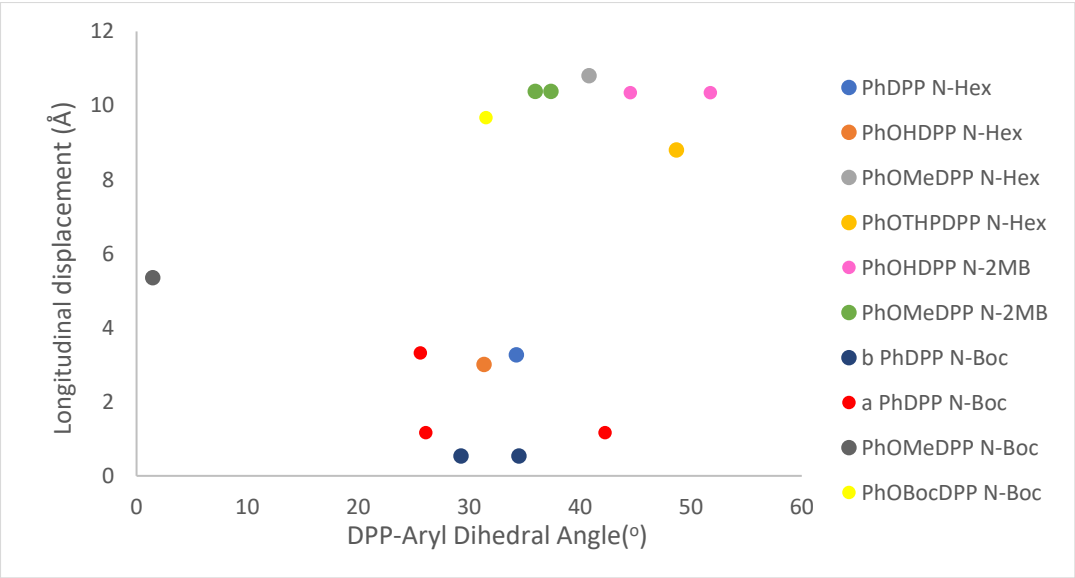

Fig. S9 Plot of DPP-Alkyl Dihedral Angle vs DPP-Aryl Dihedral Angle for **PhDPP *N*-Hex**, **PhOMeDPP *N*-Hex**, **PhOHDPP *N*-Hex, PhOTHPDPP *N*-Hex, PhOHDPP *N*-2MB**, **PhOMeDPP *N*-2MB**,**PhDPP *N*-Boc, PhOMeDPP *N*-Boc** and **PhOBocDPP *N*-Boc**

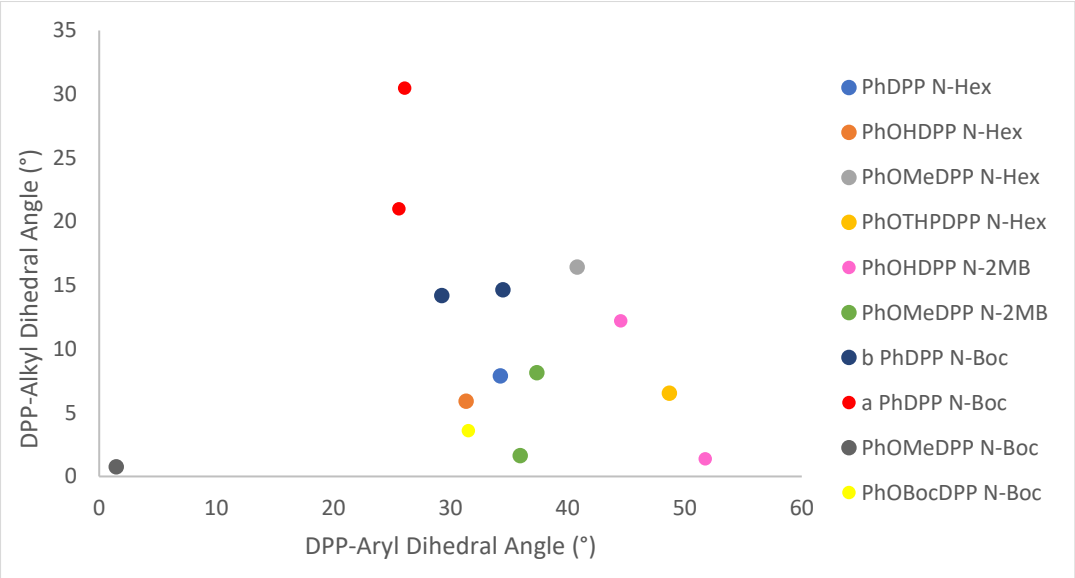

Fig. S10 Plot of Torsion Angle vs Overall Displacement for **PhDPP *N*-Hex**, **PhOMeDPP *N*-Hex**, **PhOHDPP *N*-Hex, PhOTHPDPP *N*-Hex, PhOHDPP *N*-2MB**, **PhOMeDPP *N*-2MB**,**PhDPP *N*-Boc, PhOMeDPP *N*-Boc** and **PhOBocDPP *N*-Boc**

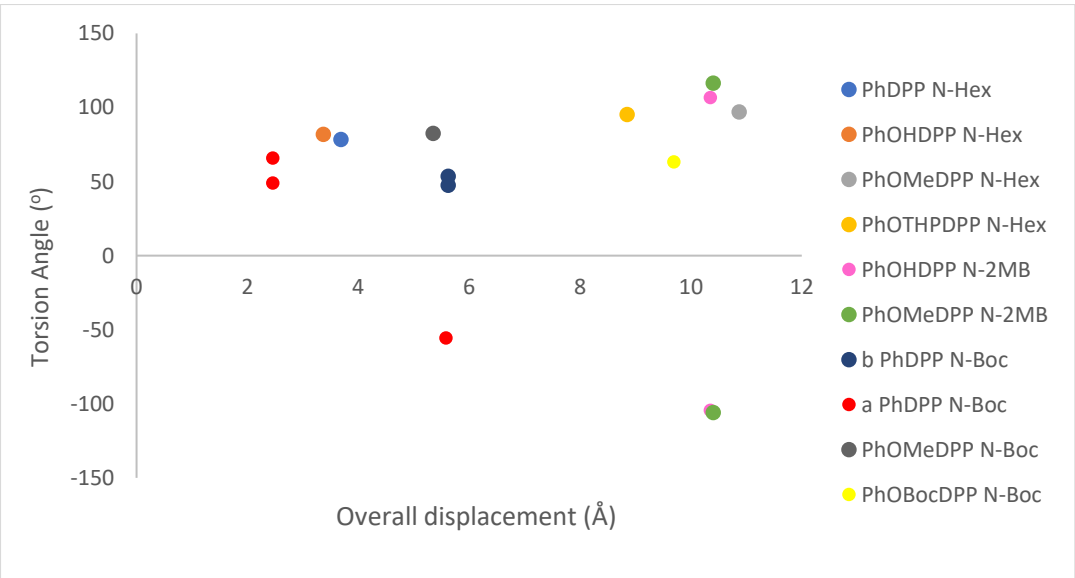

Fig. S11 Plot of Torsion Angle vs Vertical Displacement for **PhDPP *N*-Hex**, **PhOMeDPP *N*-Hex**, **PhOHDPP *N*-Hex, PhOTHPDPP *N*-Hex, PhOHDPP *N*-2MB**, **PhOMeDPP *N*-2MB**,**PhDPP *N*-Boc, PhOMeDPP *N*-Boc** and **PhOBocDPP *N*-Boc**

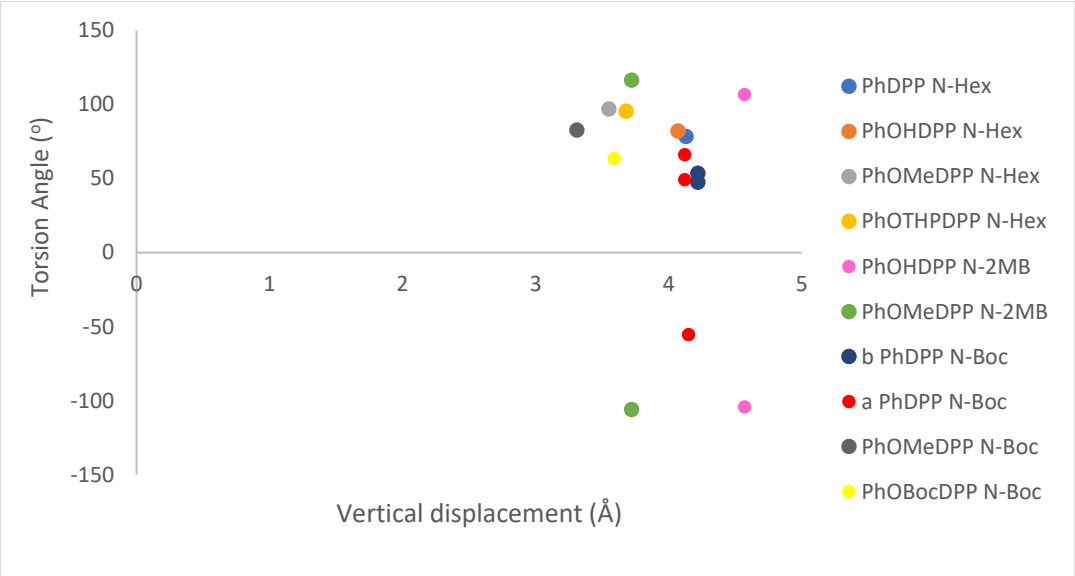

Fig. S12 Plot of Torsion Angle vs Longitudinal Displacement for **PhDPP *N*-Hex**, **PhOMeDPP *N*-Hex**, **PhOHDPP *N*-Hex, PhOTHPDPP *N*-Hex, PhOHDPP *N*-2MB**, **PhOMeDPP *N*-2MB**,**PhDPP *N*-Boc, PhOMeDPP *N*-Boc** and **PhOBocDPP *N*-Boc**

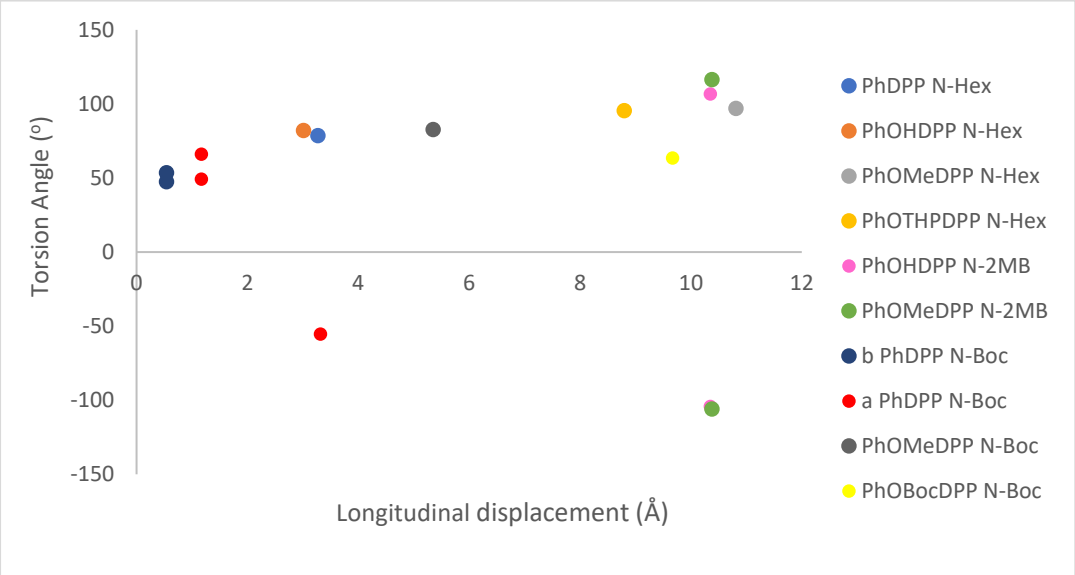

Fig. S13 Plot of Torsion Angle vs Lateral Displacement for **PhDPP *N*-Hex**, **PhOMeDPP *N*-Hex**, **PhOHDPP *N*-Hex, PhOTHPDPP *N*-Hex, PhOHDPP *N*-2MB**, **PhOMeDPP *N*-2MB**,**PhDPP *N*-Boc, PhOMeDPP *N*-Boc** and **PhOBocDPP *N*-Boc**

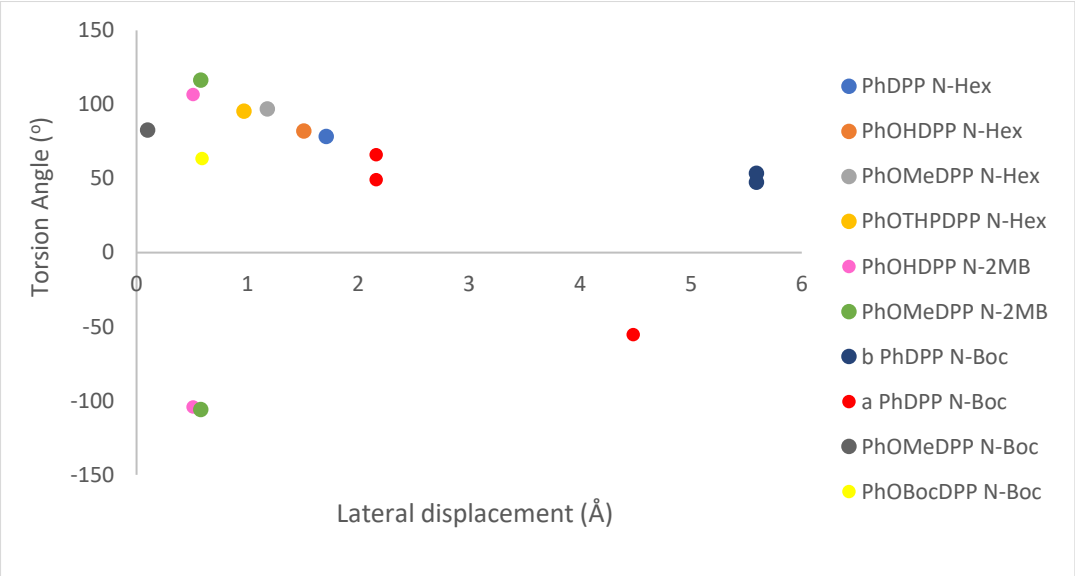

Fig. S14 Plot of Torsion Angle vs DPP-Aryl Dihedral Angle for **PhDPP *N*-Hex**, **PhOMeDPP *N*-Hex**, **PhOHDPP *N*-Hex, PhOTHPDPP *N*-Hex, PhOHDPP *N*-2MB**, **PhOMeDPP *N*-2MB**,**PhDPP *N*-Boc, PhOMeDPP *N*-Boc** and **PhOBocDPP *N*-Boc**

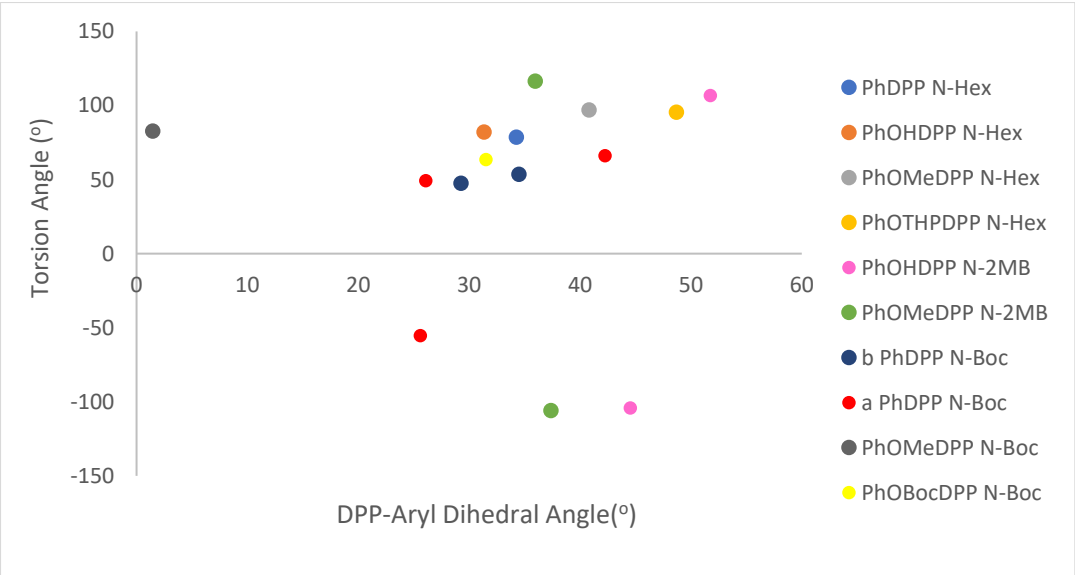

Fig. S15 Plot of Torsion Angle vs DPP-Alkyl Dihedral Angle for **PhDPP *N*-Hex**, **PhOMeDPP *N*-Hex**, **PhOHDPP *N*-Hex, PhOTHPDPP *N*-Hex, PhOHDPP *N*-2MB**, **PhOMeDPP *N*-2MB**,**PhDPP *N*-Boc, PhOMeDPP *N*-Boc** and **PhOBocDPP *N*-Boc**

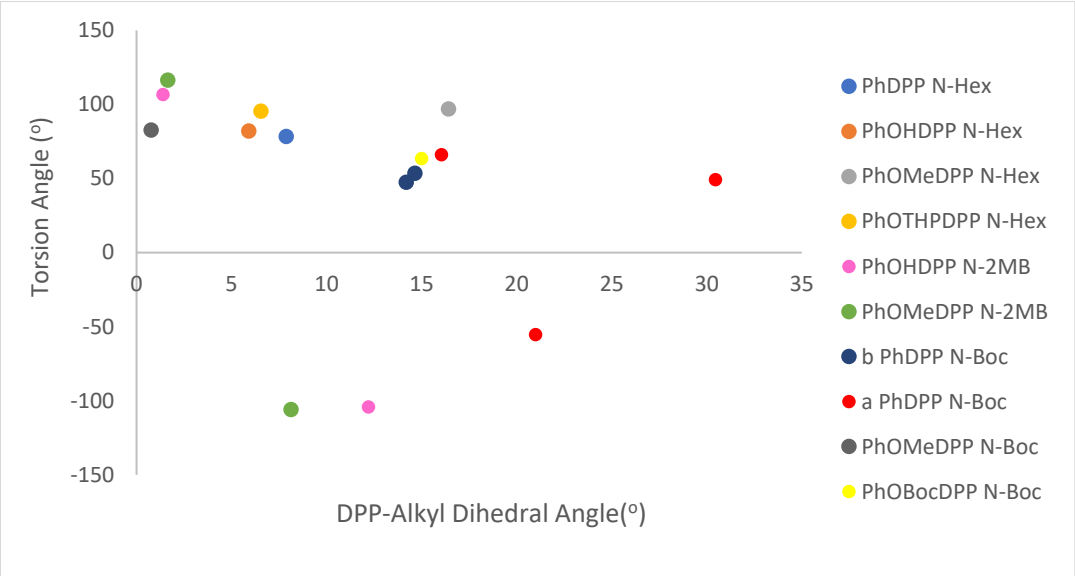

Fig. S16 Plot of DPP-Alkyl Dihedral Angle(°)vs Longitudinal Displacement for **PhDPP *N*-Hex**, **PhOMeDPP *N*-Hex**, **PhOHDPP *N*-Hex, PhOTHPDPP *N*-Hex, PhOHDPP *N*-2MB**, **PhOMeDPP *N*-2MB**,**PhDPP *N*-Boc, PhOMeDPP *N*-Boc** and **PhOBocDPP *N*-Boc**

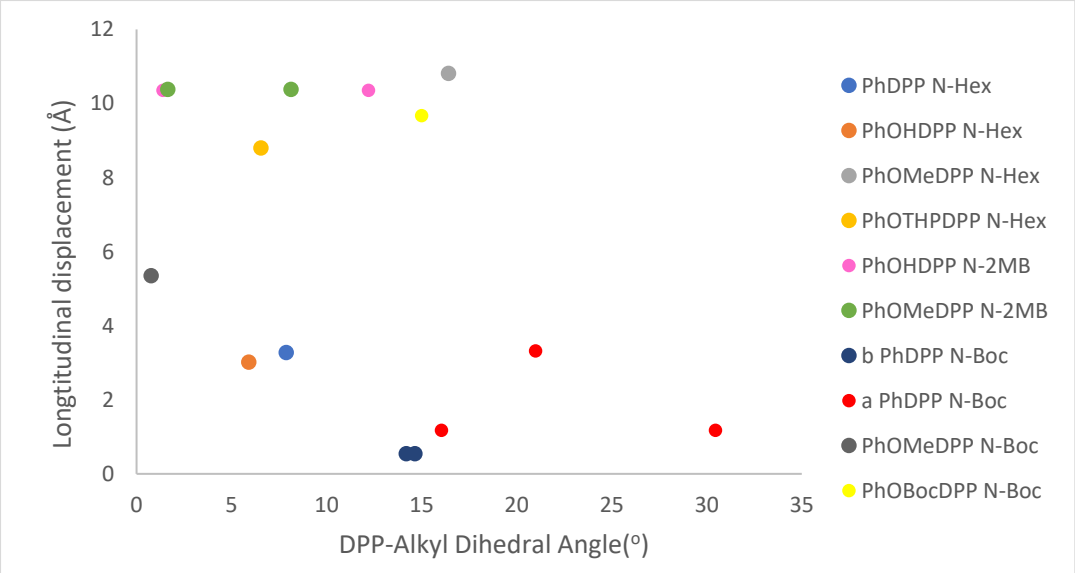

Fig. S17 Plot of Torsion Angle vs Overall Displacement for **PhDPP *N*-Hex**, **PhOMeDPP *N*-Hex**, **PhOHDPP *N*-Hex, PhOTHPDPP *N*-Hex, PhOHDPP *N*-2MB**, **PhOMeDPP *N*-2MB**,**PhDPP *N*-Boc, PhOMeDPP *N*-Boc** and **PhOBocDPP *N*-Boc**

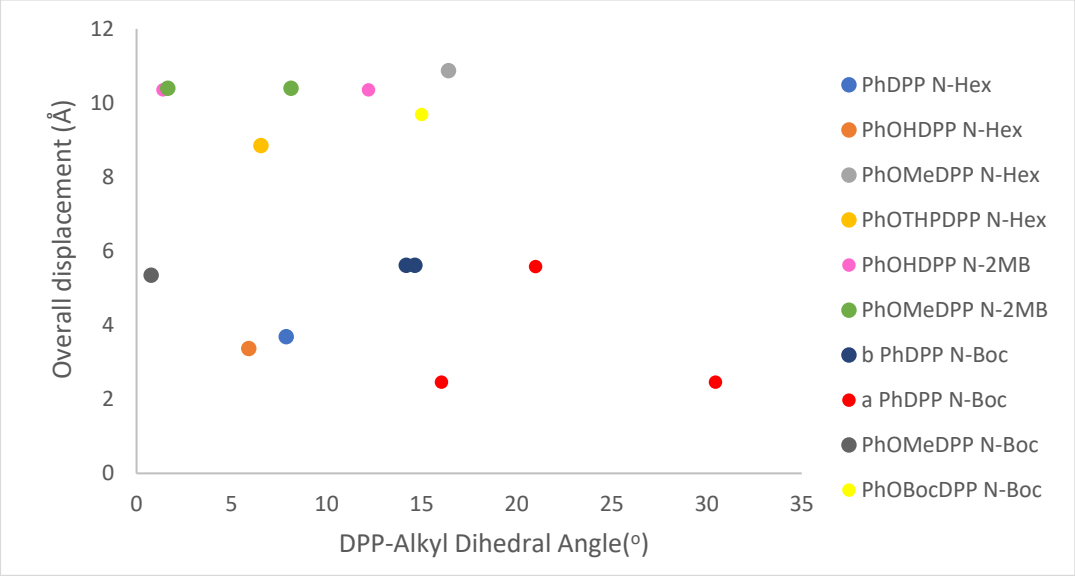

Fig. S18 Plot of DPP-Alkyl Dihedral Angle vs Vertical Displacement for **PhDPP *N*-Hex**, **PhOMeDPP *N*-Hex**, **PhOHDPP *N*-Hex, PhOTHPDPP *N*-Hex, PhOHDPP *N*-2MB**, **PhOMeDPP *N*-2MB**,**PhDPP *N*-Boc, PhOMeDPP *N*-Boc** and **PhOBocDPP *N*-Boc**

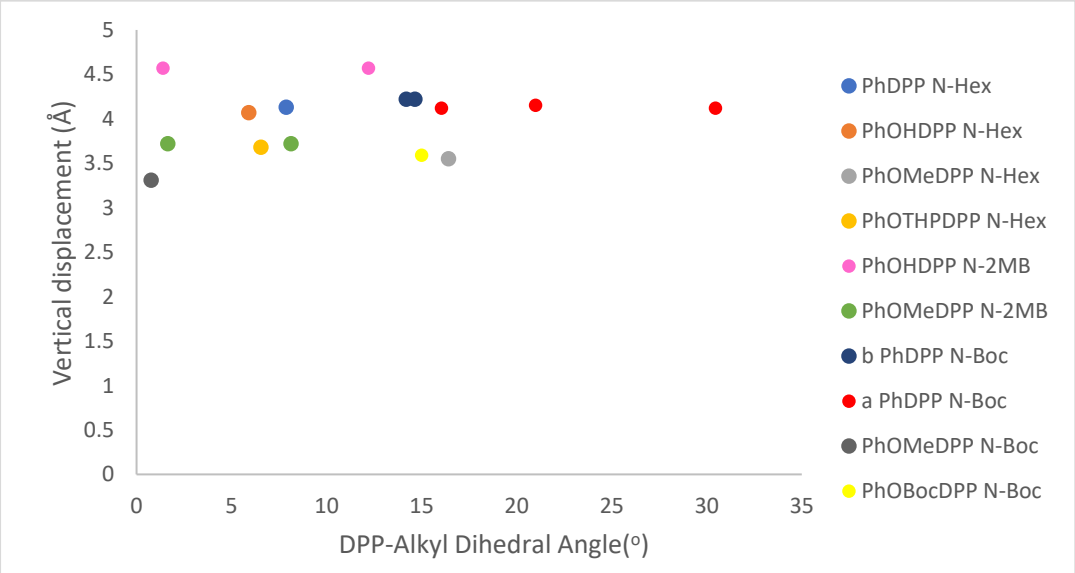

Fig. S19 Plot of DPP-Alkyl Dihedral Angle vs Lateral Displacement for **PhDPP *N*-Hex**, **PhOMeDPP *N*-Hex**, **PhOHDPP *N*-Hex, PhOTHPDPP *N*-Hex, PhOHDPP *N*-2MB**, **PhOMeDPP *N*-2MB**,**PhDPP *N*-Boc, PhOMeDPP *N*-Boc** and **PhOBocDPP *N*-Boc**

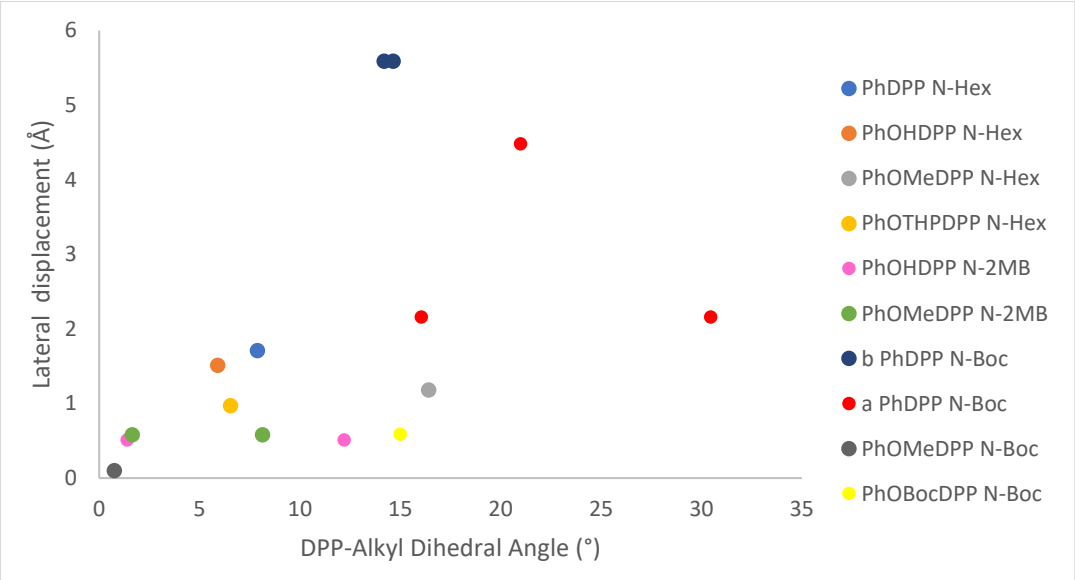

Fig. S20 Chemical structures of **PhDPP *N*-Hex** and **PhDPP *N*-MonoHex**

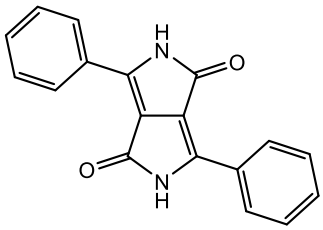

PhDPP *N*H

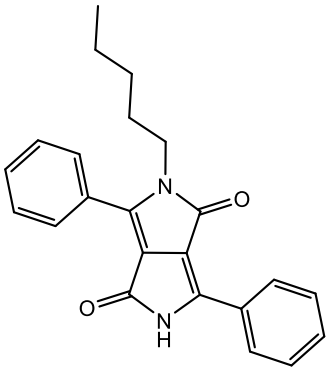

PhDPP *N*-MonoHex

Fig. S21 Hydrogen bonding interactions of **PhOHDPP *N*-Hex** and **PhOHDPP *N*-2MB**

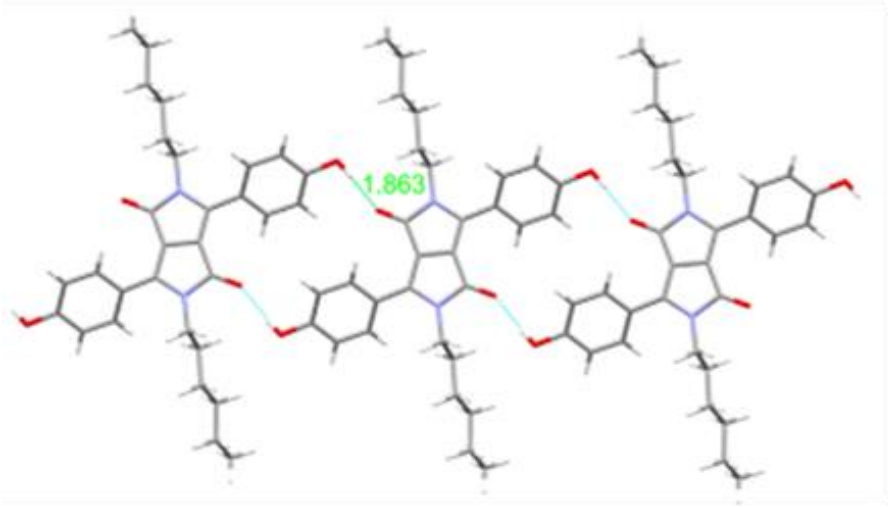

PhOHDPP *N*-Hex

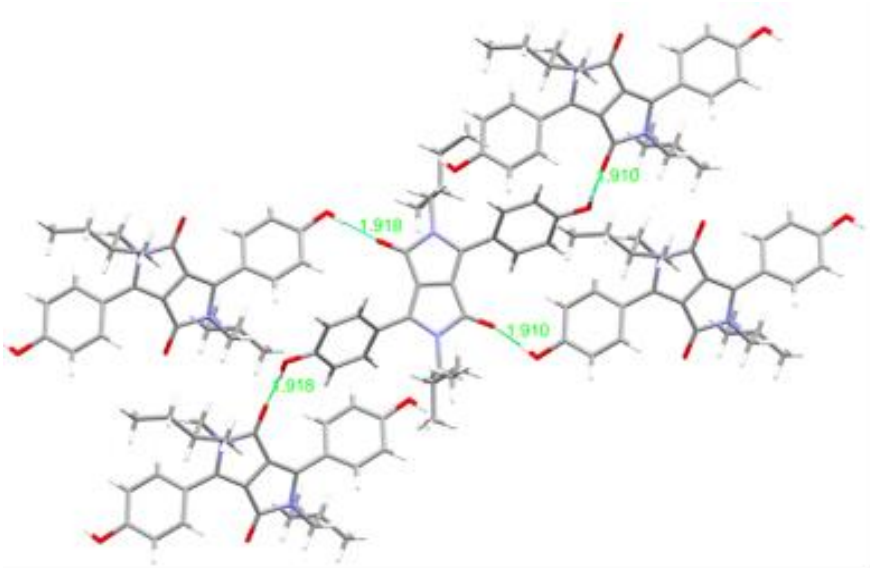

PhOHDPP *N*-2MB

Fig. S22 Solution vs solid absorption of **PhOMeDPP *N*-Hex** in THF and DCM

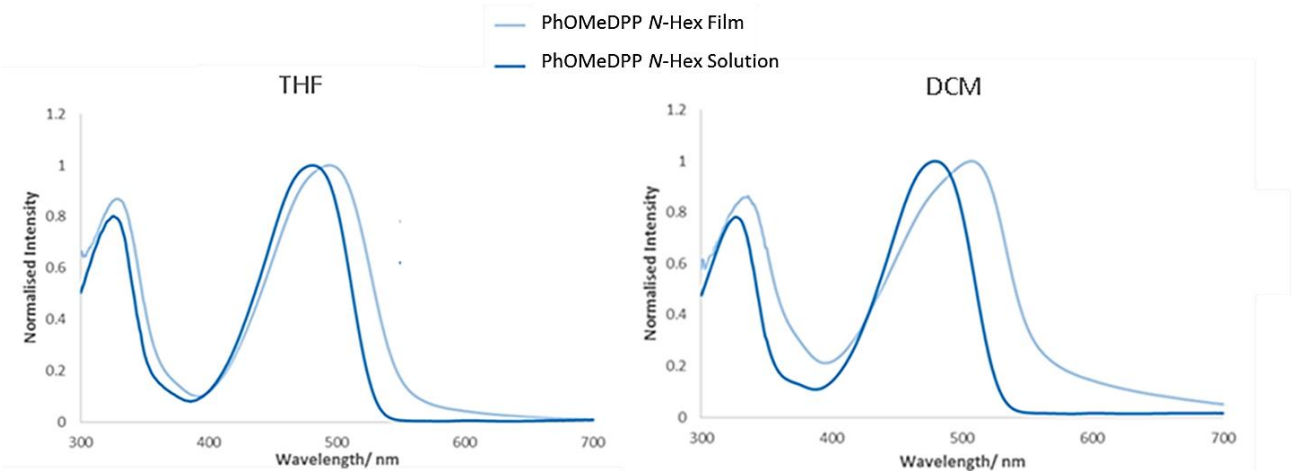

Fig. S23 Solution vs solid absorption of **PhOMeDPP *N*-2MB** in THF and DCM

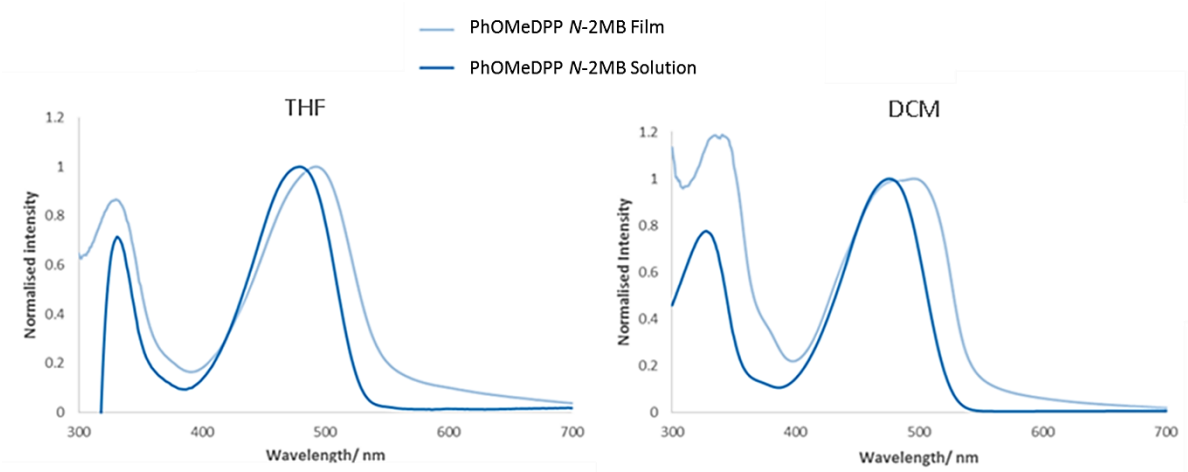

Fig. S24 Solution vs solid absorption of **PhOMeDPP *N*-Boc** in THF and DCM

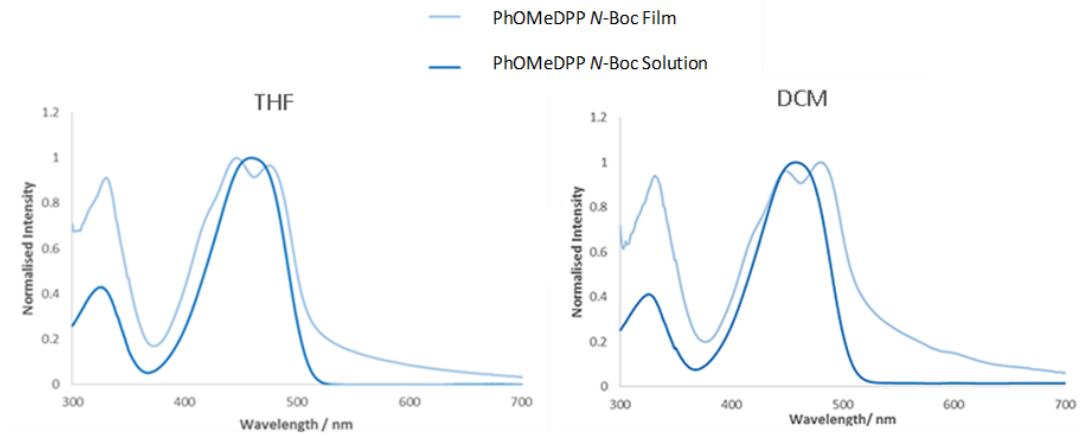

Fig. S25 Solution vs solid absorption of **PhOTHPDPP *N*-Hex** in THF and DCM

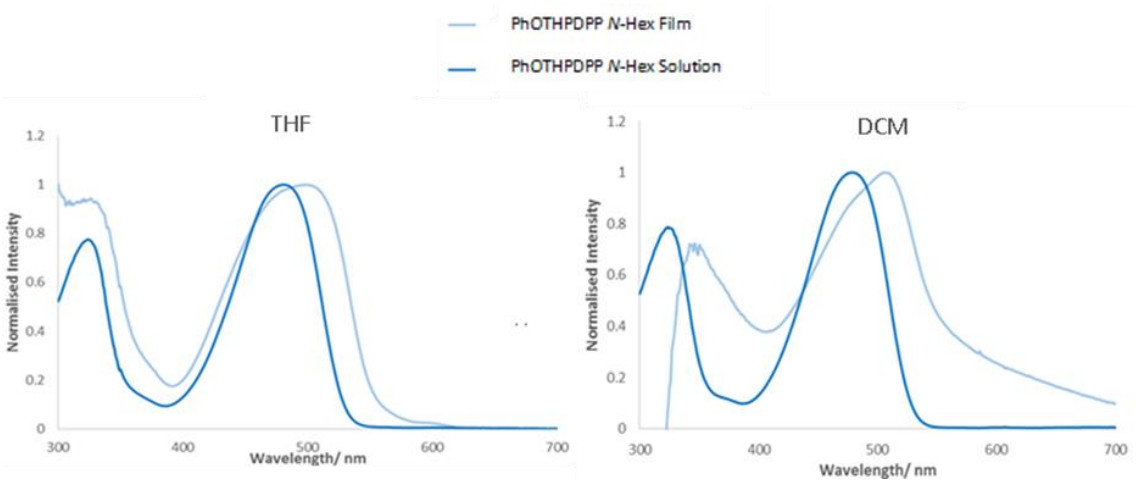

Fig. S26 Solution vs solid absorption of **PhOBocDPP *N*-Boc** in DCM

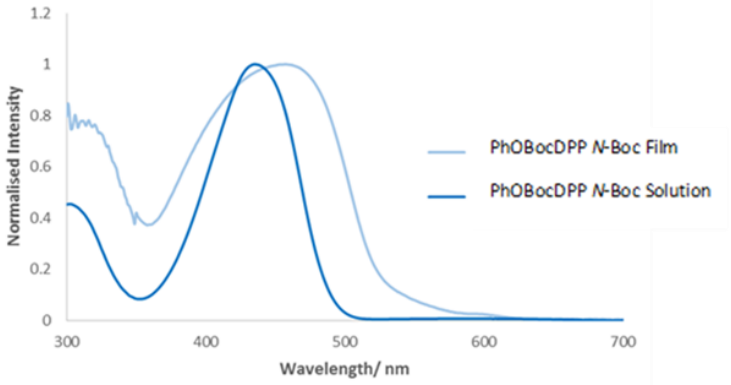

Fig. S27 Plot of solid-state absorption maxima vs. overall displacement for **PhDPP *N*-Hex**, **PhOMeDPP *N*-Hex**, **PhOMeDPP *N*-2MB**, **PhOHDPP *N*-2MB**, **PhOMeDPP *N*-Boc**, **PhOBocDPP *N*-Boc** and **PhOTHPDPP *N*-Hex**

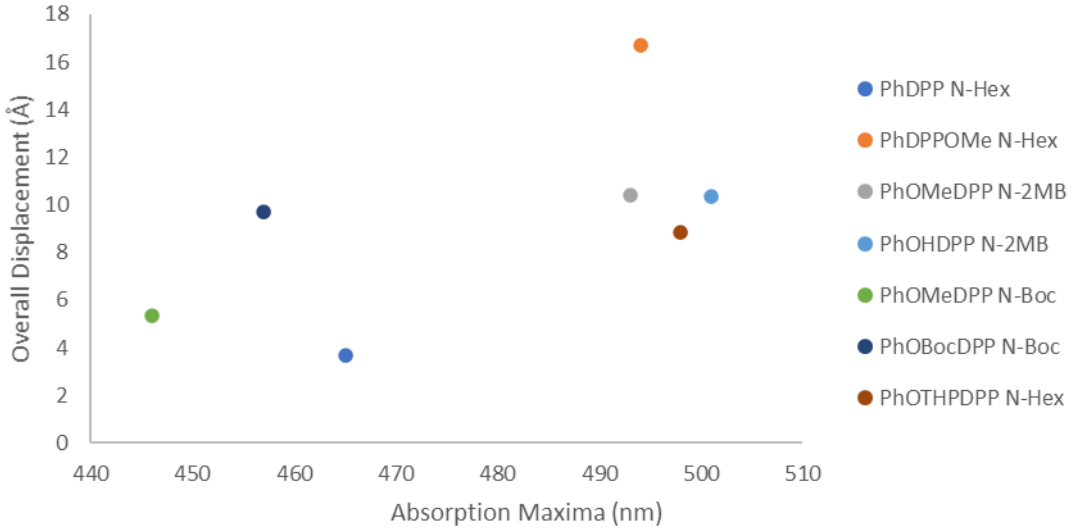

Fig. S28 Plot of solid-state absorption maxima vs. vertical displacement for **PhDPP *N*-Hex**, **PhOMeDPP *N*-Hex**, **PhOMeDPP *N*-2MB**, **PhOHDPP *N*-2MB**, **PhOMeDPP *N*-Boc**, **PhOBocDPP *N*-Boc** and **PhOTHPDPP *N*-Hex**

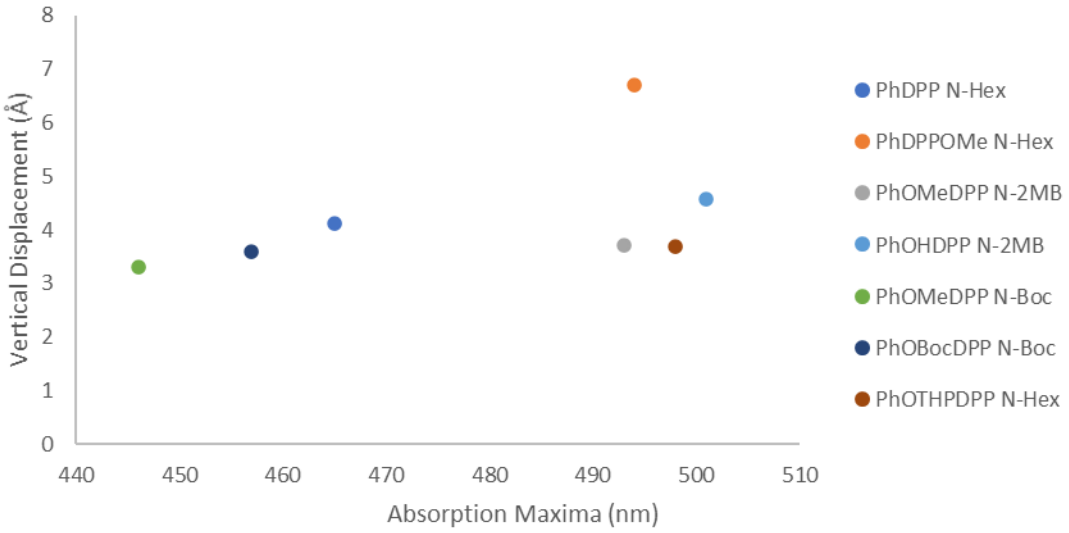

Fig. S29 Plot of solid-state absorption maxima vs. Longitudinal Displacement for **PhDPP *N*-Hex**, **PhOMeDPP *N*-Hex**, **PhOMeDPP *N*-2MB**, **PhOHDPP *N*-2MB**, **PhOMeDPP *N*-Boc**, **PhOBocDPP *N*-Boc** and **PhOTHPDPP *N*-Hex**

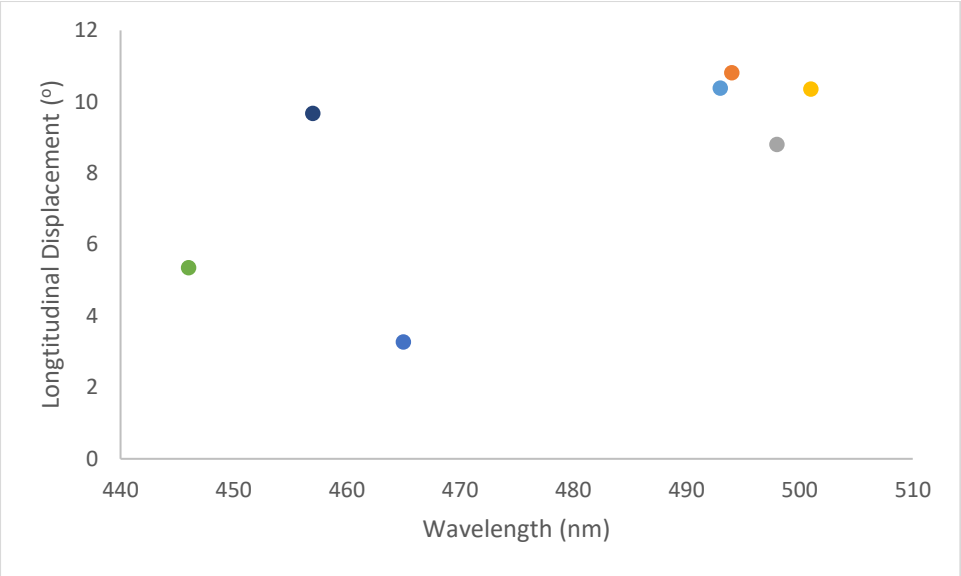

Fig. S30 Plot of solid-state absorption maxima vs. Lareral Displacement for **PhDPP *N*-Hex**, **PhOMeDPP *N*-Hex**, **PhOMeDPP *N*-2MB**, **PhOHDPP *N*-2MB**, **PhOMeDPP *N*-Boc**, **PhOBocDPP *N*-Boc** and **PhOTHPDPP *N*-Hex**

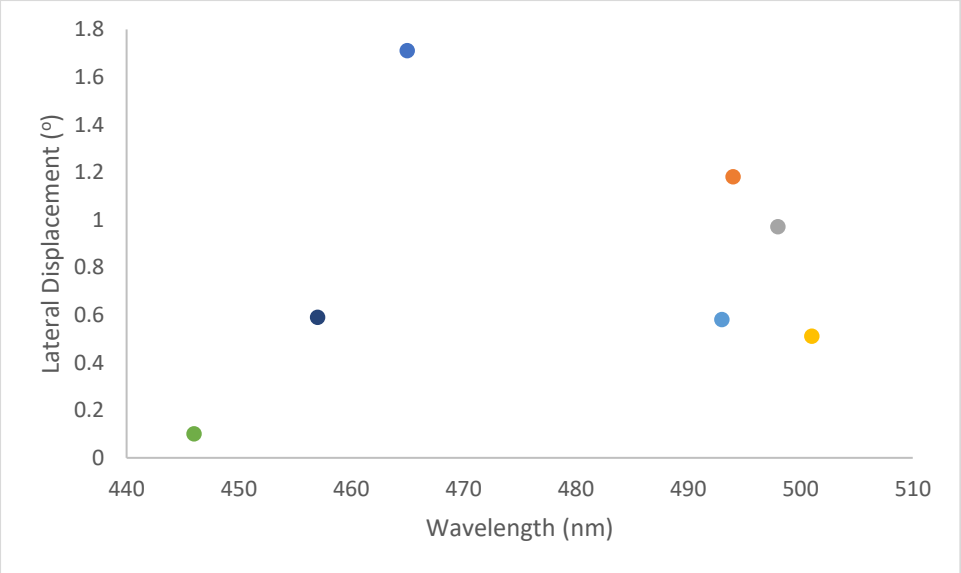

Fig. S31 Plot of solid-state absorption maxima vs. DPP-Alkyl Dihedral Angle for **PhDPP *N*-Hex**, **PhOMeDPP *N*-Hex**, **PhOMeDPP *N*-2MB**, **PhOHDPP *N*-2MB**, **PhOMeDPP *N*-Boc**, **PhOBocDPP *N*-Boc** and **PhOTHPDPP *N*-Hex**

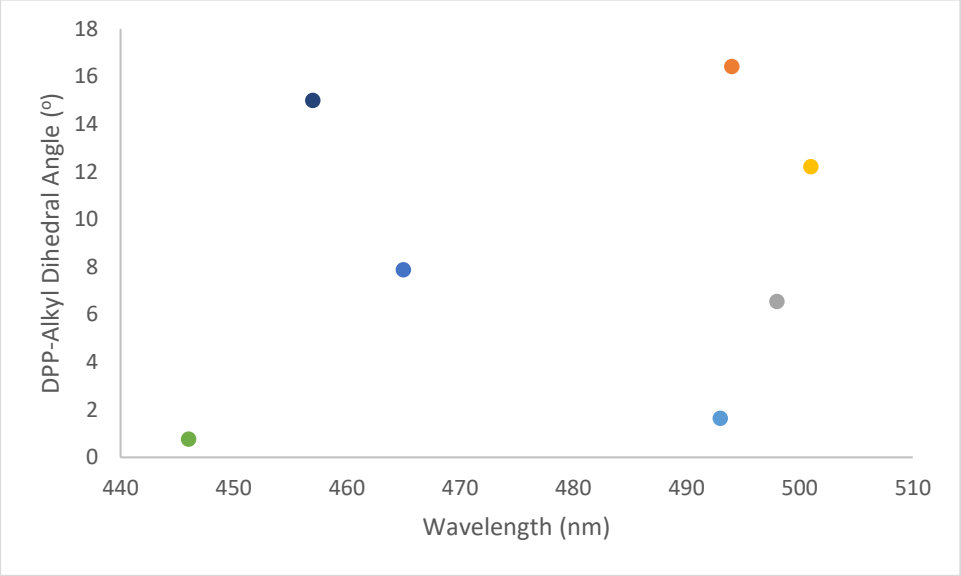

Fig. S32 Plot of Torsion Anglw vs. DPP-Alkyl Dihedral Angle for **PhDPP *N*-Hex**, **PhOMeDPP *N*-Hex**, **PhOMeDPP *N*-2MB**, **PhOHDPP *N*-2MB**, **PhOMeDPP *N*-Boc**, **PhOBocDPP *N*-Boc** and **PhOTHPDPP *N*-Hex**

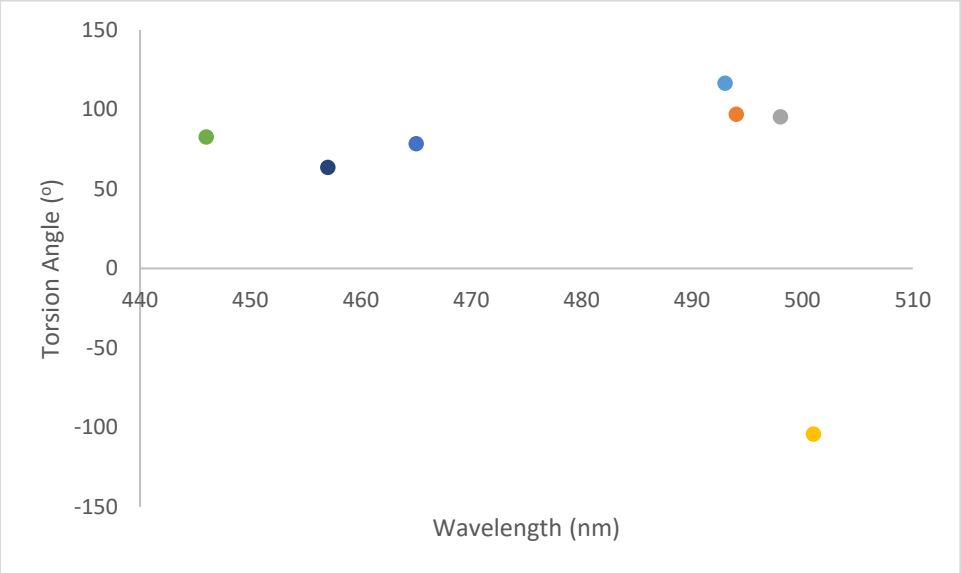

Fig. S33 Plot of solid-state absorption maxima vs. DPP-aryl angle for **PhDPP *N*-Hex**, **PhOMeDPP *N*-Hex**, **PhOMeDPP *N*-2MB**, **PhOHDPP *N*-2MB**, **PhOMeDPP *N*-Boc**, **PhOBocDPP *N*-Boc** and **PhOTHPDPP *N*-Hex**

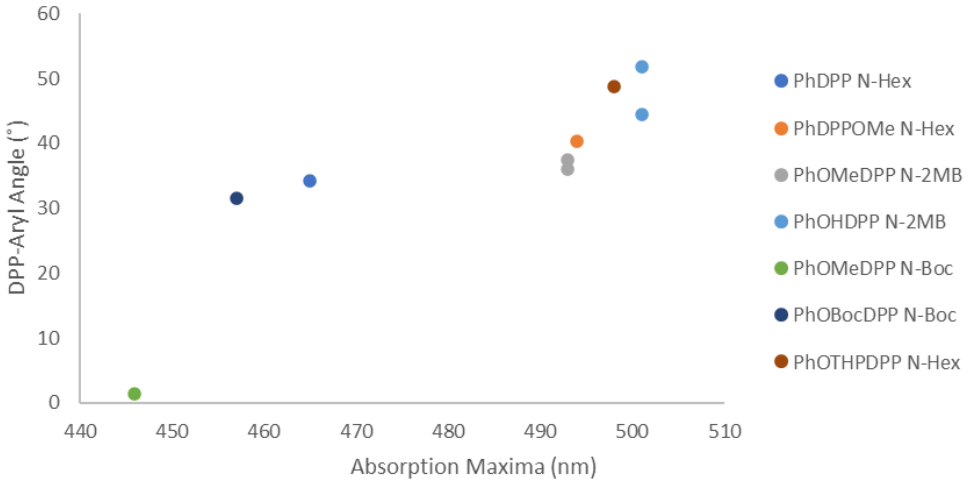

Fig. S34 Plot of absorption maxima shift vs. overall displacement for **PhDPP *N*-Hex**, **PhOMeDPP *N*-Hex**, **PhOMeDPP *N*-2MB**, **PhOHDPP *N*-2MB**, **PhOMeDPP *N*-Boc**, **PhOBocDPP *N*-Boc** and **PhOTHPDPP *N*-Hex**

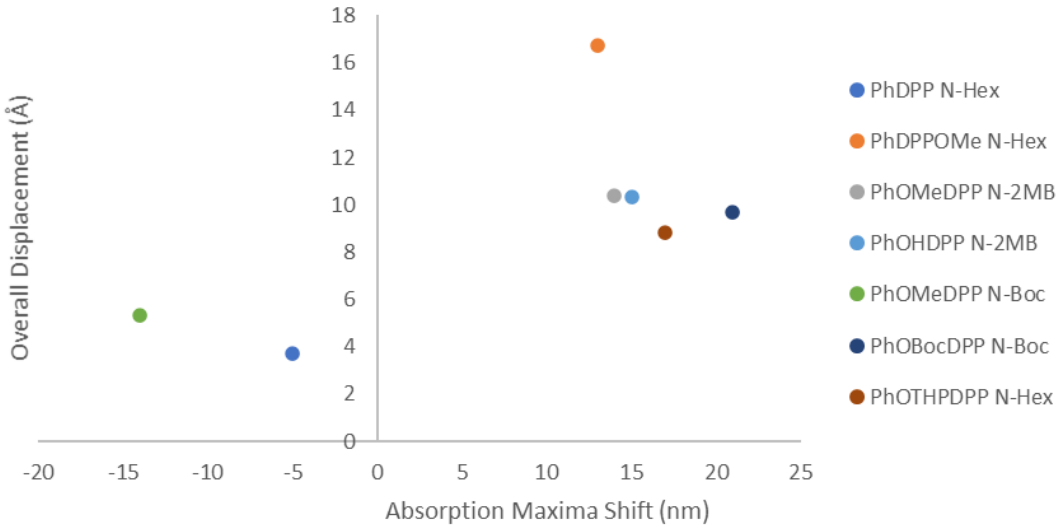

Fig. S35 Solution vs solid emission and solid absorption of **PhDPP *N*-Hex** in THF

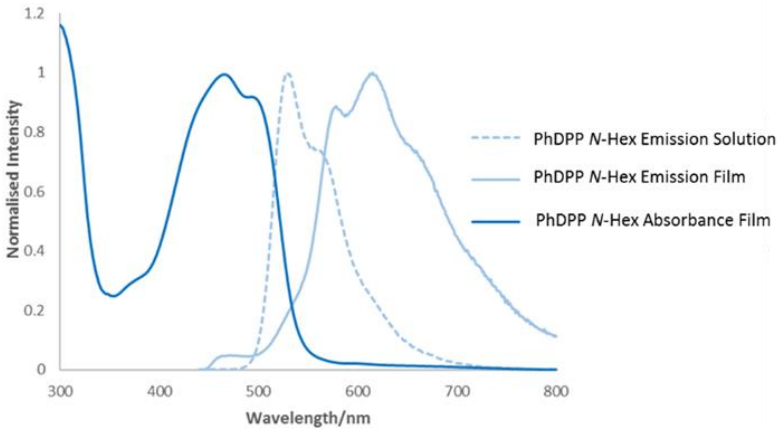

Fig. S36 Solution vs solid emission and solid absorption of **PhOMeDPP *N*-Hex** in THF

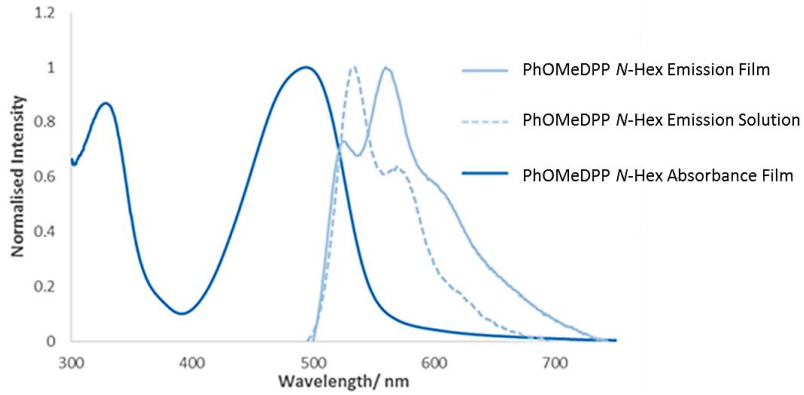

Fig. S37 Solution vs solid emission and solid absorption of **PhOMeDPP *N*-Boc** in THF and DCM

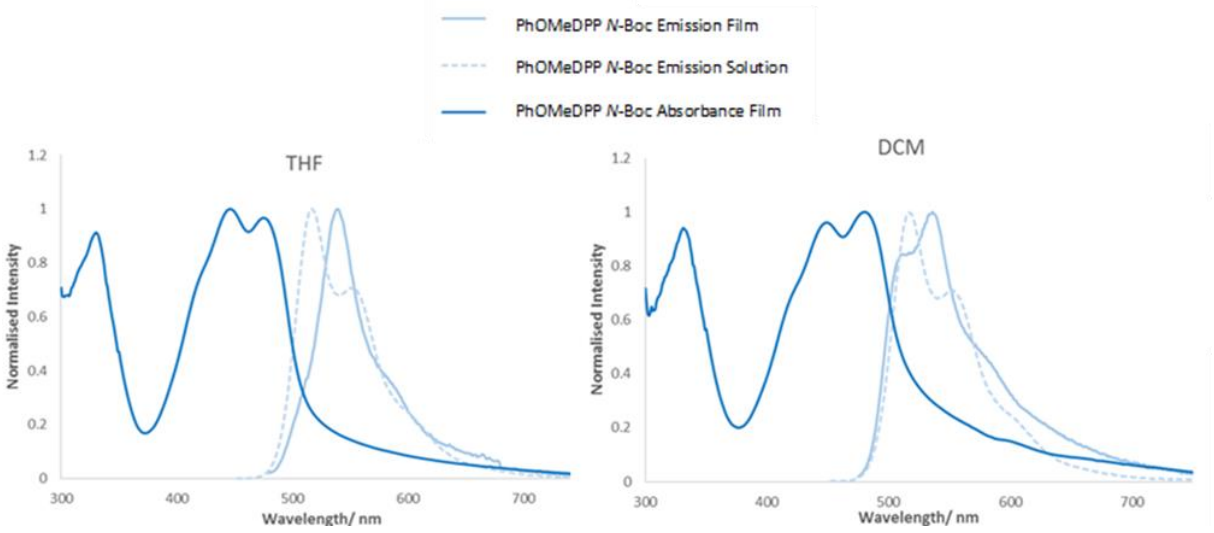

Fig. S38 Solution vs solid emission and solid absorption of **PhOBocDPP *N*-Boc** in THF

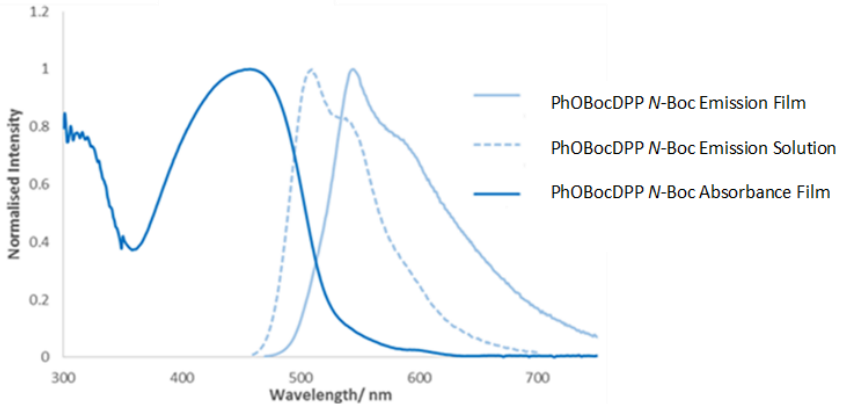

Fig. S39 Solution vs solid emission and solid absorption of **PhOTHPDPP *N*-Hex** in THF

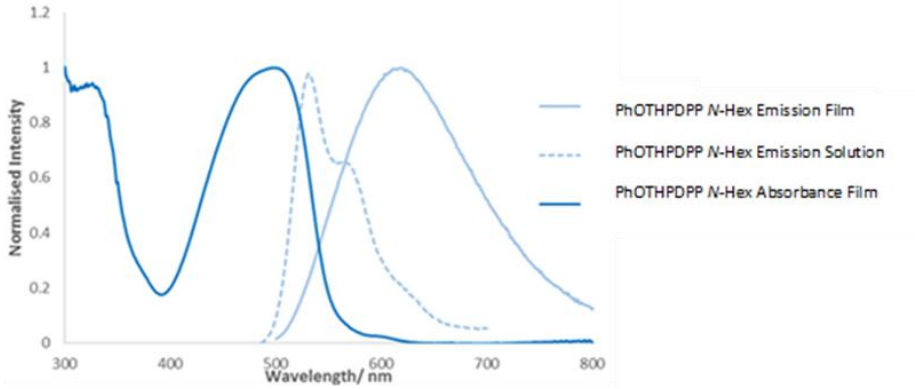

Fig. S40 Plot of solid-state emission maxima vs. vertical displacement for **PhDPP *N*-Hex**, **PhOMeDPP *N*-Hex**, **PhOMeDPP *N*-2MB**, **PhOMeDPP *N*-Boc**, **PhOBocDPP *N*-Boc** and **PhOTHPDPP *N*-Hex**

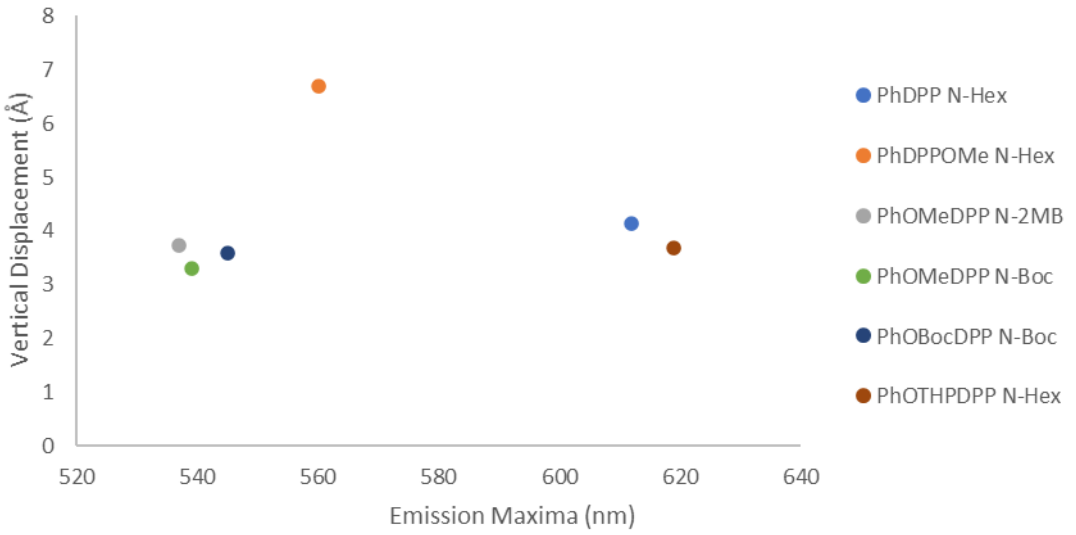

Fig. S41 Plot of solid-state emission maxima vs. overall displacement for **PhDPP *N*-Hex**, **PhOMeDPP *N*-Hex**, **PhOMeDPP *N*-2MB**, **PhOMeDPP *N*-Boc**, **PhOBocDPP *N*-Boc** and **PhOTHPDPP *N*-Hex**

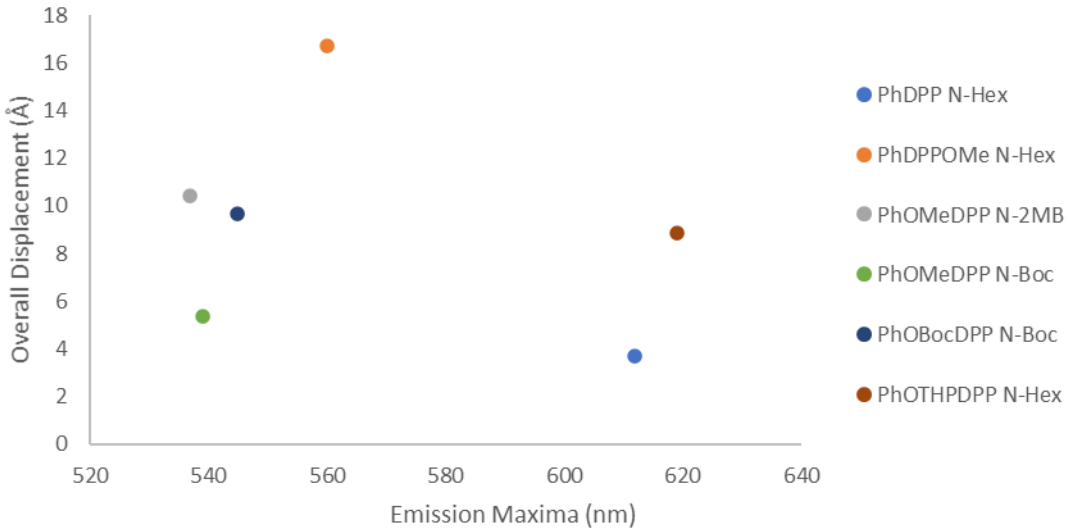

Fig. S42 Plot of solid-state emission maxima vs. DPP-aryl angle for **PhDPP *N*-Hex**, **PhOMeDPP *N*-Hex**, **PhOMeDPP *N*-2MB**, **PhOMeDPP *N*-Boc**, **PhOBocDPP *N*-Boc** and **PhOTHPDPP *N*-Hex**

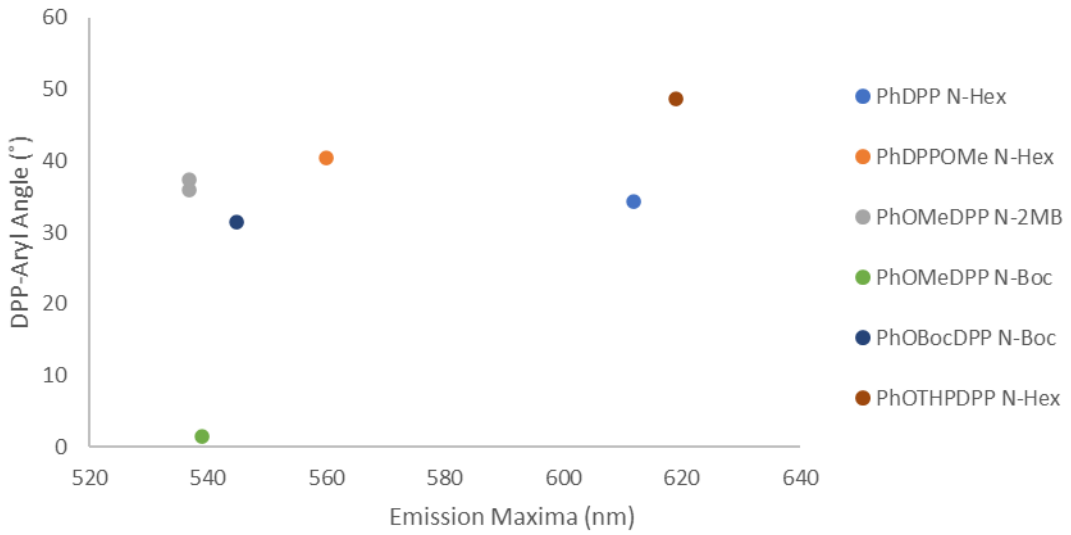

9. Supporting Tables

Table S1

PhDPP *N*-Hex			
Number	Atom1	Atom2	Length (Å)
1	C3	H4	2.868
2	O1	H3	2.494

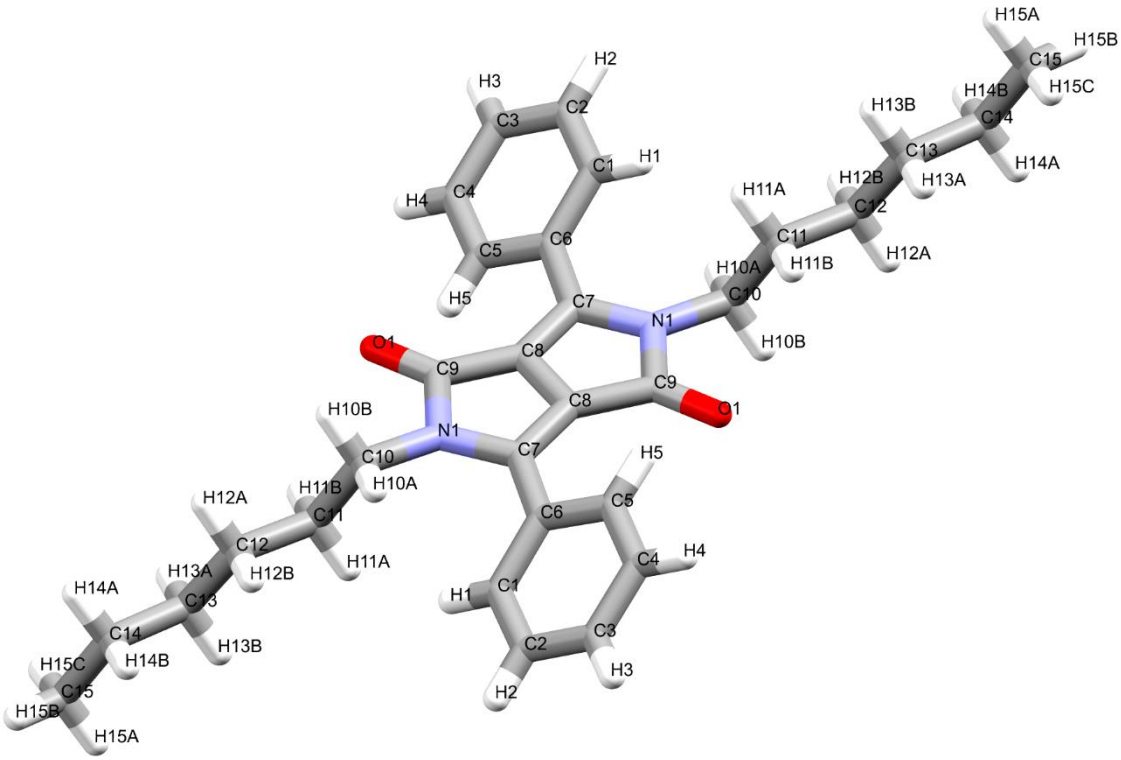

Table S2

PhOMeDPP *N*-2MB			
Number	Atom1	Atom2	Length (Å)
1	C14	H13A	2.876
2	H20C	O1	2.687
3	H20C	C7	2.816
4	H8	O4	2.634
5	C15	O2	3.120
6	H15	O2	2.279
7	O1	C9	3.183
8	O1	H9	2.276
9	O1	H26B	2.472
10	O3	H16	2.595

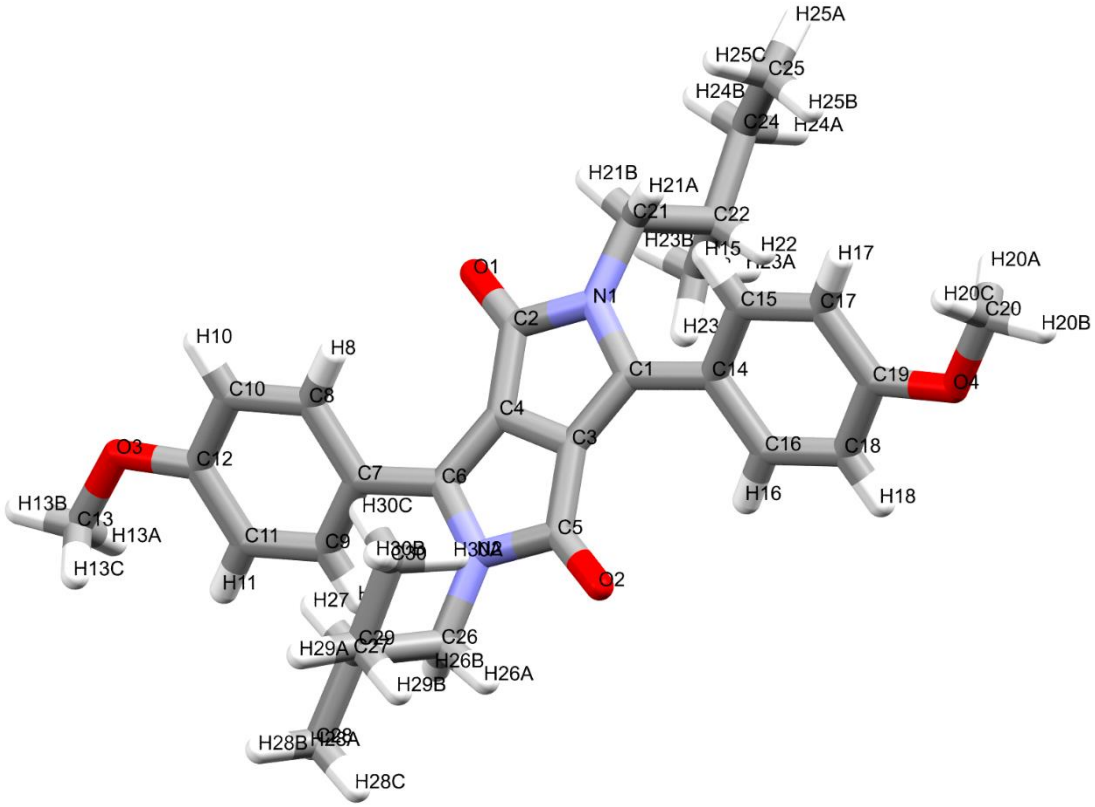

Table S3

PhOMeDPP *N*-Hex			
Number	Atom1	Atom2	Length (Å)
1	O001	H00Q	2.690
2	H00C	C00J	2.893
3	H00C	H00Q	2.380
4	O001	C009	3.217
5	O001	H009	2.395
6	O002	H008	2.621

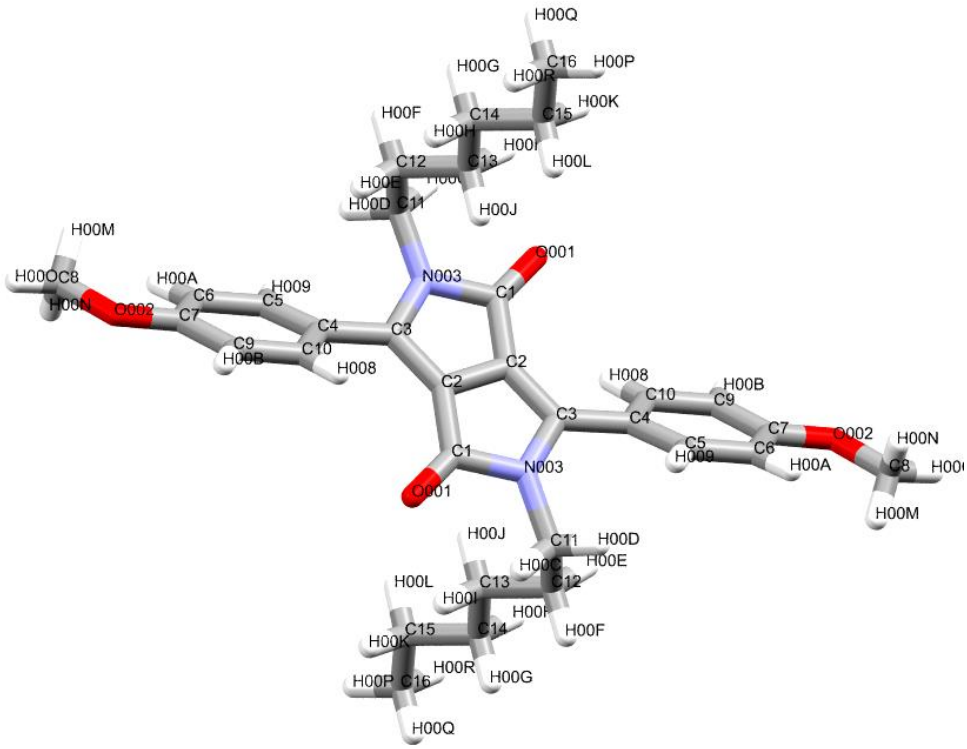

Table S4

PhOMeDPP *N*-Boc			
Number	Atom1	Atom2	Length (Å)
1	H6	H10B	2.355
2	C10	C10	2.171
3	C10	H10A	1.775
4	C10	H10B	2.369
5	C10	H10C	2.068
6	H10A	H10A	1.874
7	H10A	H10B	1.847
8	H10A	H10C	1.441
9	H10B	H10C	2.13
10	C3	C5	3.343
11	C7	C2	3.325
12	C8	C1	3.342
13	H15C	O1	2.641

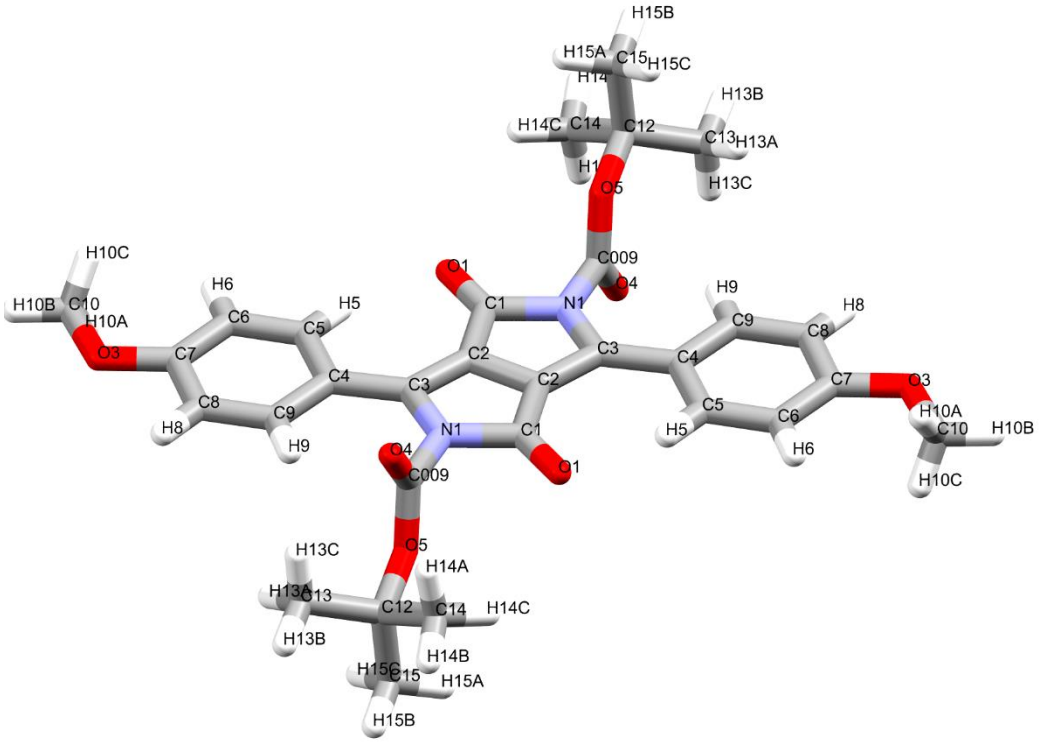

Table S5

PhOTHPDPP *N*-Hex			
Number	Atom1	Atom2	Length (Å)
1	H15A	O66	2.712
2	C2	H63A	2.888
3	C3	H63A	2.83
4	O5	H33	2.717
5	O5	H11B	2.485
6	H11A	C33	2.845
7	H11A	H33	2.298
8	H13B	C33	2.898

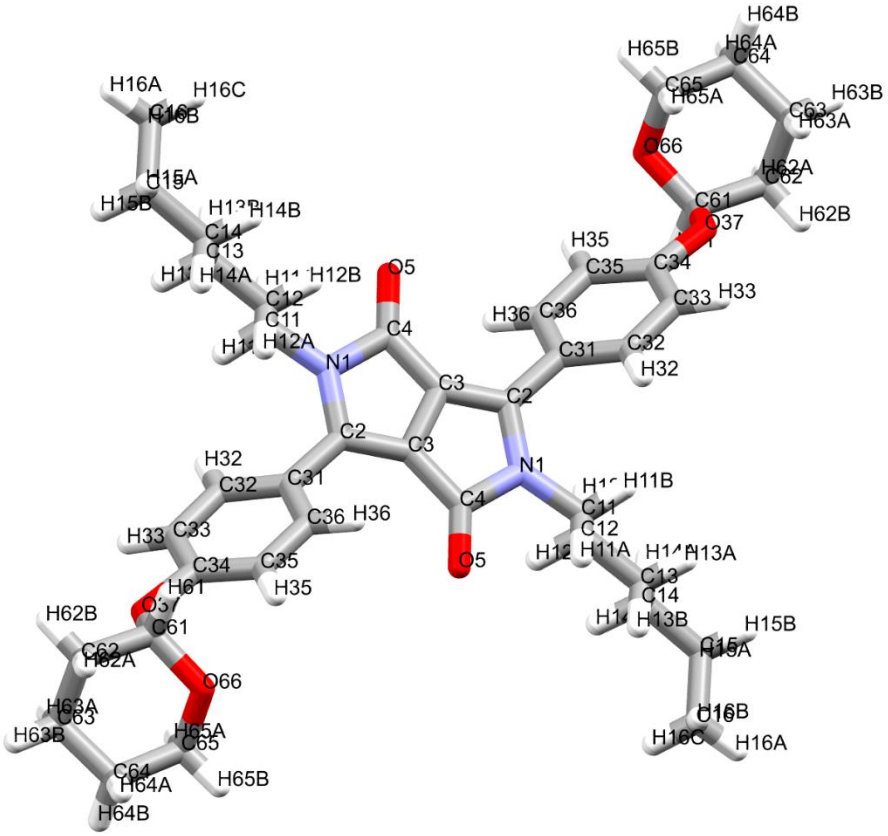

Table S6

PhOHDPP *N*-Hex			
Number	Atom1	Atom2	Length (Å)
1	O1	O2	2.681
2	O1	H11B	2.672
3	H1	O2	1.843
4	H1	H11B	2.385
5	H6	O2	2.595
6	O1	H10A	2.647
7	C1	H10A	2.831
8	C2	H10A	2.841
9	O1	H15A	2.572

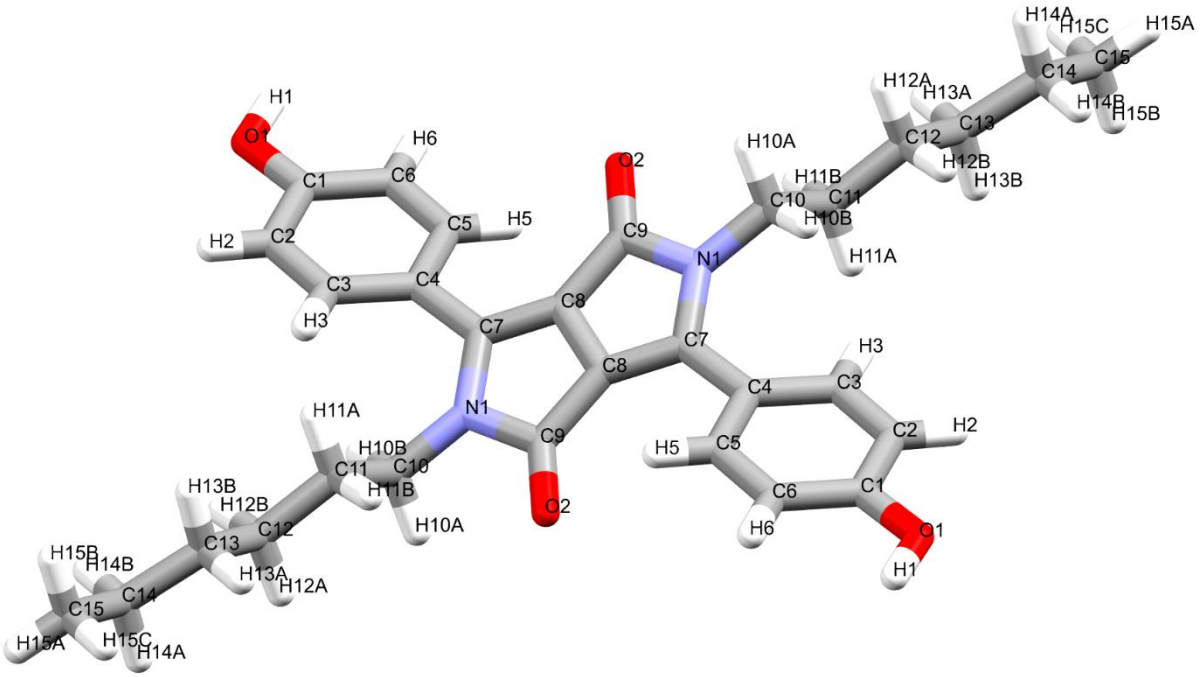

Table S7

PhOHDPP *N*-2MB			
Number	Atom1	Atom2	Length (Å)
1	C17	C6	3.369
2	H28C	O1	2.587
3	O2	O4	2.73
4	O2	H4	1.897
5	O2	H15	2.641
6	C16	H14	2.85
7	O1	O3	2.713
8	H1	O3	1.889
9	H21B	C12	2.857

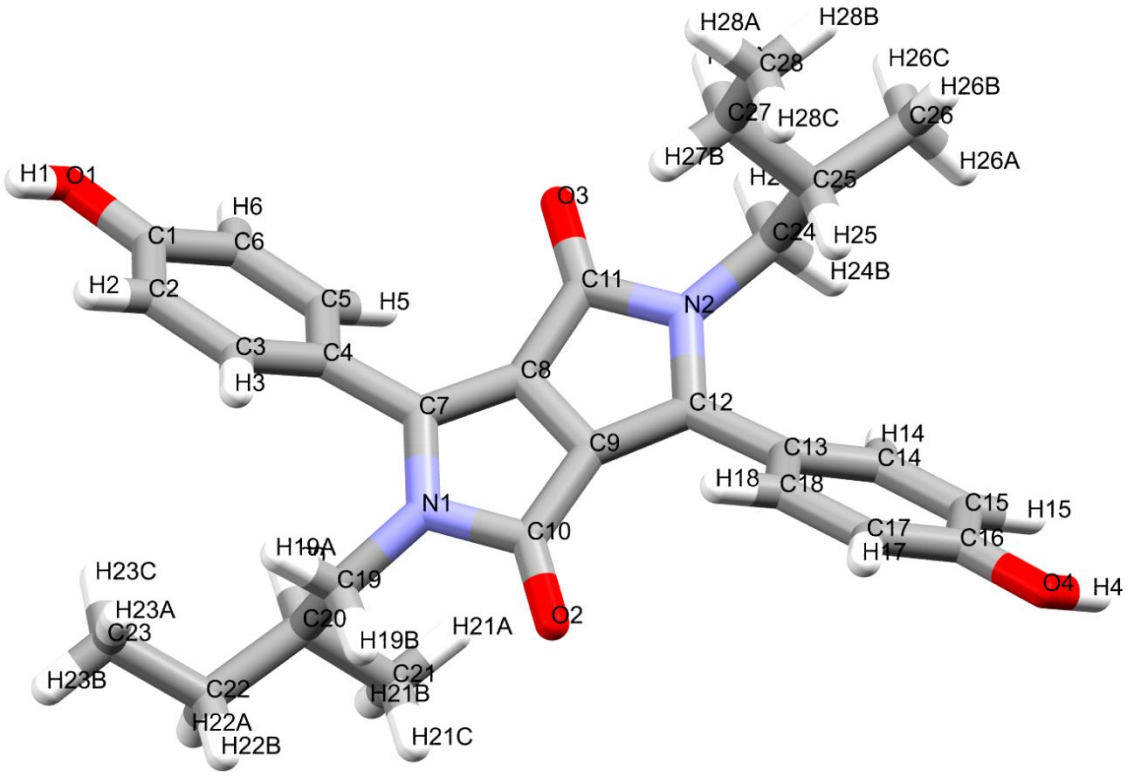

Table S8

PhOBocDPP *N*-Boc			
Number	Atom1	Atom2	Length (Å)
1	O5	C10	3.108
2	O5	H6	2.477
3	C5	C7	3.302
4	O3	H8	2.422
5	C10	H8	2.883
6	O1	H18B	2.534
7	O1	H19B	2.679

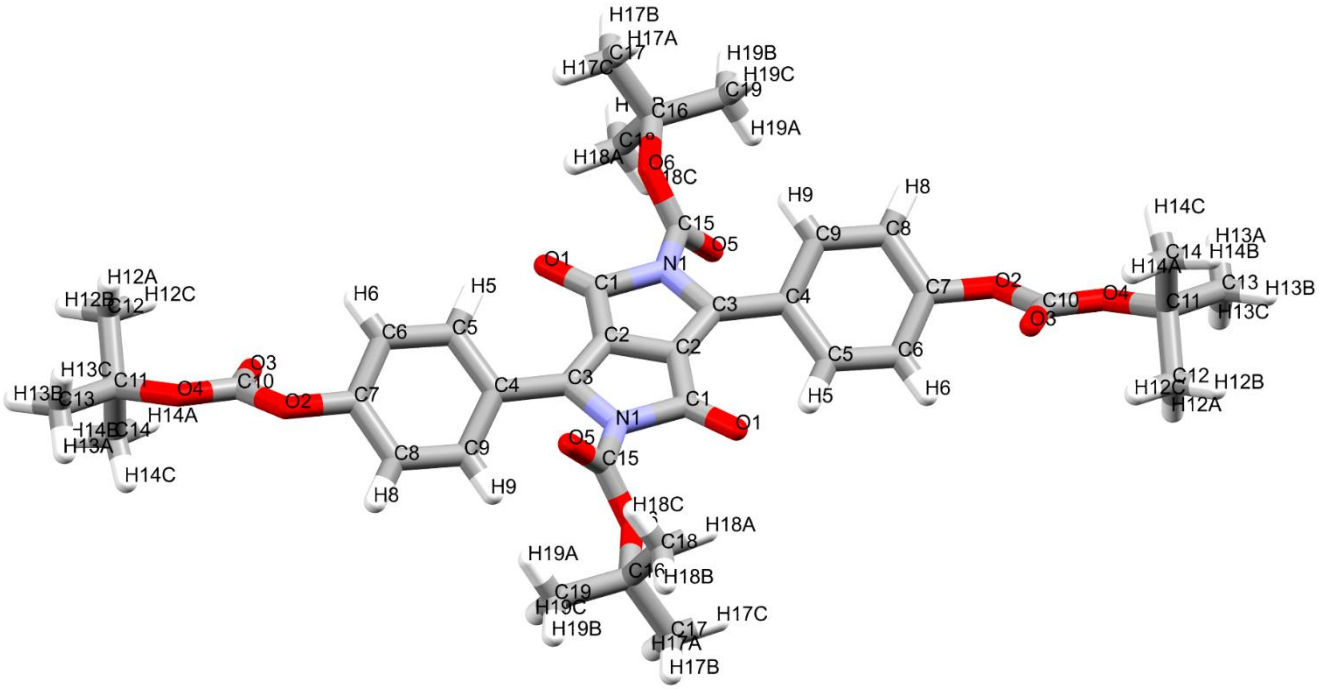

Table S9

PhDPP *N*-Boc			
Number	Atom1	Atom2	Length(Å)
1	O1	H3	2.645
2	H8	H13	2.334
3	H9	O2	2.543
4	H9	C12	2.898
5	H22	C9	2.839
6	C16	C16	3.310
7	O6	H10	2.716
8	O6	H4	2.582
9	C12	C12	3.342
10	C8	O3	3.217
11	H1	O3	2.628
12	H20	C3	2.858

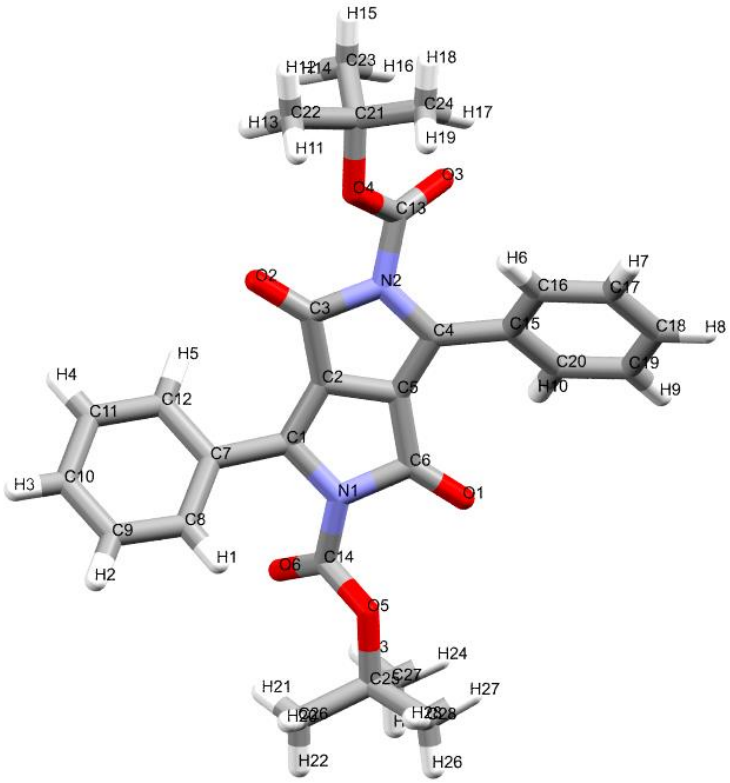

Table S10

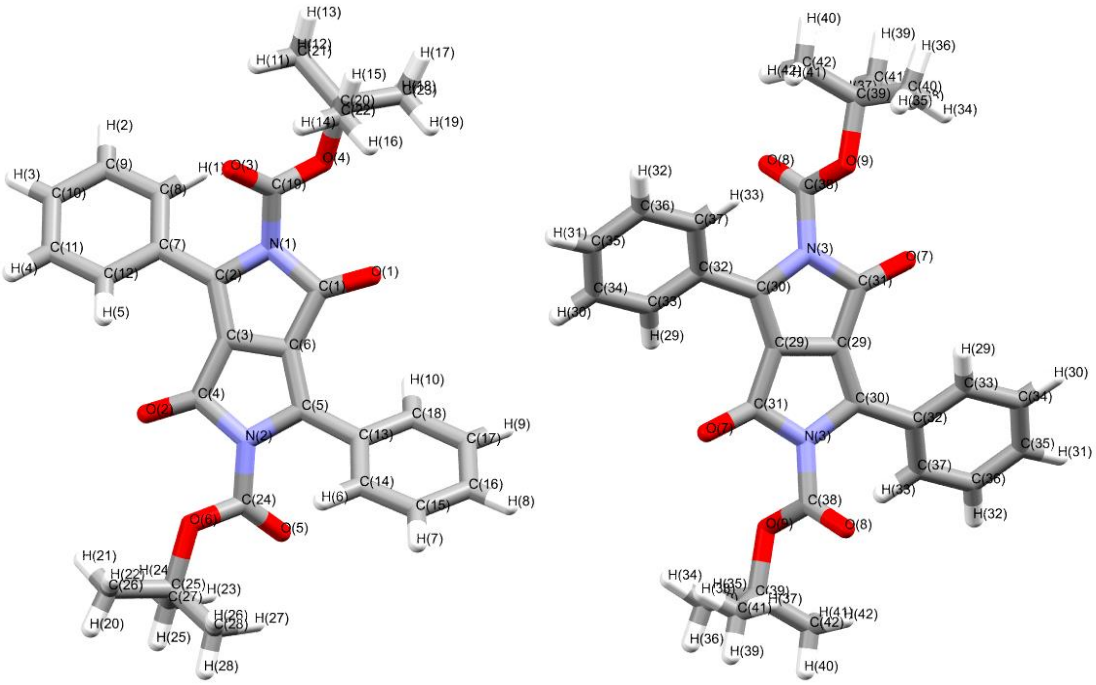

PhDPP *N*-Boc			
Number	**Atom1**	**Atom2**	**Length**(Å)
1	O(2)	C(16)	3.140
2	O(2)	H(8)	2.423
3	C(10)	O(1)	3.209
4	C(11)	O(1)	3.213
5	H(3)	O(1)	2.576
6	H(3)	H(19)	2.291
7	H(4)	O(1)	2.581
8	H(17)	O(5)	2.688
9	C(1)	H(26)	2.773
10	C(6)	H(26)	2.750
11	C(10)	H(30)	2.843
12	O(2)	H(37)	2.595
13	C(3)	O(8)	3.011
14	C(4)	O(8)	3.002
15	C(5)	O(8)	3.080
16	C(6)	O(8)	3.030

References

1 J. Cosier and A. M. Glazer, *J. Appl. Crystallogr.*, 1986, **19**, 105–107.

2 Rigaku Oxford Diffraction, (2018), CrysAlisPro Software system, version 1.171.40.45a, Rigaku Corporation, Oxford, UK.

3 O. V. Dolomanov, L. J. Bourhis, R. J. Gildea, J. A. K. Howard and H. Puschmann, *J. Appl. Crystallogr.*, 2009, **42**, 339–341.

4 G. M. Sheldrick, *Acta Crystallogr. Sect. A*, 2015, **71**, 3–8.

5 G. M. Sheldrick, *Acta Crystallogr. Sect. C Struct. Chem.*, 2015, **71**, 3–8.

6 "CheckCIF," can be found under http://checkcif.iucr.org.

7 D. . Allan, H. Nowell, S. Barnett, M. Warren, A. Wilcox, J. Christensen, L. Saunders, A. Peach, M. Hooper, L. Zaja, S. Patel, L. Cahill, R. Marshall, S. Trimnell, A. Foster, T. Bates, S. Lay, M. Williams, P. Hathaway, G. Winter, M. Gerstel and R. Wooley, *Crystals*, 2017, **7**, 336.

8 G. Winter, D. G. Waterman, J. M. Parkhurst, A. S. Brewster, R. J. Gildea, M. Gerstel, L. Fuentes-Montero, M. Vollmar, T. Michels-Clark, I. D. Young, N. K. Sauter and G. Evans, *Acta Crystallogr. Sect. D, Struct. Biol.*, 2018, **74**, 85–97.

9 Journal, 2018, CCP4 7.0.062 AIMLESS, version 060.067.062 027/005/018.

10 A. M. Brouwer, *Pure Appl. Chem.*, 2011, **83**, 2213–2228.

11 R. R. Gagne, C. A. Koval and G. C. Lisensky, *Inorg. Chem.*, 1980, **19**, 2854–2855.

12 A. Riaño, P. Mayorga Burrezo, M. J. Mancheño, A. Timalsina, J. Smith, A. Facchetti, T. J. Marks, J. T. López Navarrete, J. L. Segura, J. Casado and R. Ponce Ortiz, *J. Mater. Chem. C*, 2014, **2**, 6376–86.

13 M. J. Frisch, G. W. Trucks, H. B. Schlegel, G. E. Scuseria, M. A. Robb, J. R. Cheeseman, G. Scalmani, V. Barone, B. Mennucci, G. A. Petersson, H. Nakatsuji, M. Caricato, X. Li, H. P. Hratchian, A. F. Izmaylov, J. Bloino, G. Zheng, J. L. Sonnenberg, M. Hada, M. Ehara, K. Toyota, R. Fukuda, J. Hasegawa, M. Ishida, T. Nakajima, Y. Honda, O. Kitao, H. Nakai, T. Vreven, J. A. Montgomery, J. E. Peralta, F. Ogliaro, M. Bearpark, J. J. Heyd, E. Brothers, K. N. Kudin, V. N. Staroverov, R. Kobayashi, J. Normand, K. Raghavachari, A. Rendell, J. C. Burant, S. S. Iyengar, J. Tomasi, M. Cossi, N. Rega, J. M. Millam, M. Klene, J. E. Knox, J. B. Cross, V. Bakken, C. Adamo, J. Jaramillo, R. Gomperts, R. E. Stratmann, O. Yazyev, A. J. Austin, R. Cammi, C. Pomelli, J. W. Ochterski, R. L. Martin, K. Morokuma, V. G. Zakrzewski, G. A. Voth, P. Salvador, J. J. Dannenberg, S. Dapprich, A. D. Daniels, Farkas, J. B. Foresman, J. V Ortiz, J. Cioslowski and D. J. Fox, *Gaussian 09, Revis. B.01, Gaussian, Inc., Wallingford CT*, 2009.

14 B. Baumeier, J. Kirkpatrick and D. Andrienko, *Phys. Chem. Chem. Phys.*, 2010, **12**, 11103–11113.

15 E. F. Valeev, V. Coropceanu, D. A. da Silva Filho, S. Salman and J.-L. Brédas, *J. Am. Chem. Soc.*, 2006, **128**, 9882–9886.

16 T. Liu and A. Troisi, *J. Phys. Chem. C*, 2011, **115**, 2406–2415.

17 A. N. Sokolov, S. Atahan-Evrenk, R. Mondal, H. B. Akkerman, R. S. Sánchez-Carrera, S. Granados-Focil, J. Schrier, S. C. B. Mannsfeld, A. P. Zoombelt, Z. Bao and A. Aspuru-Guzik, *Nat. Commun.*, 2011, **2:437**, 1–8.

18 W. K. Chan, Y. Chen, Z. Peng and L. Yu, *J. Am. Chem. Soc.*, 1993, **115**, 11735–11743.

19 A. Shaabani, M. Dabiri, A. Bazgir and K. Gharanjig, *Dye. Pigm.*, 2006, **71**, 68–72.

20 Ciba Specialty Chemicals Corporation, USPat.,5969154, 1999.